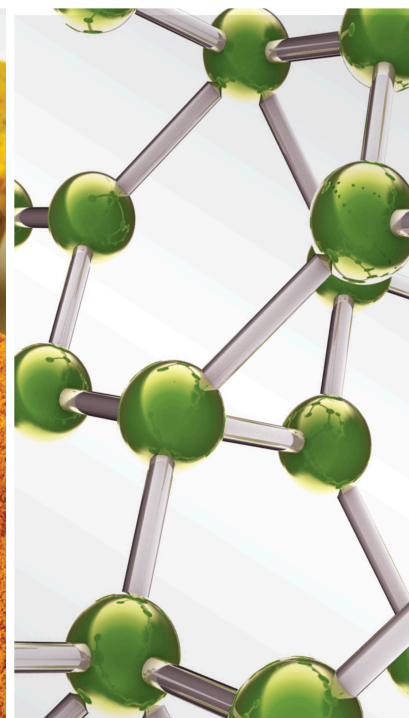# Natural Products as Sources of New Analgesic Drugs

Lead Guest Editor: Arielle Cristina Arena
Guest Editors: Candida Aparecida Leite Kassuya, Elisabete Castelon Konkiewitz, and Edward Benjamin Ziff

Natural Products as Sources of New Analgesic Drugs

Natural Products as Sources of New Analgesic Drugs

Lead Guest Editor: Arielle Cristina Arena
Guest Editors: Candida Aparecida Leite Kassuya,
Elisabete Castelon Konkiewitz, and Edward
Benjamin Ziff

Editorial Board

Daniel Collado-Mateo, Spain
Marisa Colone, Italy
Lisa A. Conboy, USA
Kieran Cooley, Canada
Edwin L. Cooper, USA
José Otávio do Amaral Corrêa, Brazil
Maria T. Cruz, Portugal
Roberto K. N. Cuman, Brazil
Ademar A. Da Silva Filho, Brazil
Chongshan Dai, China
Giuseppe D'Antona, Italy
Nawab John Dar, USA
Vincenzo De Feo, Italy
Rocío De la Puerta, Spain
marinella de leo, Italy
Laura De Martino, Italy
Josué De Moraes, Brazil
Mozaniel de Oliveira, Brazil
Arthur De Sá Ferreira, Brazil
Nunziatina De Tommasi, Italy
Gourav Dey, India
Dinesh Dhamecha, USA
Claudia Di Giacomo, Italy
Antonella Di Sotto, Italy
Gabriel O. Dida, Japan
Mario Dioguardi, Italy
Vishal Diwan, Australia
Caigan Du, Canada
Shizheng Du, China
Lin-Rui Duan, China
Jeng-Ren Duann, USA
Nativ Dudai, Israel
Thomas Efferth, Germany
Abir El-Alfy, USA
Mohamed Ahmed El-Esawi, Egypt
Mohd Ramli Elvy Suhana, Malaysia
Talha Bin Emran, Japan
Roger Engel, Australia
Karim Ennouri, Tunisia
Giuseppe Esposito, Italy
Tahereh Eteraf-Oskouei, Iran
Mohammad Faisal, Saudi Arabia
Sharida Fakurazi, Malaysia
Robson Xavier Faria, Brazil
Mohammad Fattahi, Iran
Keturah R. Faurot, USA
Piergiorgio Fedeli, Italy

Nianping Feng, China
Yibin Feng, Hong Kong
Glaura Fernandes, Brazil
Laura Ferraro, Italy
Antonella Fioravanti, Italy
Johannes Fleckenstein, Germany
Carmen Formisano, Italy
Harquin Simplice Foyet, Cameroon
Filippo Fratini, Italy
Huiying Fu, China
Hua-Lin Fu, China
Liz G Müller, Brazil
Jian-Li Gao, China
Dolores García Giménez, Spain
Gabino Garrido, Chile
Safoora Gharibzadeh, Iran
Muhammad N. Ghayur, USA
Roxana Ghiulai, Romania
Angelica Oliveira Gomes, Brazil
Yuewen Gong, Canada
Elena González-Burgos, Spain
Susana Gorzalczany, Argentina
Sebastian Granica, Poland
Jiangyong Gu, China
Maruti Ram Gudavalli, USA
Shanshan Guo, China
Jianming GUO, China
Shuzhen Guo, China
Jian-You Guo, China
Hai-dong Guo, China
Zihu Guo, China
Narcís Gusi, Spain
Svein Haavik, Norway
Fernando Hallwass, Brazil
Gajin Han, Republic of Korea
Ihsan Ul Haq, Pakistan
Md. Areeful Haque, India
Hicham Harhar, Morocco
Kuzhuvelil B. Harikumar, India
Mohammad Hashem Hashempur, Iran
Muhammad Ali Hashmi, Pakistan
Waseem Hassan, Pakistan
Sandrina A. Heleno, Portugal
Pablo Herrero, Spain
Soon S. Hong, Republic of Korea
Md. Akil Hossain, Republic of Korea
Muhammad Jahangir Hossen, Bangladesh

Shih-Min Hsia, Taiwan
Ching-Liang Hsieh, Taiwan
Weicheng Hu, China
Sen Hu, China
Changmin Hu, China
Tao Hu, China
Sheng-Teng Huang, Taiwan
Wei Huang, China
Ciara Hughes, Ireland
Attila Hunyadi, Hungary
Tarique Hussain, Pakistan
Maria-Carmen Iglesias-Osma, Spain
Elisha R. Injeti, USA
H. Stephen Injeyan, Canada
Amjad Iqbal, Pakistan
Chie Ishikawa, Japan
Angelo A. Izzo, Italy
Mohieddin Jafari, Finland
Rana Jamous, Palestinian Authority
Muhammad Saeed Jan, Pakistan
G. K. Jayaprakasha, USA
Kamani Ayoma Perera Wijewardana
Jayatilaka, Sri Lanka
Kyu Shik Jeong, Republic of Korea
Qing Ji, China
Yanxia Jin, China
Hualiang Jin, China
Leopold Jirovetz, Austria
Won-Kyo Jung, Republic of Korea
Jeeyoun Jung, Republic of Korea
Atul Kabra, India
Sleman Kadan, Israel
Takahide Kagawa, Japan
Nurkhalida Kamal, Saint Vincent and the
Grenadines
Atsushi Kameyama, Japan
Wenyi Kang, China
Kyungsu Kang, Republic of Korea
Shao-Hsuan Kao, Taiwan
Juntra Karbwang, Japan
Nasiara Karim, Pakistan
Morimasa Kato, Japan
Deborah A. Kennedy, Canada
Asaad Khalid Khalid, Saudi Arabia
Haroon Khan, Pakistan
Washim Khan, USA
Bonglee Kim, Republic of Korea

Yun Jin Kim, Malaysia
Junghyun Kim, Republic of Korea
Dong Hyun Kim, Republic of Korea
Kyungho Kim, Republic of Korea
Youn-Chul Kim, Republic of Korea
Cheorl-Ho Kim, Republic of Korea
Jin-Kyung Kim, Republic of Korea
Kibong Kim, Republic of Korea
Woojin Kim, Republic of Korea
Yoshiyuki Kimura, Japan
Nebojša Kladar, Serbia
Mi Mi Ko, Republic of Korea
Toshiaki Kogure, Japan
Jian Kong, USA
Malcolm Koo, Taiwan
Yu-Hsiang Kuan, Taiwan
Robert Kubina, Poland
Omer Kucuk, USA
Victor Kuete, Cameroon
Woon-Man Kung, Taiwan
Chan-Yen Kuo, Taiwan
Joey S. W. Kwong, China
Kuang C. Lai, Taiwan
Fanuel Lampiao, Malawi
Ilaria Lampronti, Italy
Chou-Chin Lan, Taiwan
Mario Ledda, Italy
Sang Yeoup Lee, Republic of Korea
Dong-Sung Lee, Republic of Korea
Kyu Pil Lee, Republic of Korea
Jeong-Sang Lee, Republic of Korea
Byung-Cheol Lee, Republic of Korea
Namhun Lee, Republic of Korea
Yun Jung Lee, Republic of Korea
Gihyun Lee, Republic of Korea
Harry Lee, China
Ju Ah Lee, Republic of Korea
Christian Lehmann, Canada
Marivane Lemos, Brazil
George B. Lenon, Australia
Marco Leonti, Italy
Xing Li, China
Min Li, China
XiuMin Li, Armenia
Chun-Guang Li, Australia
Xuqi Li, China
Hua Li, China

Yi-Rong Li, Taiwan
Yu-cui Li, China
Xi-Wen Liao, China
Vuanghao Lim, Malaysia
Shuibin Lin, China
Bi-Fong Lin, Taiwan
Shih-Chao Lin, Taiwan
Ho Lin, Taiwan
Kuo-Tong Liou, Taiwan
Chian-Jiun Liou, Taiwan
Christopher G. Lis, USA
Gerhard Litscher, Austria
I-Min Liu, Taiwan
Jingping Liu, China
Xiaosong Liu, Australia
Suhuan Liu, China, China
Yujun Liu, China
Emilio Lizarraga, Argentina
Monica Loizzo, Italy
Nguyen Phuoc Long, Republic of Korea
Víctor López, Spain
Zaira López, Mexico
Chunhua Lu, China
Ângelo Luís, Portugal
Anderson Luiz-Ferreira, Brazil
Jian-Guang Luo, China
Ivan Luzardo Luzardo-Ocampo, Mexico
Zheng-tao Lv, China
Michel Mansur Machado, Brazil
Filippo Maggi, Italy
Jamal A. Mahajna, Israel
Juraj Majtan, Slovakia
Toshiaki Makino, Japan
Nicola Malafronte, Italy
Giuseppe Malfa, Italy
Francesca Mancianti, Italy
Subashani Maniam, Australia
Carmen Mannucci, Italy
Arroyo-Morales Manuel, Spain
Juan M. Manzaneque, Spain
Fatima Martel, Portugal
Simona Martinotti, Italy
Carlos H. G. Martins, Brazil
Stefania Marzocco, Italy
Maulidiani Maulidiani, Malaysia
Andrea Maxia, Italy
Avijit Mazumder, India

Isac Medeiros, Brazil
Ahmed Mediani, Malaysia
Lewis Mehl-Madrona, USA
Ayikoé Guy Mensah-Nyagan, France
Oliver Micke, Germany
Maria G. Miguel, Portugal
Luigi Milella, Italy
Roberto Miniero, Italy
Letteria Minutoli, Italy
Prashant Modi, India
Daniel Kam-Wah Mok, Hong Kong
Changjong Moon, Republic of Korea
Albert Moraska, USA
Mark Moss, United Kingdom
Yoshiharu Motoo, Japan
Kamal D. Moudgil, USA
Yoshiki Mukudai, Japan
Sakthivel Muniyan, USA
Laura Muñoz-Bermejo, Spain
Saima Muzammil, Pakistan
Massimo Nabissi, Italy
Siddavaram Nagini, India
Hajime Nakae, Japan
Takao Namiki, Japan
Srinivas Nammi, Australia
Krishnadas Nandakumar, India
Vitaly Napadow, USA
Derek Tantoh Ndinteh, South Africa
Pratibha V. Nerurkar, USA
Jorddy Neves Cruz, Brazil
Benoit Banga N'guessan, Ghana
Marcello Nicoletti, Italy
Eliud Nyaga Mwaniki Njagi, Kenya
Cristina Nogueira, Brazil
Sakineh Kazemi Noureini, Iran
Rômulo Dias Novaes, Brazil
Martin Offenbaecher, Germany
Yoshiji Ohta, Japan
Oluwafemi Adeleke Ojo, Nigeria
Olumayokun A. Olajide, United Kingdom
Olufunmiso Olusola Olajuyigbe, Nigeria
Luís Flávio Oliveira, Brazil
Atolani Olubunmi, Nigeria
Abimbola Peter Oluyori, Nigeria
Vahidreza Ostadmohammadi, Iran
Chiagoziem Anariochi Otuechere, Nigeria
Mustafa Ozyurek, Turkey

Ester Pagano, Italy
Sokcheon Pak, Australia
Antônio Palumbo Jr, Brazil
Zongfu Pan, China
Yunbao Pan, China
Siyaram Pandey, Canada
Gunhyuk Park, Republic of Korea
Bong-Soo Park, Republic of Korea
Wansu Park, Republic of Korea
Rodolfo Parreira, Brazil
Matheus Pasquali, Brazil
Luiz Felipe Passero, Brazil
Visweswara Rao Pasupuleti, Malaysia
Bhushan Patwardhan, India
Claudia Helena Pellizzon, Brazil
Weijun Peng, China
Cheng Peng, Australia
Shagufta Perveen, Saudi Arabia
Raffaele Pezzani, Italy
Florian Pfab, Germany
Sonia Piacente, Italy
Andrea Pieroni, Italy
Richard Pietras, USA
Haifa Qiao, USA
Sheng Qin, China
Cláudia Quintino Rocha, Brazil
Khalid Rahman, United Kingdom
Nor Fadilah Rajab, Malaysia
Elia Ranzato, Italy
Manzoor A. Rather, India
Valentina Razmovski-Naumovski, Australia
Julita Regula, Poland
Kanwal Rehman, Pakistan
Gauhar Rehman, Pakistan
Ke Ren, USA
Man Hee Rhee, Republic of Korea
Daniela Rigano, Italy
José L. Rios, Spain
Francisca Rius Diaz, Spain
Eliana Rodrigues, Brazil
Maan Bahadur Rokaya, Czech Republic
Barbara Romano, Italy
Mariangela Rondanelli, Italy
Antonietta Rossi, Italy
DANIELA RUSSO, Italy
Mi Heon Ryu, Republic of Korea
Bashar Saad, Palestinian Authority

Abdul Sadiq, Pakistan
Sabiu Saheed, South Africa
Mohamed Z.M. Salem, Egypt
Avni Sali, Australia
Andreas Sandner-Kiesling, Austria
Manel Santafe, Spain
José Roberto Santin, Brazil
Antonietta Santoro, Italy
Tadaaki Satou, Japan
Roland Schoop, Switzerland
Sven Schröder, Germany
Sindy Seara-Paz, Spain
Veronique Seidel, United Kingdom
Terry Selfe, USA
Senthamil R. Selvan PhD, USA
Arham Shabbir, Pakistan
Suzana Shahar, Malaysia
Hongcai Shang, China
Wen-Bin Shang, China
Ronald Sherman, USA
Karen J. Sherman, USA
She-Po Shi, China
San-Jun Shi, China
Insop Shim, Republic of Korea
Im Hee Shin, Republic of Korea
Yukihiro Shoyama, Japan
Morry Silberstein, Australia
Samuel Martins Silvestre, Portugal
Moganavelli Singh, South Africa
Kuttulebbai N. S. Sirajudeen, Malaysia
Slim Smaoui, Tunisia
Eun Jung Sohn, Republic of Korea
Francisco Solano, Spain
Maxim A. Solovchuk, Taiwan
Young-Jin Son, Republic of Korea
Chang G. Son, Republic of Korea
Yanting Song, China
Chengwu Song, China
Klaokwan Srisook, Thailand
Vanessa Steenkamp, South Africa
Annarita Stringaro, Italy
Dan Su, China
Shan-Yu Su, Taiwan
Keiichiro Sugimoto, Japan
Valeria Sulsen, Argentina
Zewei Sun, China
Amir Syahir, Malaysia

Xiaobin Zeng, Shenzhen People's Hospital,
2nd Clinical Medical College of Jinan
University, Shenzhen 518120, Guangdong
Province,China, China
Bimeng Zhang, China
Zhiqian Zhang, China
Jianliang Zhang, China
Mingbo Zhang, China
Jiu-Liang Zhang, China
Fangbo Zhang, China
RONGJIE ZHAO, China
Jing Zhao, China
Zhangfeng Zhong, Macau
Yan Zhu, USA
Guoqi Zhu, China
Suzanna M. Zick, USA
Stephane Zingue, Cameroon

Contents

Editorial

Natural Products as Sources of New Analgesic Drugs

Arielle Cristina Arena ,[1] Candida Aparecida Leite Kassuya,[2] Elisabete Castelon Konkiewitz,[2] and Edward Benjamin Ziff[3]

[1]*Universidade Estadual Paulista, São Paulo, Brazil*
[2]*Universidade Federal da Grande Dourados, Dourados, Brazil*
[3]*New York University Grossman School of Medicine, New York, NY, USA*

Correspondence should be addressed to Arielle Cristina Arena; arielle.arena@unesp.br

At the same time, as conventional therapies for the treatment of pain are losing their effectiveness, more and more pharmacological studies are showing that products of natural origin are promising for the development of new molecules or therapies. The idea for this special issue emerged from the considerable interest in identifying new therapeutic agents obtained from plants used in popular medicine for the treatment and/or management of pain. New drugs and therapies that are highly effective, low cost, safe, and available may be developed through comprehensive investigation of the bioactivities of a number of natural compounds. With this in mind, researchers from different countries were invited to contribute original research and review articles about new natural products with analgesic properties. After the review process, 5 high-quality articles were accepted for publication. The topics included in this issue comprise effects of new medicinal plants with analgesic properties studied using animal models of chronic pain, the safety and/or adverse effects of medicinal plants with analgesic activities, effects of new medicinal plants in pain management, and the mode of action of plants with analgesic activities. A brief summary of each of the accepted articles is provided as follows.

The paper by H. Ilmi et al. evaluated the analgesic and antipyretic effects of a tablet obtained from *Andrographis paniculata* ethyl acetate fraction, in animal models. *A. paniculata* is an herbaceous plant belonging to the Acanthaceae family, found especially in India, Sri Lanka, Pakistan, and Indonesia. The authors observed that the *A. paniculata* ethyl acetate fraction exhibited analgesic and antipyretic activities in the tablet dosage form. The results revealed that this species could be an excellent candidate as an herbal medicine for the treatment of pain and fever.

C. C. Liao et al. studied the effects of *Scutellaria baicalensis* (SB), a traditional Chinese medicine used for the treatment of inflammatory and painful conditions, on migraine by behavioral analysis of systemic administration to rats using the nitroglycerin (NTG) induced migraine rat model. The authors observed that pretreatment with 1.0 g/kg SB alleviated migraine-related behaviors in the NTG-induced experimental model. Thus, SB may be a promising natural product for the treatment of migraine.

In another paper, J. Chang et al. investigated the molecular mechanism as well as the effective compounds present in the Gu-tong formula. Gu-tong formula (GTF) is used in treatment of cancer-related pain and includes nine traditional Chinese medicines. The authors revealed the potential pharmacological mechanism of GTF in cancer pain treatment, from a systematic perspective, which may involve the secretion of inflammatory cytokines, membrane potential, bone protection, and other biological processes through the regulation of chemokines, MAPK, and TRP channels. Cholesterol and stigmasterol in GTF have been suggested to be the key pharmacodynamic molecules for analgesia, as seen in molecular docking screening. These findings provide insights into comprehending the synergistic effect of GTF on cancer pain relief.

The paper by S. A. Richard et al. focuses explicitly on an analgesic-antitumor peptide (AGAP) extracted from the venom of Scorpion BmK, with the aim of elucidating the

cardinal analgesic and antitumor potentials of AGAP, with the emphasis on the key signaling mechanisms through which it functions. This review clearly points to the fact that AGAP has analgesic and antitumor potentials. Studies have shown that AGAP has a strong inhibitory influence on both viscera and soma pain. In addition, AGAP enhances the effects of MAPK inhibitors in neuropathic and inflammation-associated pain. In cancers such as colon cancer, breast cancer, lymphoma, and glioma, AGAP was effective in blocking proliferation. This molecule has more affinity for tumor cells and has less harmful effects on healthy cells. Thus, AGAP can represent a promising analgesic and antitumor therapy for some types of tumors.

In addition to therapeutic tests, products of natural origin should be evaluated for their safety, and toxicity tests are required by international regulatory agencies. W. A. S. S. Weerakoon et al. investigated the safety profile of the Sudarshana powder (SP) and its novel preparation, Sudarshana suspension (SS), in male Wistar rats, and tolerance studies were conducted with healthy adult volunteers. Sudarshana powder is an effective antipyretic Ayurvedic preparation, widely used in Sri Lanka as well as in India from the very early beginning of Ayurveda treatment. The data collected revealed that the extract of SP and novel preparation SS given orally to male Wistar rats and healthy volunteers did not cause toxicity at the therapeutic dose level, which demonstrates its safety after oral administration.

We hope that this issue of *Evidence-Based Complementary and Alternative Medicine* will be truly special for researchers studying the effects of natural products as sources of new analgesic drugs.

Conflicts of Interest

The editors declare that they have no conflicts of interest regarding the publication of this special issue.

Acknowledgments

Arielle Cristina Arena
Candida Aparecida Leite Kassuya
Elisabete Castelon Konkiewitz
Edward Benjamin Ziff

Research Article

Analgesic and Antipyretic Activities of Ethyl Acetate Fraction Tablet of *Andrographis paniculata* in Animal Models

Hilkatul Ilmi [ID],[1] **Irfan Rayi Pamungkas** [ID],[2] **Lidya Tumewu** [ID],[1] **Achmad Fuad Hafid** [ID],[1,3] **and Aty Widyawaruyanti** [ID][1,3]

[1]*Center of Natural Product Medicine Research and Development, Institute of Tropical Disease, Universitas Airlangga, Surabaya 60115, Indonesia*
[2]*Undergraduate Student, Universitas Airlangga, Surabaya 60115, Indonesia*
[3]*Department of Pharmaceutical Sciences, Faculty of Pharmacy, Universitas Airlangga, Surabaya 60115, Indonesia*

Correspondence should be addressed to Aty Widyawaruyanti; aty-w@ff.unair.ac.id

Objectives. To determine the analgesic and antipyretic activities of a tablet derived from *Andrographis paniculata* ethyl acetate fraction (AS201-01) in animal models. *Methods*. The tablet derived from AS201-01 contains an equivalent of 35 mg andrographolide per tablet. Analgesic activity was determined using an acetic acid-induced writhing test on adult male mice. A writhe was recorded by a stopwatch and was defined as the stretching of the abdomen and/or stretching of at least one hind limb. For the determination of antipyretic activity, pyrexia was induced by subcutaneous injection of 15% w/v Brewer's yeast into adult male rats. Rectal temperature was monitored at 1, 2, 3, and 4 hours after treatment. *Results*. The results showed that the AS201-01 tablet had analgesic and antipyretic activity. In the acetic acid-induced writhing model, AS201-01 tablet exhibited significant analgesic effect with a 66.73% reduction in writhing response at a dose of 50 mg andrographolide/kg body weight compared to the negative control group. The tablet also showed a significant antipyretic effect. The maximum antipyretic effect was observed after the third hour of administration of the AS201-01 tablet at a dose of 100 mg andrographolide/kg body weight. *Conclusion*. Tablet of *Andrographis paniculata* ethyl acetate fraction (AS201-01) exhibited analgesic and antipyretic activities.

1. Introduction

Nonsteroidal anti-inflammatory drugs (NSAID) are used worldwide to treat inflammation, pain, and fever. However, they often produce significant side effects and are toxic to various organs of the body, causing problems such as kidney failure, allergic reactions, reduced auditory ability, and increased risk of hemorrhage due to interference with platelet function [1, 2]. Therefore, the development of novel compounds with analgesic and antipyretic activities without side effects are needed [3].

Traditional uses of medicinal plants provide suitable sources for the development of new drugs [4]. *Andrographis paniculata*, commonly known as the "king of bitters", is an herbaceous plant belonging to the Acanthaceae family. This plant is widely grown in the tropics, especially in India, Sri Lanka, Pakistan, and Indonesia [5]. *Andrographis paniculata* is one of the most popular medicinal plants used traditionally to treat fever and infectious diseases. This plant has been reported to have anti-inflammatory, antibacterial, antioxidant, anticancer, antidiabetic, antimalarial, hepatoprotective, immunostimulant, antiallergic, analgesic, and antipyretic effects [6–10].

Several studies have been conducted to determine the analgesic and antipyretic activity of *A. paniculata*. The compounds isolated from *A. paniculata*, namely, andrographolide and 14-deoxy-11,12-didehydroandrographolide, as well as the derivatives of both, showed analgesic and antipyretic activities [11]. Analgesic activity was determined *in vivo* in mice using the hot plate and writhing test, while antipyretic activity was determined *in vivo* in rats using the Baker's yeast-induced fever test. Andrographolide produced

a significant analgesic effect at a dose of 4 mg/kg body weight given intraperitoneally [11–13]. Ethanol extract of *A. paniculata* showed the analgesic activity in the writhing test in mice [2]. The ethanol extract of *A. paniculata* was introduced orally in the mice, and the results showed that the *A. paniculata* ethanol extract had an analgesic activity of 34%. Sodium diclofenac, the positive control, had an analgesic activity of 76%.

Previous studies have reported that the ethyl acetate fraction of *A. paniculata* contains 27.22% higher andrographolide compared to the ethanol extract [14]. Therefore, an increased likelihood that the ethyl acetate fraction of *A. paniculata* will have stronger analgesic and antipyretic effects than the ethanol extract. However, this has never been tested. Here we show the first investigation into the analgesic and antipyretic activities of the ethyl acetate fraction tablet of *A. paniculata*.

2. Materials and Methods

2.1. Materials. The plant material used in this study was *Andrographis paniculata* powder with 1.82% andrographolide content obtained from Pharmaceutical Industry PT Kimia Farma (Persero) Tbk., Indonesia. The tablet derived from *A. paniculata* ethyl acetate fraction (AS201-01) contained an equivalent of 35 mg andrographolide per tablet and was produced at Faculty of Pharmacy, Universitas Airlangga.

2.2. Extraction and Fractionation. Andrographolide is the major active compound found in *A. paniculata*. It was optimally soluble in methanol and ethanol, and the solubility increased with an increase of temperature in the range of 15–50°C [15]. Ethanol can be used as an extraction solvent and safe for human consumption [16]. Therefore, the extraction was conducted using ethanol at temperature 50°C to optimize the extraction result. The *A. paniculata* powder as much as 1 kg was extracted using 6 L of 96% ethanol as a solvent. The extraction was conducted by stirring for 60 minutes at temperature of 50°C. The extract was filtered, and residue was further extracted again using 6 L of 96% ethanol. The second extract was filtered and gathered with the first extract. Total solvent used for extraction was 12 L. The collected liquid extract then evaporated to 40% of its initial volume to obtain a concentrated extract. The concentrated extract was then fractionated with water-ethyl acetate (2 : 1) mixture to obtain the ethyl acetate fraction. The liquid fraction was then evaporated to obtain a dried ethyl acetate fraction [14].

2.3. Determination of Andrographolide Content in Ethyl Acetate Fraction and Tablet. Andrographolide content in ethyl acetate fraction and tablet was determined by thin layer chromatography (TLC)-densitometry. Andrographolide standard (Aldrich 365645-100 MG) and samples (ethyl acetate fraction and AS201-01 tablet) were spotted on a TLC silica gel 60 GF254 plates. A chloroform-methanol solution (9 : 1) was used in the mobile phase. TLC plate was then analyzed under UV wavelength of 200–400 nm with CAMAG TLC scanner 3, and maximum absorbance was found to be 228 nm. The regression curve of the andrographolide standards was determined, and then it was used to calculate the andrographolide content in fraction and tablet [14].

2.4. Formulation and Production of Ethyl Acetate Fraction Tablet. The ethyl acetate fraction tablet was produced to contain 35 mg andrographolide. The amount of ethyl acetate fraction per tablet was calculated based on andrographolide content which was determined previously. Tablet composition was as follows: ethyl acetate fraction (equivalent to 35 mg andrographolide) 167.5 mg, PVP K-30 13 mg, microcrystalline cellulose (MCC) 150 mg, amylum manihot 150 mg, lactose 120 mg, PEG-4000 13.75 mg, sodium starch glycolate (SSG) 26 mg, talk 4.875 mg, and Mg stearate 4.875 mg. The total weight of the tablet was 650 mg.

Tablets were produced on the laboratory scale, 100 tablets per batch. To produce the tablet, first, the ethyl acetate fraction was dissolved in a sufficient quantity of ethanol. PEG-4000 and PVP K-30 were then added and mixed. MCC was then added as a diluent, followed by amylum manihot and lactose. The mixture was then dried at temperature 40°C for 12 hours and sifted through an 18-mesh sieve (1 mm). SSG, talk, and Mg stearate were added as a diluent and lubricant, respectively, and then mixed well for 15 min. The prepared mixture was compressed into a tablet using a 13 mm punch on a tablet machine.

2.5. Evaluation of Tablet. The tablet of *A. paniculata* ethyl acetate fraction (AS201-01) was evaluated for following parameters [17].

2.6. Tablet Weight Variation. The high weight variation of the tablet had the ability to influence the dose. Therefore, a weight variation test was carried out. Twenty tablets were weighed individually using an electronic balance (Precisa), and the average weight was calculated.

2.7. Hardness. Tablets must have a certain hardness to withstand mechanical shocks. Tablet hardness can also affect the dissolution release, influencing the bioavailability of the drug. Therefore, a hardness test was conducted using a hardness tester (Schleuniger). A runway driven by an electric motor pressed the tablet until the tablet breaks, a scale instruction gives the breaking strength value (kg/cm^2). The recommended value is 4–8 kg/cm^2 which indicates hardness of tablets.

2.8. Friability. The tablets are weighed, and placed on a device (Friabilator) then operate device as much as 100 revolutions (25 rpm). Then, the tablets were dedusted and reweighed. Weight loss should not exceed 0.5–1%. Percent friability (%*F*) was calculated as follows:

$$\%F = \frac{\text{loss in weight}}{\text{initial weight}} \times 100. \qquad (1)$$

2.9. Disintegration Time.

Disintegration time was assessed using disintegration apparatus at $37 \pm 2^{\circ}$C. We placed 1 tablet in each of the 6 tubes of basket-rack assembly, and the apparatus was operate using water. We observed the time needed for tablets to disintegrate completely. After 30 minutes, the basket-rack assembly from fluid was lifted, and we observed the tablets. All of the tablets should have disintegrated completely. If 1 or 2 tablets fail to disintegrate, we repeated the test on 12 additional tablets. No less than 16 of 18 tested tablets must be completely disintegrated after 30 minutes.

2.10. Experimental Animal.

Male mice (BALB/C strain, 25–30 g) were used for the analgesics activity test, and male rats (Wistar strain, 100–150 g) were used for the antipyretics activity test. The animals were maintained on a standard animal pellets diet (NUVO pellets) and water *ad libitum* at the Animal Laboratory of the Institute of Tropical Disease, Universitas Airlangga, Surabaya. The animals were kept at standard temperature ($25 \pm 1^{\circ}$C) and a 12/12 h light/dark cycle. All the animals were acclimatized for seven days before the study [4]. Permission and approval for animal studies were obtained from the Faculty of Veterinary Medicine, Universitas Airlangga, with approval number 753-KE.

2.11. Analgesic Activity Test Using Acetic Acid-Induced Writhing Test.

The analgesic activity was determined by the acetic acid abdominal constriction test [18, 19]. Twenty-five male mice were randomly divided into 5 groups, where each group consisted of 5 mice. Group 1 was treated with carboxymethyl cellulose (CMC-Na 0.5%) (as negative control). Group 2 was treated with standard drug diclofenac sodium at a dose of 40 mg/kg body weight [2]. Groups 3, 4, and 5 were treated with AS201-01 tablets at a dose equal to 12.5, 25, and 50 mg andrographolide/kg body weight, respectively. All treatments were administered orally. Thirty minutes after administration of all treatments, each mouse was injected with 1% acetic acid at a dose of 10 ml/kg body weight intraperitoneally [20, 21]. At 5, 15, 25, 35, and 45 minutes after acetic acid injection, the number of writhing responses observed during a 5-minute period were counted and recorded [11].

The percentage of analgesic activity was calculated as follows:

$$\% \text{ inhibition } = \frac{\text{Wc} - \text{Wt}}{\text{Wc}} \times 100\%, \qquad (2)$$

where W is the number of writhing, c is the negative control, and t is the test.

2.12. Antipyretic Activity Test Using Yeast-Induced Hyperthermia in Rats.

The antipyretic activity was evaluated with a fever induced by Brewer's yeast (Sigma 51475) following the established method in rats with some modifications [13]. The normal temperature was recorded before injection of Brewer's yeast using the rectal route using a digital probe thermometer for rats (BIOSEP®) to a depth of 3 cm into the rectum. Pyrexia was induced by subcutaneous injection of 20% w/v suspension of Brewer's yeast in distilled water at a dose of 10 mg/kg body weight. After 18 hours, the rise in rectal temperature was recorded, and only animals showing an increase in temperature of at least 0.6°C were selected for the study. The animals were randomly divided into six groups, each group containing five rats. Group 1 was treated with CMC-Na 0.5% (as negative control). Group 2 was treated with standard drug paracetamol at a dose of 150 mg/kg body weight [21]. Groups 3, 4, 5, and 6 were treated with AS201-01 tablets at a dose equal to 12.5, 25, 50, and 100 mg andrographolide/kg body weight, respectively. All treatments were administered orally. After the treatments, the rectal temperature of each animal was again recorded at 1 hour intervals up to 4 hours. The percentage reduction in pyrexia was calculated using the following formula:

$$\% \text{ reduction} = \frac{B - \text{Cn}}{B - A} \times 100\%, \qquad (3)$$

where A is the normal temperature, B is the rectal temperature after 18 h of yeast injection, and Cn is the rectal temperature after 1, 2, 3, and 4 h.

2.13. Data Analysis.

The results obtained were expressed as the mean ± SEM (standard error of mean) of six animals. For statistical analysis, one-way ANOVA was followed by post-hoc Dunnett's test for multiple comparisons. An effect was considered to be significant at the $P < 0.05$ level. GraphPad Prism 7.0 software (GraphPad Co., Ltd., San Diego, CA, USA) was used in statistical analysis.

3. Results

3.1. Determination of Andrographolide Content in Ethyl Acetate Fraction and Tablet.

Andrographolide content in ethyl acetate fraction was determined by the TLC-densitometry method using andrographolide (Aldrich 365645-100 MG) as a standard. Andrographolide content in the pure ethyl acetate fraction was $20.90 \pm 2.72\%$ and $6.51 \pm 0.20\%$ in the AS201-01 tablet manufactured from this fraction (Tables 1 and 2). This result was used when preparing doses of 12.5 mg andrographolide/kg body weight.

3.2. Formulation, Production, and Evaluation of Ethyl Acetate Fraction Tablet.

Several physical characteristics of the AS201-01 tablet were assessed according to the method of Depkes RI, 2014 [17]. The AS201-01 tablet has specifications which are shown in Table 3. The tablet meets the specification requirements by Farmakope Indonesia.

3.3. Analgesic Activity.

The effect of AS201-01 tablet on acetic acid-induced writhing in mice is presented in Table 4.

TABLE 1: Andrographolide content in ethyl acetate fraction.

Andrographolide standard		Ethyl acetate fraction		
Concentration, μg (x)	Area (y)	Area	Concentration (% w/w)	Average concentration (% w/w)*
0.08	1042.45	3000.27	23.48	20.90 ± 2.72
0.1	1196.10	2399.68	18.05	
0.2	2531.88	2778.27	21.15	
0.3	3171.55			
0.4	4046.33			
0.6	5954.67			

Regression: $y = 9327.3x + 378.86$; *data represent mean ± SD.

TABLE 2: Andrographolide content in AS201-01 tablet.

Andrographolide standard		AS201-01 tablet		
Concentration, μg (x)	Area (y)	Area	Concentration (% w/w)	Average concentration (% w/w)*
0.08	912.82	3098.30	6.31	6.51 ± 0.20
0.1	1204.85	3171.69	6.51	
0.2	2223.54	3259.70	6.71	
0.3	3152.31			
0.4	3989.96			
0.6	5591.52			

Regression: $y = 8948x + 340.39$; *data represent mean ± SD.

TABLE 3: Physical characteristics of AS201-01 tablet.

Tablet weight (mg)				Hardness (kg/cm^2)	Friability (%)	Disintegration time
643.2	649.4	646.6	642.2	6.26	0.80	17 min 28 sec
647.8	645.5	643.8	642.6	6.23	0.80	15 min 29 sec
645.3	643.1	643.5	642.8	6.60	0.70	
647.0	645.9	644.8	648.5			
645.8	649.1	642.1	648.6			
	Average 645.38 ± 0.2			6.36 ± 0.21	0.77 ± 0.06	16 min 28.5 sec

The results indicated that AS201-01 tablet significantly reduced ($P < 0.0001$) in the writhes count after oral administration in a dose-dependent manner when compared to the negative control. The maximum inhibition was observed at 50 mg andrographolide/kg dose of AS201-01 tablet (66.73%). However, diclofenac sodium (reference drug) reduced the number of abdominal writhes by 74.62%. Statistical analysis showed a significant difference in the three doses compared to diclofenac sodium ($P < 0.05$). The inhibitory effect of diclofenac sodium was greater than that of the highest dose of the AS201-01 tablet.

3.4. Antipyretic Activity. The effect of AS201-01 tablet and paracetamol in yeast-induced pyrexia in rats is shown in Table 5. The subcutaneous injection of yeast increased the rectal temperature by 1.26–2°C after 18 hours of injection.

The AS201-01 exhibited an antipyretic effect during the first hour after administration in a dose-dependent manner which was significantly different ($P < 0.05$) from the negative control. The dose of 50 and 100 mg/kg body weight significantly attenuated pyrexia in rats after 1 hour ($P < 0.05$), and the lowering of temperature was even more significant ($P < 0.001$) from 2 h to 3 h in comparison to the negative control. The maximum reduction was observed at 100 mg

andrographolide/kg dose of AS201-01 tablet after the third hour of administration (100%). The data are shown in Figure 1. Meanwhile, the maximum reduction was showed by paracetamol (reference drug) after the second hour of administration (100%). The percentage of reduction was decreased during the third hour and showed the lowest after the fourth hour of paracetamol administration. This activity profile was probably attributed to their pharmacokinetics characteristics.

4. Discussion

Medicinal plants are important sources for the development of new drugs because most of these products are believed to have bioactive compounds responsible for healing various diseases without any side effects and at a lower cost [22]. *Andrographis paniculata* is one of the most popular medicinal plants used traditionally and known to exhibit a wide range of pharmacological effects. Andrographolide is a major constituent of *A. paniculata* and is likely to be responsible for the analgesic and antipyretic effect of *A. paniculata* [11]. Madav et al. have reported that 300 mg/kg of andrographolide, administered orally, had a significant analgesic activity on acetic-induced writhing in mice at doses of 100 and 300 mg/kg body weight [12]. In addition,

TABLE 4: Analgesic activity of AS201-01 tablet by acetic acid-induced writhing in mice.

Group	Dose (mg/kg)	Number of writhes in 45 min (Mean ± SEM)	Inhibition (%)
Negative control	—	106.4 ± 1.1	—
Positive control	40	$27 \pm 1.9^{****}$	74.62
	12.5	$81 \pm 1.0^{****}$	23.87
AS201-01 tablet	25	$47.2 \pm 2.1^{****}$	55.64
	50	$35.4 \pm 1.2^{****}$	66.73

Data are reported as mean ± SEM for all groups. The data were analyzed by ANOVA followed by Dunnett's test. Asterisks (*) indicate statistically significant value from negative control, $^{****}P < 0.0001$.

TABLE 5: Antipyretic activity of AS201-01 tablet in yeast-induced pyrexia in rats.

Group (mg/kg)	Rectal temperature (°C)					
	Normal	Initial temperature (after 18 h)	After treatment			
			1 h	2 h	3 h	4 h
Negative control	36.48 ± 0.28	38.48 ± 0.22	38.16 ± 0.19	38.18 ± 0.19	38.32 ± 0.15	38.36 ± 0.19
AS201-01 tablet at dose 12.5	36.16 ± 0.14	37.78 ± 0.15	38.14 ± 0.19	37.62 ± 0.22	37.68 ± 0.32	37.62 ± 0.33
AS201-01 tablet at dose 25	36.20 ± 0.09	37.62 ± 0.21	$37.22 \pm 0.08^*$	$37.46 \pm 0.17^*$	$37.36 \pm 0.12^*$	$37.46 \pm 0.07^*$
AS201-01 tablet at dose 50	36.36 ± 0.09	38.06 ± 0.15	$37.36 \pm 0.31^*$	$36.92 \pm 0.31^*$	$36.80 \pm 0.39^{***}$	$37.36 \pm 0.24^*$
AS201-01 tablet at dose 100	36.30 ± 0.19	38.10 ± 0.10	$37.26 \pm 0.18^*$	$36.66 \pm 0.17^{**}$	$36.22 \pm 0.10^{***}$	$36.98 \pm 0.24^{**}$
Paracetamol at dose 150	36.68 ± 0.13	37.94 ± 0.21	$36.72 \pm 0.31^{***}$	$36.64 \pm 0.27^{**}$	$37.16 \pm 0.14^{**}$	37.56 ± 0.25

Data are reported as mean ± SEM ($n = 5$). The data were analyzed by ANOVA followed by Dunnett's test. Asterisks (*) indicate statistically significant value compared to the negative control, $^*P < 0.05$; $^{**}P < 0.01$; and $^{***}P < 0.001$.
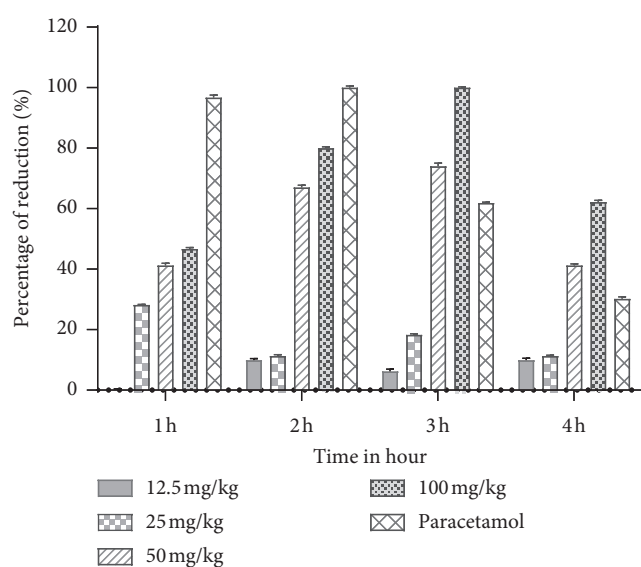
FIGURE 1: Percentage reduction of AS201-01 tablet and standard drug (paracetamol) in yeast-induced pyrexia in rats.

doses of 180 and 360 mg/kg body weight of andrographolide were also found to be able to relieve fever in humans by the third day after administration [23].

A. paniculata is widely used in traditional medicine and safely consumed. Oral acute toxicity evaluation reported an ethanolic extract of *A. paniculata* with an upper fixed dose of 5000 mg/kg body weight, which has no significant acute toxicological effects [24]. Meanwhile, andrographolide as a bioactive compound of *A. paniculata* was reported to have LD_{50} higher than 5 g/kg body weight by oral treatment both in male and female mice [25]. These

data support the safe use of *A. paniculata* as alternative medicine.

Previous studies have reported that the ethyl acetate fraction of *A. paniculata* has a higher andrographolide content than the ethanol extract [14]. Based on the results, ethyl acetate fraction was further developed as a tablet dosage form, namely, AS201-01 tablet. The determination of andrographolide content in ethyl acetate fraction was conducted by the TLC-densitometry method. The data were used to manufacture AS201-01 tablet using ethyl acetate fraction as an active ingredient which is equal to 35 mg of andrographolide per tablet. Ethyl acetate fraction (167.5 mg) which was containing 35 mg andrographolide, was needed to produce one tablet. Ethyl acetate fraction possibly contains other diterpenoids, flavonoids, and polyphenol compounds. *A. paniculata* is known as a source of 2′-oxygenated flavonoids and labdane type diterpenoids [26–28]. This study used andrographolide as the active marker of *A. paniculata* due to its abundance and various bioactive properties. Therefore, the characterization of other compounds contained in ethyl acetate was not performed.

AS201-01 tablet was then investigated for its analgesic and antipyretic activities. Analgesic activity was determined using an acetic acid-induced writhing test. Acetic acid-induced writhing reflex model in mice is a widely accepted, simple, sensitive, and effective pain model for evaluating peripherally acting analgesics [29, 30]. The characteristic of pain activity generated by intraperitoneal injection of acetic acid is presented with contraction of the abdominal muscle followed by extension of hind limbs and elongation of body parts, and such constriction is thought to be mediated by the local peritoneal receptor [31]. Acetic acid induces inflammatory pain by impelling capillary permeability [32] and releasing substances that excite pain nerve endings such as

serotonin, histamine, bradykinins, and prostaglandins (PGE2 and PG2α) from arachidonic acid through cyclooxygenase (COX) enzymes [33, 34]. When prostaglandin is released, the nerve endings respond to it through prostaglandin $E2$ (PGE2) receptor by picking up and transmitting the pain and injury messages through the nervous system to the brain and cause visceral writhing stimuli in mice. The inhibition of prostaglandin synthesis is remarkably efficient as an antinociceptive mechanism in visceral pain [35, 36]. Diclofenac sodium was used as the positive control. It is a nonsteroidal anti-inflammatory drug (NSAID) that has analgesic, antipyretic, and anti-inflammatory activity. Diclofenac performs its action via inhibition of prostaglandin synthesis by inhibiting COX-1 and COX-2[37]. In our study, the *A. paniculata* tablet significantly reduced the number of writhing in a dose-dependent manner. The maximum inhibition was observed at 50 mg andrographolide/kg dose of AS201-01 tablet (66.73%). These findings strongly suggest that AS201-01 tablet showed its analgesic activity through a peripheral mechanism, which is the inhibition of prostaglandin biosynthesis by acting on visceral receptors sensitive to acetic acid [38].

The present study was also conducted to evaluate the antipyretic activity of the AS201-01 tablet on animal models (rats). The baker's yeast-induced fever test, which simulates a pathogenic fever, is a low-cost and reliable method for assessing new antipyretics [13, 39]. Fever is known to be caused by several endogenous pyrogens such as interleukin-1β (IL-1β) and IL-6, interferon-α (IFN-α), tumor necrosis factor-α (TNF-α), macrophage protein-1, and prostaglandins such as PGE2 and PGI2. Brewer's yeast induces both TNF-α and prostaglandin synthesis [40, 41].

The oral administration of the AS201-01 tablet significantly attenuated rectal temperature of yeast-induced pyrexia in rats. The efficacy of the antipyretic effect of the AS201-01 tablet was observed to have increased in a dose-dependent manner. The maximum reduction was observed at 100 mg andrographolide/kg dose of the AS201-01 tablet after the third hour of administration (100%). The inhibition of prostaglandin synthesis and the inhibition of cytokine release could be the possible mechanism of antipyretic actions of AS201-01 tablet. Andrographolide is the major compound of *A. paniculata* was reported to have analgesic, antipyretic, and anti-inflammatory activity, but the exact mechanism remains unknown. Shen et al. reported that the anti-inflammatory effect of andrographolide was explained by its ability to inhibit neutrophil adhesion/transmigration through suppression of Mac-1 upregulation [42].

Paracetamol was used as a positive control in this study. It is a standard drug with a central analgesic effect and is due to activation of descending serotonergic pathway [43]. The maximum reduction of pyrexia was showed by paracetamol as a reference drug after the second hour of administration (100%). Paracetamol is extensively metabolized and excreted unchanged in the urine, only 2–5% of its therapeutic dose. It is rapidly and relatively uniformly distributed in the tissues, and the plasma half-life is 1.5–2 hours [44]. The rapid absorption of paracetamol resulted in a high percentage of reduction pyrexia in the first hour after drug administration and reached the maximum reduction after the second hour of administration. The activity of paracetamol was decreased during the third hour and showed the lowest activity after the fourth hour of administration. The activity profile of paracetamol was in accordance with its pharmacokinetics characteristics. On the other hand, andrographolide takes a longer time to reach maximum reduction compared to paracetamol. The pharmacokinetics and oral bioavailability of andrographolide in rats and humans were studied by Panossian et al. The study reported that the maximum concentration of andrographolide in rat's plasma is estimated at 2 hours after administration, and the plasma half-life is 3 hours. Furthermore, a large part (55%) of andrographolide is bound to plasma proteins, and only a limited amount can enter the cells [45]. The Biopharmaceutics Classification System (BCS) classified andrographolide as class III drug which has low solubility and low permeability [46]. It showed poor oral bioavailability due to its high lipophilicity, low aqueous solubility rapid transformation, and efflux by P-glycoprotein [47]. This andrographolide pharmacokinetics profile indicated that AS201-01 tablet possibly needed more time to produce the maximum antipyretic activity compared to paracetamol. AS201-01 tablet still showed higher activity during the fourth administration compared to paracetamol. It was suggested that the AS201-01 tablet was potential an antipyretic drug.

Various studies reported the analgesic and antipyretic activity of *A. paniculata* extract or its compounds. On the other hand, little attention has been directed toward the development of *A. paniculata* as a herbal medicine product. This study demonstrated the analgesic and antipyretic activity of formulated ethyl acetate fraction of *A. paniculata* in the tablet dosage form. The formulation study of ethyl acetate fraction as a dosage form needed to be further conducted specially to enhance the bioavailability and reduce time to achieve maximum concentration in the plasma.

5. Conclusions

The ethyl acetate fraction tablet of *A. paniculata* exhibited analgesic and antipyretic activities. The maximum analgesic and antipyretic activity was observed at 50 mg andrographolide/kg and 100 mg andrographolide/kg dose of ethyl acetate fraction tablet of *A. paniculata*.

Data Availability

The data used to support the findings of this study are included within the article.

Conflicts of Interest

The authors declare that there are no conflicts of interest in this study.

Acknowledgments

References

[1] M. C. Thomas, "Diuretics, ACE inhibitors and NSAIDs—the triple whammy," *Medical Journal of Australia*, vol. 172, no. 4, pp. 184-185, 2000.

[2] M. Hassan, S. Khan, A. Shaikat et al., "Analgesic and anti-inflammatory effects of ethanol extracted leaves of selected medicinal plants in animal model," *Veterinary World*, vol. 6, no. 2, pp. 68–71, 2013.

[3] J. S. M. Pasin, A. P. O. Ferreira, A. L. L. Saraiva et al., "Antipyretic and antioxidant activities of 5-trifluoromethyl-4,5-dihydro-1H-pyrazoles in rats," *Brazilian Journal of Medical and Biological Research*, vol. 43, no. 12, pp. 1193–1202, 2010.

[4] N. K. Subedi, S. M. A. Rahman, and M. A. Akbar, "Analgesic and antipyretic activities of methanol extract and its fraction from the root of schoenoplectus grossus," *Evidence-Based Complementary and Alternative Medicine*, vol. 2016, Article ID 3820704, 8 pages, 2016.

[5] A. Valdiani, M. A. Kadir, S. G. Tan et al., "Nain-e Havandi Andrographis paniculata present yesterday, absent today: a plenary review on underutilized herb of Iran's pharmaceutical plants," *Molecular Biology Reports*, vol. 39, no. 5, pp. 5409–5424, 2012.

[6] K. Jarukamjorn and N. Nemoto, "Pharmacological aspects of Andrographis paniculata on health and its major diterpenoid constituent andrographolide," *Journal of Health Science*, vol. 54, no. 4, pp. 370–381, 2008.

[7] S. Akbar, "Andrographis paniculata: a review of pharmacological activities and clinical effects," *Alternative Medicine Review*, vol. 16, no. 1, 2011.

[8] T. Jayakumar, C. Y. Hsieh, J. J. Lee, and J. J. Sheu, "Review article: experimental and clinical pharmacology of andrographis paniculata and its major bioactive phytoconstituent andrographolide," *Evidence-Based Complementary and Alternative Medicine*, vol. 2013, Article ID 846740, 16 pages, 2013.

[9] J. Joselin and J. Jeeva, "Andrographis paniculata: a review of its traditional uses, phytochemistry and pharmacology," *Medicinal and Aromatic Plants*, vol. 3, no. 4, 2014.

[10] A. Okhuarobo, J. Ehizogie Falodun, O. Erharuyi, V. Imieje, A. Falodun, and P. Langer, "Harnessing the medicinal properties of Andrographis paniculata for diseases and beyond: a review of its phytochemistry and pharmacology," *Asian Pacific Journal of Tropical Disease*, vol. 4, no. 3, pp. 213–222, 2014.

[11] S. Suebsasana, P. Pongnaratorn, J. Sattayasai, T. Arkaravichien, S. Tiamkao, and C. Aromdee, "Analgesic, antipyretic, anti-inflammatory and toxic effects of andrographolide derivatives in experimental animals," *Archives of Pharmacal Research*, vol. 32, no. 9, pp. 1191–1200, 2009.

[12] S. Madav, H. C. Tripathi, Tandan, and S. K. Mishra, "Analgesic, antipyretic and antiulcerogenic effects of andrographolide," *Indian Journal of Pharmaceutical Sciences*, vol. 57, no. 3, pp. 121–125, 1995.

[13] J. Tomazetti, D. S. Ávila, A. P. O. Ferreira et al., "Baker yeast-induced fever in young rats: characterization and validation of an animal model for antipyretics screening," *Journal of Neuroscience Methods*, vol. 147, no. 1, pp. 29–35, 2005.

[14] A. F. Hafid, B. Rifai, L. Tumewu et al., "Andrographolide determination of Andrographis paniculata extracts, ethyl acetate fractions and tablets by thin layer chromatography," *Journal of Chemical and Pharmaceutical Research*, vol. 7, no. 12, pp. 557–561, 2015.

[15] M. Chen, C. Xie, and L. Liu, "Solubility of andrographolide in various solvents from (288.2 to 323.2) K," *Journal of Chemical and Engineering Data*, vol. 55, no. 11, pp. 5297-5298, 2010.

[16] J. Shi, H. Nawaz, J. Pohorly, G. Mittal, Y. Kakuda, and Y. Jiang, "Extraction of polyphenolics from plant material for functional foods-engineering and technology," *Food Reviews International*, vol. 21, no. 1, pp. 139–166, 2005.

[17] Departmen Kesehatan Republik Indonesia, *Farmakope Indonesia Edisi V*, Departemen Kesehatan Republik Indonesia, Jakarta, Indonesia, 2014.

[18] R. Koster, M. Anderson, and E. J. De Beer, "Acetic acid for analgesic screening," *Federation Proceedings*, vol. 18, pp. 412–417, 1959.

[19] M. Hijazi, A. El-Mallah, M. Aboul-Ela, and A. Ellakany, "Evaluation of analgesic activity of papaver libanoticum extract in mice: involvement of opioids receptors," *Evidence-Based Complementary and Alternative Medicine*, vol. 2017, Article ID 8935085, 13 pages, 2017.

[20] S. C. Chou, Y. Chiu, C. Chen et al., "Analgesic and anti-inflammatory activities of the ethanolic extract of artemisia morrisonensis hayata in mice," *Evidence-Based Complementary and Alternative Medicine*, vol. 79, Article ID 138954, 11 pages, 2012.

[21] M. A. Khan, H. Khan, S. Khan, T. Mahmood, P. M. Khan, and A. Jabar, "Anti-inflammatory, analgesic and antipyretic activities of Physalis minima Linn," *Journal of Enzyme Inhibition and Medicinal Chemistry*, vol. 24, no. 3, pp. 632–637, 2009.

[22] S. C. Koech, R. O. Ouko, N. M. Michael, M. M. Ireri, M. P. Ngugi, and N. M. Njagi, "Analgesic activity of dichloromethanolic root extract of clutia abyssinica in Swiss albino mice," *Natural Products Chemistry and Research*, vol. 5, no. 2, 2017.

[23] V. Thamlikitkul, T. Dechatiwongse, S. Theerapong et al., "Efficacy of Andrographis paniculata, Nees for pharyngotonsillitis in adults," *Journal of the Medical Association of Thailand = Chotmaihet Thangphaet*, vol. 74, no. 10, pp. 437–442, 1991.

[24] L. Worasuttayangkurn, W. Nakareangrit, J. Kwangjai et al., "Acute oral toxicity evaluation of Andrographis paniculata-standardized first true leaf ethanolic extract," *Toxicology Reports*, vol. 6, pp. 426–430, 2019.

[25] C. Bothiraja, A. P. Pawar, V. S. Shende, and P. P. Joshi, "Acute and subacute toxicity study of andrographolide bioactive in rodents: evidence for the medicinal use as an alternative medicine," *Comparative Clinical Pathology*, vol. 22, no. 6, pp. 1123–1128, 2013.

[26] M. Kuroyanagi, M. Sato, A. Ueno, and K. Nishi, "Flavonoids from Andrographis paniculata," *Chemical & Pharmaceutical Bulletin*, vol. 35, no. 11, pp. 4429–4435, 1987.

[27] I. Jantan and P. G. Waterman, "Ent-14β-hydroxy-8(17),12-labdadien-16,15-olide-3β,19-oxide: a diterpene from the aerial parts of Andrographis paniculata," *Phytochemistry*, vol. 37, no. 5, pp. 1477–1479, 1994.

[28] K. R. Munta, M. V. B. Reddy, D. Gunasekar, M. M. Murthy, C. Caux, and B. Bodo, "A flavone and an unusual 23-carbon terpenoid from Andrographis paniculata," *Phytochemistry*, vol. 62, pp. 1271–1275, 2003.

[29] H. O. J. Collier, L. C. Dinneen, C. A. Johnson, and C. Schneider, "The abdominal constriction response and its suppression by analgesic drugs in the mouse," *British Journal of Pharmacology and Chemotherapy*, vol. 32, no. 2, pp. 295–310, 1968.

[30] A. Zulfiker, M. M. Rahman, M. K. Hossain, K. Hamid, M. Mazumder, and M. S. Rana, "In vivo analgesic activity of ethanolic extracts of two medicinal plants-*Scoparia dulcis* L. and *Ficus racemosa* Linn," *Biology and Medicine*, vol. 2, no. 2, pp. 42–48, 2010.

[31] G. A. Bentley, S. H. Newton, and J. Starr, "Studies on the antinociceptive action of α agonist drugs and their interactions with opioid mechanisms," *British Journal of Pharmacology*, vol. 79, no. 1, pp. 125–134, 1983.

[32] M. Amico-Roxas, A. Caruso, S. Trombadore, R. Scifo, and U. Scapagnini, "Gangliosides antinociceptive effects in rodents," *Archives Internationales de Pharmacodynamie et de therapie*, vol. 272, pp. 103–117, 1984.

[33] R. M. Gené, L. Segura, T. Adzet, E. Marin, and J. Iglesias, "Heterotheca inuloides: anti-inflammatory and analgesic effect," *Journal of Ethnopharmacology*, vol. 60, no. 2, pp. 157–162, 1998.

[34] T.-C. Lu, Y.-Z. Ko, H.-W. Huang, Y.-C. Hung, Y.-C. Lin, and W.-H. Peng, "Analgesic and anti-inflammatory activities of aqueous extract from Glycine tomentella root in mice," *Journal of Ethnopharmacology*, vol. 113, no. 1, pp. 142–148, 2007.

[35] J. B. Da Silva, V. d. S. Temponi, F. V. Fernandes et al., "New approaches to clarify antinociceptive and anti-inflammatory effects of the ethanol extract from vernonia condensata leaves," *International Journal of Molecular Sciences*, vol. 12, no. 12, pp. 8993–9008, 2011.

[36] E. M. Franzotti, C. V. Santos, H. M. Rodrigues, R. H. Mourao, M. R. Andrade, and A. R. Antoniolli, "Anti-inflammatory, analgesic and acute toxicity of Sida cadifolia L," *Journal Ethnopharmacology*, vol. 72, no. 1-2, pp. 273–277, 2000.

[37] T. J. Gan, "Diclofenac: an update on its mechanism of action and safety profile," *Current Medical Research and Opinion*, vol. 26, no. 7, pp. 1715–1731, 2010.

[38] B. Y. Sheikh, S. M. N. K. Zihad, N. Sifat et al., "Comparative study of neuropharmacological, analgesic properties and phenolic profile of Ajwah, Safawy and Sukkari cultivars of date palm (Phoenix dactylifera)," *Oriental Pharmacy and Experimental Medicine*, vol. 16, no. 3, pp. 175–183, 2016.

[39] K. M. A. Wonder, B. L. Stanley, A. Stephen, B. G. Eric, U. U. Ruth, and E. Woode, "An evaluation of the anti-inflammatory, antipyretic and analgesic effects of hydroethanol leaf extract of Albizia zygia in animal models," *Pharmaceutical Biology*, vol. 55, no. 1, pp. 338–348, 2017.

[40] W. Rititid, P. Ruangsang, W. Reanmongkol, and M. Wongnawa, "Studies of the anti-inflammatory and antipyretic activities of the methanolic extract of Piper sarmentosum Roxb. Leaves in rats," *Songklanakarin Journal of Science and Technology*, vol. 29, no. 6, pp. 1519–1526, 2007.

[41] J. S. M. Pasin, A. P. O. Ferreira, A. L. L. Saraiva et al., "Diacerein decreases TNF-α and IL-1β levels in peritoneal fluid and prevents Baker's yeast-induced fever in young rats," *Inflammation Research*, vol. 59, no. 3, pp. 189–196, 2010.

[42] Y.-C. Shen, C.-F. Chen, and W.-F. Chiou, "Andrographolide prevents oxygen radical production by human neutrophils: possible mechanism(s) involved in its anti-inflammatory effect," *British Journal of Pharmacology*, vol. 135, no. 2, pp. 399–406, 2002.

[43] G. G. Graham and K. F. Scott, "Mechanism of action of paracetamol," *American Journal of Therapeutics*, vol. 12, no. 1, pp. 46–55, 2005.

[44] L. Prescott, "Kinetics and metabolism of paracetamol and phenacetin," *British Journal of Clinical Pharmacology*, vol. 10, no. S2, pp. 291S–298S, 1980.

[45] A. Panossian, A. Hovhannisyan, G. Mamikonyan et al., "Pharmacokinetic and oral bioavailability of andrographolide from Andrographis paniculata fixed combination Kan Jang in rats and human," *Phytomedicine*, vol. 7, no. 5, pp. 351–364, 2000.

[46] S. Y. K. Fong, M. Liu, H. Wei et al., "Establishing the pharmaceutical quality of Chinese herbal medicine: a provisional BCS classification," *Molecular Pharmaceutics*, vol. 10, no. 5, pp. 1623–1643, 2013.

[47] L. Ye, T. Wang, L. Tang et al., "Poor oral bioavailability of a promising anticancer agent andrographolide is due to extensive metabolism and efflux by P-glycoprotein," *Journal of Pharmaceutical Sciences*, vol. 100, no. 11, pp. 5007–5017, 2011.

Research Article

The Effectiveness of *Scutellaria baicalensis* on Migraine: Implications from Clinical Use and Experimental Proof

Chung-Chih Liao [iD],[1] **Ke-Ru Liao** [iD],[2] **Cheng-Li Lin** [iD],[3,4] **and Jung-Miao Li** [iD][1,5]

[1]*Graduate Institute of Chinese Medicine, College of Chinese Medicine, China Medical University, Taichung 40402, Taiwan*
[2]*Department of Neurology, Yuanlin Christian Hospital, Yuanlin 51052, Taiwan*
[3]*Management Office for Health Data, China Medical University Hospital, Taichung 40447, Taiwan*
[4]*College of Medicine, China Medical University, Taichung 40402, Taiwan*
[5]*Department of Chinese Medicine, Show Chwan Memorial Hospital, Changhua 50008, Taiwan*

Correspondence should be addressed to Jung-Miao Li; rung-miau@hotmail.com

Background. Scutellaria baicalensis (SB), a traditional Chinese medicine, is commonly used for the treatment of inflammatory and painful conditions. The purpose of the present study was to examine the effects of SB on migraine. *Materials and Methods.* We examined the clinical applications of SB based on the data obtained from Taiwan's National Health Insurance Research Database and confirmed that it was frequently used in Taiwan for the treatment of headaches. An experimental migraine model was established in rats by an intraperitoneal injection of nitroglycerin (NTG, 10 mg/kg). Pretreatment with SB was given orally 30 min before NTG administration. The rats were subjected to migraine-related behaviour tests that were video-recorded and analysed using EthoVision XT 12.0 software. *Results.* The frequency of exploratory and locomotor behaviour was comparatively lower in the NTG group than that in the control group, while the frequency of resting and grooming behaviour increased. These phenomena were ameliorated by pretreatment with 1.0 g/kg SB. The total time spent on the smooth surface was longer in the NTG group than that in the control group, but the time was shortened by pretreatment with 1.0 g/kg SB. *Conclusions.* Pretreatment with 1.0 g/kg SB relieved migraine-related behaviours in the experimental NTG-induced migraine model. The outcome therefore demonstrated that pretreatment with 1.0 g/kg SB is beneficial for migraine treatment.

1. Introduction

Migraine is a prevalent and complex neurological disorder, characterized by recurrent unilateral, pulsating, moderate-to-severe pain, aggravated by routine physical activity, and associated with nausea, photophobia, or phonophobia [1]. According to large-scale recent research, migraine affects approximately 12% of the population worldwide and has a higher prevalence among the female population, school/college students, and urban residents [2, 3].

Traditional Chinese medicine (TCM) has been used for the treatment of migraine for thousands of years by using TCM theory experience. Recently, a large body of basic and clinical research confirmed the scientific benefit of TCM for

the treatment of migraine [4–7]. The root of *Scutellaria baicalensis* (SB, known in Chinese medicine as Huang Qin) is a TCM herb, distributed in countries such as China, Japan, North Korea, Russia, and Mongolia [8]. It is known, from the experience of traditional Chinese doctors, to have analgesic, anti-inflammatory, and neuroprotective effects [9, 10]. Migraine is now known as an inflammatory neurovascular disorder [11]. Although SB has anti-inflammatory and neuroprotective potency, clinical or experimental research on SB in TCM academia for the treatment of migraine has hardly been reported.

As a result, the present study first explored the clinical use of SB in Taiwan. Systemic administration of nitroglycerin (NTG) in rodents to induce hyperalgesia or migraine-

related behaviours is one of the most widely accepted experimental migraine models [12–15]. Thereafter, we studied the effects of SB on migraine by behavioural analysis of an NTG-induced migraine rat model.

2. Materials and Methods

2.1. Clinical Applications of SB. The National Health Insurance program in Taiwan, which is an integration of all public insurance systems, offers insurance for conventional Western medicine and TCM [16, 17]. Detailed information about TCM utilization was collected from the National Health Insurance Research Database (NHIRD).

We conducted an analysis of Longitudinal Health Insurance Database 2000 (LHID 2000), which is a random sample of one million enrollees from the NHIRD's longitudinal data spanning the period of 1997 to 2013. Diagnostic codes were collected from the International Classification of Diseases, Ninth Revision, Clinical Modification (ICD-9-CM). We extracted the top ten most common indications for SB from the primary diagnosis codes. This study was approved by the Institutional Review Board of China Medical University in central Taiwan (CMUH-104-REC2-115-R3).

2.2. Animals. Male Sprague Dawley rats, purchased from BioLASCO (Taipei, Taiwan), weighing 225–300 g were used in this study. A light-dark cycle of 12:12 h, relative humidity of 55% ± 5%, and room temperature of 23°C ± 1°C were maintained. Food and tap water were provided *ad libitum*. Animal use was approved by the Institutional Animal Care and Use Committee of Show Chwan Memorial Hospital (no. 106021) and followed the Guide for the Use of Laboratory Animals (National Academy Press).

2.3. SB Preparation. SB extract subtle granules were produced by Ko Da Pharmaceutical Co., Ltd. (Taoyuan, Taiwan). Scutellariae radix, the dried root of *Scutellaria baicalensis* Georgi (Fam. Labiatae), was purchased from Gansu province, People's Republic of China (Figure 1(a)). The origin and voucher specimens were identified and kept by Ko Da Pharmaceutical Co., Ltd. In brief, 210 kg of Scutellariae radix was extracted in 10-fold (w/v) boiled water for 1 h followed by filtration through a 40-mesh sieve. The filtrates were collected and subjected to vacuum concentration to produce 70 kg of extracts. The excipients, including 40.6 kg of starch, 28 kg of Scutellariae radix powder, and 1.4 kg of sodium carboxymethyl cellulose, were dried in a granulator, and then the extracts were added followed by granulation. The ratio of extracts and starch in SB extract subtle granules was 1 : 1 (w/w).

Analytical high-performance liquid chromatography was performed using a Hitachi D-7000 interface equipped with an L-7100 pump, L-7455 detector, and L-7200 autosampler (Tokyo, Japan) to examine the baicalin content in the SB extract subtle granules. The test solution was prepared by mixing approximately 0.5 g of SB extract subtle granules with 30 mL mixture of acetonitrile and diluted phosphoric acid in a ratio of 28 and 72 (v/v) under heating reflux for

30 min. After centrifugation at 4000 rpm for 10 min, the supernatant was collected and added to a mixture of acetonitrile and diluted phosphoric acid at a ratio of 28 to 72 (v/v) to make up a final volume of 100 mL and then passed through a $0.45 \mu m$ filter. Around 5 mg of baicalin, with purity higher than 98% as claimed by the supplier (ChemFaces, Hubei, China), was mixed with 10 mL to obtain a stock standard solution, and 2 mL of stock standard solution was added to the mixture of acetonitrile and diluted phosphoric acid at a ratio of 28 to 72 (v/v) for a final volume of 20 mL to obtain the working standard solution. Chromatographic separation was carried out on a Mightysil RP-18 column (250×4.6 mm, $5 \mu m$) using an isocratic solvent system comprising a mixture of acetonitrile and diluted phosphoric acid at a ratio of 28 to 72 (v/v). The ultraviolet wavelength, flow rate, injection volume, and stop time were set at 270 nm, 1.0 mL/min, $10 \mu L$, and 30 min, respectively. The content of baicalin in the SB extract subtle granules was 148.51 mg/g (Figure 1(b)).

2.4. Grouping. To induce migraine attacks, the rats were given an intraperitoneal (i.p.) injection of NTG (10 mg/kg) [14]. A total of 24 rats were randomly allocated into four groups ($n = 6$) as follows:

(1) Control group: i.p. injection of normal saline only

(2) NTG group: i.p. injection of NTG only

(3) Placebo group: oral administration of 1.0 g/kg starch 30 min before i.p. injection of NTG

(4) SB-1.0 group: oral administration of 1.0 g/kg SB 30 min before i.p. injection of NTG

The dose of SB used in the present study was calculated based on the report by Nair and Jacob [18]. They reported that rat equivalent dose (mg/g) = human dose (mg/g) × 6.2. We considered that an average human weighs 60 kg. Therefore, based on the clinical human dosage of 9.6 g, which is the rational dose commonly used in clinical TCM practice and suggested by pharmaceutical companies in Taiwan, we calculated the appropriate SB dosage for rats to be 1.0 g/kg.

The experimental procedure is shown in Figure 2.

2.5. Rat Behaviour Tests

2.5.1. Assessment of Spontaneous Nociceptive Behaviour. Thirty minutes after i.p. injection with NTG, spontaneous nociceptive behaviour was observed using a transparent acrylic apparatus ($45 \times 45 \times 35$ cm^3). A camera was placed 1 m in front of the apparatus, and the behaviour of the rats was video-recorded for 20 min. The rats' behaviour was analysed automatically using the rat behaviour recognition module of EthoVision XT 12.0 software (Noldus Information Technology, Leesburg, VA, United States).

Rat behaviour information and analysis were referenced from the descriptions in previous studies [19, 20]. In brief, rat behaviour was categorized into five types: exploratory behaviour (including rearing up and sniffing), locomotor

(a)   (b)
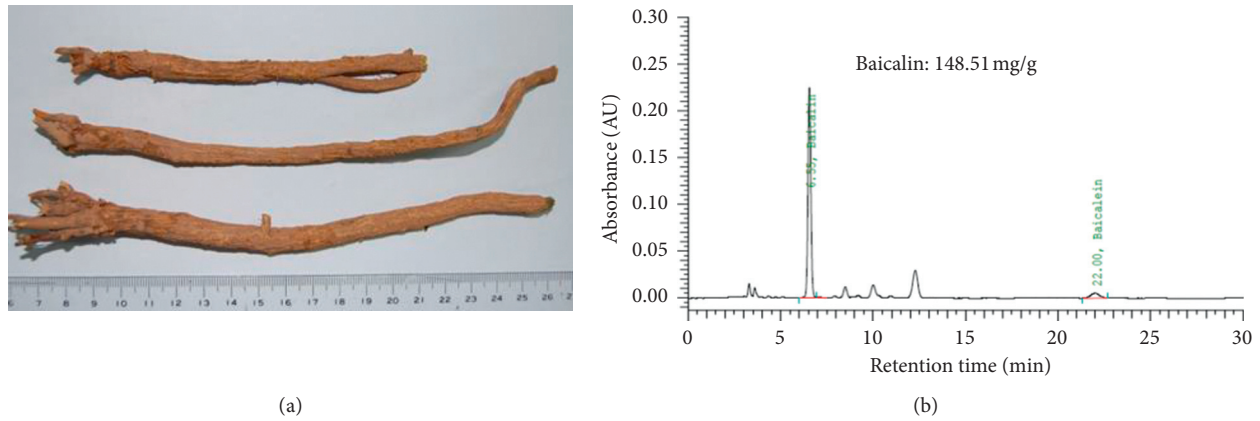
FIGURE 1: (a) Morphology of *Scutellaria baicalensis* (Huang Qin). (b) High-performance liquid chromatography (HPLC) fingerprint of *Scutellaria baicalensis* extract subtle granules.
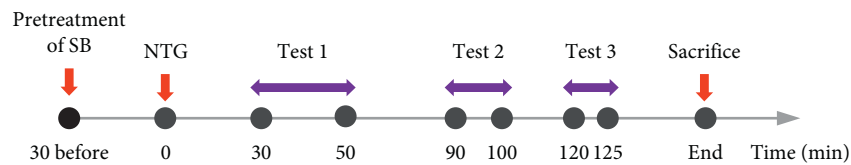
FIGURE 2: Experimental procedure. Pretreatment with *Scutellaria baicalensis* (SB): oral administration of *Scutellaria baicalensis* (SB) 30 min prior to i.p. injection with NTG; NTG: nitroglycerin (10 mg/kg) i.p. injection; test 1: rat behaviour recognition module test video recordings; test 2: light/dark box test video recordings; test 3: rough/smooth surface apparatus test video recordings.

behaviour (including walking and jumping), freezing behaviour (including twitching), resting behaviour, and grooming behaviour.

For the aforementioned behaviours, the frequency of engaging in the behaviour was calculated.

2.5.2. Assessment of Light-Aversive Behaviour. Ninety minutes after i.p. injection of NTG, light-aversive behaviour was tested using a light/dark box. The light/dark box was made of two identical compartments ($30 \times 30 \times 22.5$ cm^3), where the light chamber was placed under a bright environment without a cover, and the dark box was fully black with a lid. A small opening gate (10 cm $\times 10$ cm^3) connected the two chambers, and the rats could freely move across the two chambers. At the start of the assessment, the rats were placed in the centre of the light chamber and allowed to freely move across the two chambers for 10 min. The test was video-taped and analysed using EthoVision XT 12.0. The parameter of total time spent in the light chamber was further analysed.

2.5.3. Assessment of Spontaneous Tactile Allodynia. One hundred and twenty minutes after the i.p. injection of NTG, spontaneous tactile allodynia was tested using a rough/smooth surface apparatus, which was modified from a previous research [21]. The apparatus consisted of a transparent acrylic box ($45 \times 45 \times 35$ cm^3), in which the floor was divided into two identical arenas (22.5×45 cm^3 each). The left-side floor surface was covered by smooth sandpaper

(P1000 grit), and the right-side floor surface was covered by rough sandpaper (P40 grit). At the beginning of the test, the rats were placed in the centre of the apparatus and allowed to freely move across both arenas for 5 min. The test was video-taped and analysed using EthoVision XT 12.0. The total time spent in the smooth surface arena and heat map plots of the mean locations of the groups were calculated.

All rats were sacrificed after the completion of all behavioural tests.

2.6. Statistical Analysis. All the data are shown as mean ± SEM. Statistical significance between the control, NTG, placebo, and SB-1.0 groups was analysed using one-way ANOVA followed by a Tukey's post hoc test. A p value <0.05 was considered statistically significant. GraphPad Prism 7.0 software (San Diego, CA, USA) was used for the statistical analysis.

3. Results

3.1. Clinical Applications of SB in Taiwan. To investigate the clinical application of SB by TCM doctors in Taiwan, we conducted a population-based analysis using LHID 2000, which comprises a random sample of one million participants from the NHIRD between 1997 and 2013. The top 10 most frequent clinical applications of SB between 1997 and 2013 in Taiwan are shown in Table 1. The use of SB to treat headache ($N = 4849$, 2.51%) was the fourth most common clinical application.

TABLE 1: Top 10 clinical applications of *Scutellaria baicalensis* by traditional Chinese medicine doctors from 1997 to 2013 in Taiwan.

Ranking	ICD-9-CM	Indications	Usage number (N)	Percentage (%)
1	460	Acute nasopharyngitis (common cold)	25828	13.37
2	786.2	Cough	15476	8.01
3	477.9	Allergic rhinitis cause unspecified	4869	2.52
4	784.0	Headache	4849	2.51
5	780.59	Other sleep disturbances	2655	1.37
6	490	Bronchitis, not specified as acute or chronic	2483	1.29
7	472.0	Chronic rhinitis	2472	1.28
8	780.50	Sleep disturbances, unspecified	2445	1.27
9	536.9	Unspecified functional disorder of stomach	2339	1.21
10	536.8	Dyspepsia and other specified disorders of function of stomach	2255	1.17

ICD-9-CM: International Classification of Diseases, Ninth Revision, Clinical Modification.

3.2. Effect of Pretreatment with SB on NTG-Induced Spontaneous Nociceptive Behaviour in Rats

3.2.1. Exploratory Behaviour including Rearing Up and Sniffing. Notably, the rats in the NTG group engaged less in rearing up behaviour than those in the control group did ($p < 0.001$; Figure 3(a) (A)). Pretreatment with 1.0 g/kg SB ($p < 0.01$; Figure 3(a) (A)), but not placebo ($p > 0.05$; Figure 3(a) (A)), resulted in relatively more frequent rearing up behaviour compared to that in the NTG group.

Similar to the above outcome, the rats in the NTG group did not engage in sniffing behaviour as frequently as those in the control group did ($p < 0.01$; Figure 3(a) (B)). Pretreatment with 1.0 g/kg SB ($p < 0.05$; Figure 3(a) (B)), but not placebo ($p > 0.05$; Figure 3(a) (B)), resulted in a more frequent sniffing behaviour compared to that of the NTG group.

3.2.2. Locomotor Behaviour including Walking and Jumping. The rats in the NTG group engaged in walking behaviour less frequently than the control group ($p < 0.001$; Figure 3(b) (A)). Pretreatment with 1.0 g/kg SB ($p < 0.001$; Figure 3(b) (A)), but not with placebo ($p > 0.05$; Figure 3(b) (A)), resulted in a higher frequency of walking behaviour in comparison with that of the NTG group.

No significant differences were noted between the control, NTG, placebo, and SB-1.0 g/kg groups (all $p > 0.05$; Figure 3(b) (B)) in the analysis of the frequency of jumping behaviour.

3.2.3. Freezing Behaviour including Twitching. The rats in the NTG group did not show significantly different twitching behaviour from that of rats in the control group ($p > 0.05$; Figure 3(c)). Pretreatment with 1.0 g/kg SB led to more frequent twitching behaviour compared to that in the NTG group ($p < 0.05$; Figure 3(c)). However, pretreatment with placebo resulted in a similar frequency of twitching behaviour as that in the NTG group ($p > 0.05$; Figure 3(c)).

3.2.4. Resting Behaviour. The prevalence of resting behaviour was higher in the rats in the NTG group than that in the control group ($p < 0.001$, Figure 3(d)). Pretreatment with 1.0 g/kg SB ($p < 0.01$; Figure 3(d)), but not placebo ($p > 0.05$;

Figure 3(d)), resulted in lower engagement in resting behaviour compared to that in the NTG group.

3.2.5. Grooming Behaviour. The rats in the NTG group exhibited grooming behaviour more frequently than the control group did, and the difference was significant ($p < 0.01$; Figure 3(e)). Pretreatment with 1.0 g/kg SB ($p < 0.01$; Figure 3(e)), but not with placebo ($p > 0.05$; Figure 3(e)), resulted in a decrease in the frequency of this behaviour.

3.2.6. Effect of Pretreatment with SB on NTG-Induced Light Aversion in Rats. The rats in the NTG group spent significantly less time in the light chamber compared to that spent by the control group ($p < 0.05$; Figure 4). Rats pretreated with 1.0 g/kg SB showed a difference in behaviour that approached marginal significance ($p = 0.054$; Figure 4), which was not observed with placebo pretreatment ($p = 0.977$; Figure 4), and spent a longer time in the light chamber than rats in the NTG group did.

3.2.7. Effect of Pretreatment with SB on NTG-Induced Spontaneous Tactile Allodynia Behaviour in Rats. The rats in the NTG group spent considerably longer time on the smooth surface than those in the control group did ($p < 0.001$; Figure 5(a)). The time spent engaging in this behaviour was decreased by pretreatment with 1.0 g/kg SB ($p < 0.05$; Figure 5(a)). Group mean location heat maps demonstrated that rats in the NTG group had a higher preference for the arena border and corners and spent more time on the smooth surfaces than those in the control group did (Figure 5(b)). This behaviour was decreased by pretreatment with 1.0 g/kg SB (Figure 5(b)).

4. Discussion

Migraine is considered a headache disorder, which involves the neural and vascular components of nociceptive transmission, and is associated with multiple pathophysiology, such as inflammation, and impaired functioning of neurotransmitters, ion channels, immune system, mitochondrial function, and oxidative stress factors [22]. Although Western medicine has rapidly developed treatments for
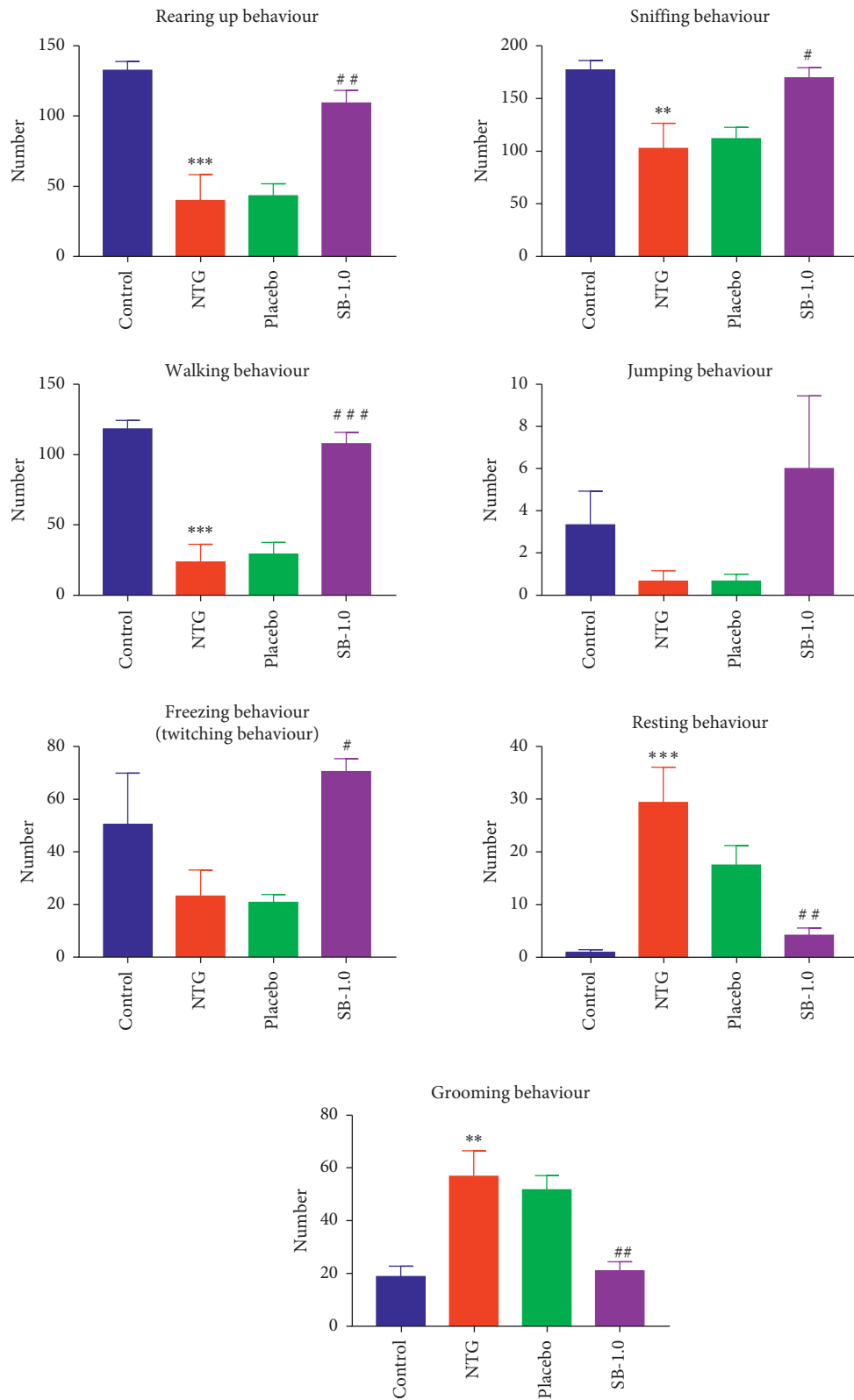
FIGURE 3: Effects of pretreatment with *Scutellaria baicalensis* (SB) on spontaneous nociceptive behaviour in a nitroglycerin-induced migraine rat model: (a) (A) the frequency of rearing up behaviour (exploratory behaviour); (B) the frequency of sniffing behaviour (exploratory behaviour). (b) (A) The frequency of walking behaviour (locomotor behaviour); (B) the frequency of jumping behaviour (locomotor behaviour). (c) The frequency of twitching behaviour (freezing behaviour). (d) The frequency of having an immobile posture or sleeping (resting behaviour). (e) The frequency of grooming the face or body (grooming behaviour). Frequency: the numbers/20 min; control: control group; NTG: NTG group; placebo: placebo group; SB-1.0: SB-1.0 group; data are presented as mean ± SEM. $*p < 0.05$, $**p < 0.01$, and $***p < 0.001$ for the NTG group versus the control group; $#p < 0.05$, $##p < 0.01$, and $###p < 0.001$ versus the NTG group.
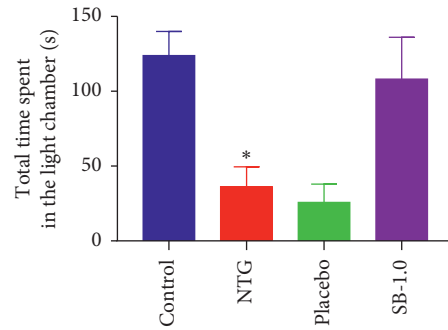
FIGURE 4: Effects of pretreatment with *Scutellaria baicalensis* (SB) on total time spent in the light chamber (s/10 min) of light-aversive behaviour in a nitroglycerin-induced migraine rat model. Control: control group; NTG: NTG group; placebo: placebo group; SB-1.0: SB-1.0 group; data are presented as mean ± SEM. $*p < 0.05$, $**p < 0.01$, and $***p < 0.001$ for the NTG group versus the control group; $\#p < 0.05$, $\#\#p < 0.01$, and $\#\#\#p < 0.001$ versus the NTG group.
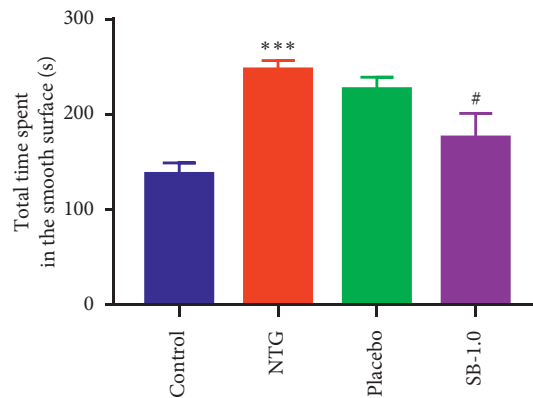
(a)
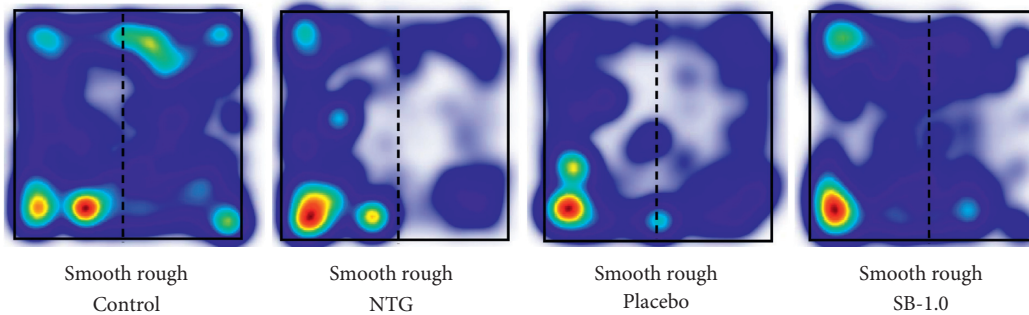
(b)

FIGURE 5: Effects of pretreatment with *Scutellaria baicalensis* (SB) on spontaneous tactile allodynia behaviour in an NTG-induced migraine rat model. (a) Total time spent engaging in spontaneous tactile allodynia behaviour on the smooth surface (s/5 min); (b) group mean heat map plot (the left side is the smooth surface arena). Control: control group; NTG: NTG group; placebo: placebo group; SB-1.0: SB-1.0 group; smooth: smooth surface; rough: rough surface. Data are presented as mean ± SEM. $*p < 0.05$, $**p < 0.01$, and $***p < 0.001$ for the NTG group versus the control group; $\#p < 0.05$, $\#\#p < 0.01$, and $\#\#\#p < 0.001$ versus the NTG group.

migraine, some patients who face adverse effects of these medications seek alternative therapies for migraine prophylaxis and treatment [23]. Based on TCM theories and records in Chinese historical book, SB is considered an excellent anti-inflammatory and analgesic drug in the experience of traditional Chinese doctors; its use can be traced to the book "*Shen Nong Ben Cao Jing*" written in the Han Dynasty [8]. Moreover, SB is not only widely used in China

but is also used as a medicinal plant in many countries around the world. For example, SB is a traditional plant medicine applied to wounds and insect bites in Nepal [8]. The chemical components, such as flavonoids, diterpenes, polyphenols, and amino acids, of SB [24] have several important biological activities, including anti-inflammatory, antitumor, antioxidant, antibacterial, and antiviral effects [25]. In addition, a recent study showed that SB has potential

therapeutic effects on coronavirus disease 2019 [26]. Moreover, baicalin and baicalein, which are the major bioactive compounds in SB, have demonstrated an important role in inhibiting the production of inflammatory cytokines [25, 27], NF-κB signalling [28, 29], and c-fos expression [30] in multiple experimental models. These mechanisms are crucial in the pathophysiological processes of migraine. Hence, we assumed that SB could be potentially effective in migraine treatment.

However, to date, there has been no large-scale exploration of the actual clinical use of SB, including the distribution and frequency of use. In Taiwan, Chinese medicine is a popular medicine system for people. We also have a robust healthcare system with complete database records. Hence, we conducted a retrospective nationwide investigation of the prescription practices of TCM doctors to understand the actual clinical application of SB. Our findings revealed that SB was recommended for a variety of diseases, mainly respiratory inflammatory disorders, headache, sleep impairments, and gastrointestinal discomfort, in Taiwan. These findings are similar to those of a previous study, which showed that SB is commonly used for and has excellent therapeutic effects in sleep disturbance, hepatitis, diarrhoea, vomiting, haemorrhage, hypertension, and respiratory infection [8]. We found that SB could be used in varied diseases and is not limited to specific conditions; hence, the percentage of top ten diseases where SB was used was not particularly high. Although only 2.51% of the indications (the fourth most common indication) of SB in Taiwan was for the treatment of headaches, including migraine, surprisingly, it was not included in the clinical or basic applications of SB in previous scientific reports. It should be noted that our clinical investigation of the indications for SB usage is very credible because we used a nationwide random sample from the NHIRD, which had minimal selection bias owing to the very high rate of insured individuals and the fact that all Chinese herbal products were prescribed by well-trained and qualified TCM practitioners in Taiwan. Hence, we further designed an animal experiment using the widely accepted NTG-induced migraine model to prove the effectiveness of SB.

In the present study, we assessed various migraine-like behaviours of NTG-induced migraine rat models by using recorded videos that were analysed by reliable automated software [31, 32]; therefore, the results of the present study could be considered more credible and more objective than manually scored behaviours.

Migraine diagnosis is based on clinical self-reported pain and attendant symptoms. Although animals are not verbal, recent studies have considered NTG-induced animal models as clinically relevant due to the translational ability of behavioural endpoints [12, 21]. Our previous studies showed that NTG-induced nociceptive behaviours in rats with migraine headache included reduced exploratory and locomotor behaviours and increased resting behaviour [33, 34]. The aforementioned nociceptive behaviours in rodents mimicked those experienced by people with migraine, who generally present with reduced involvement in routine physical activity and decreased interest in exploring new surroundings or objects during an acute migraine attack episode [34, 35]. Therefore, we could use the parameters of the rat model to test antialgesic drug potency. The results of the present study demonstrated that pretreatment with 1.0 g/kg SB could increase locomotor activity and decrease resting behaviour in NTG-induced migraine rats, suggesting that pretreatment with SB could alleviate migraine pain in humans.

Photophobia is one of the important symptoms of migraine [36]. Previous reports have shown that light aversion behaviour, tested using the light/dark box, in NTG-induced migraine rodents effectively mimics the phenomenon of photophobia [35, 37]. Our results indicated that pretreatment with 1.0 g/kg SB resulted in decreased light aversion, which approached marginal significance, implying that SB might alleviate photophobia in an individual who experiences migraine.

Cutaneous allodynia is a common symptom seen in migraineurs; it indicates cranial hypersensitivity and appears to be a predictor of migraine chronification [38, 39]. Recently, a rough/smooth apparatus test was used to evaluate spontaneous tactile allodynia in an NTG-induced migraine rodent model [21]. Our results showed that pretreatment with 1.0 g/kg SB decreased the total time spent on the smooth surface in the rough/smooth test, indicating that SB can decrease tactile allodynia in NTG-induced migraine rat models, which suggests that SB can be helpful for the clinical treatment of cutaneous allodynia in migraineurs.

There are still some limitations to the present study: (1) the animal experiment lacked a group treated with a medicine, such as ibuprofen, to compare the efficacy of SB and conventional Western medicine. In addition, a dose-dependent relationship of the bioactive agents of SB, such as baicalin, was not reported in the current animal experiment; (2) the regulatory mechanisms of SB in migraine rats were not explored, and further validation, such as by biomarker determination (NO, CGRP level) and immunohistochemistry assay, should be conducted to investigate neuronal activity in the future; and (3) although the results of the present study explain how SB was helpful for the treatment of NTG-induced migraine in rats, a well-designed clinical trial is required to evaluate the efficacy of SB in humans.

5. Conclusions

The results of the present study indicated that pretreatment with SB increased the frequency of rearing up and sniffing in exploratory behaviour and increased the frequency of walking in locomotor behaviour in NTG-induced migraine models. NTG-induced migraine rats pretreated with SB also had lower frequencies of both resting behaviour and grooming behaviour. These phenomena indicate that SB could be helpful in decreasing the migraine pain level. Additionally, NTG-induced migraine rats pretreated with SB spent less time on the smooth surface compared to the time spent by the rats that did not receive SB pretreatment, which indicates that SB could be helpful in decreasing cutaneous allodynia in migraineurs. These results support the

application of SB for the treatment of headache, as is a common practice in Taiwan.

Abbreviations

i.p.:	Intraperitoneal injection
ICD-9-CM:	International Classification of Diseases, Ninth Revision, Clinical Modification
NHIRD:	National Health Insurance Research Database
NTG:	Nitroglycerin
SB:	*Scutellaria baicalensis*
TCM:	Traditional Chinese medicine.

Data Availability

The datasets used and analysed during the current study are available from the corresponding author upon reasonable request.

Ethical Approval

1. Human data: this study was approved by the Institutional Review Board of China Medical University in central Taiwan (CMUH-104-REC2-115-R3). 2. Animals: animal use was approved by the Institutional Animal Care and Use Committee of Show Chwan Memorial Hospital (no. 106021) and followed the Guide for the Use of Laboratory Animals (National Academy Press).

Conflicts of Interest

The authors declare that they have no conflicts of interest.

Authors' Contributions

C-C Liao and K-R Liao performed the animal experiment and wrote the manuscript, C-L Lin analysed the data from the NHIRD in Taiwan, and J-M Li designed the protocol and revised the manuscript. All authors read and approved the final manuscript. Chung-Chih Liao and Ke-Ru Liao contributed equally to this work.

Acknowledgments

References

[1] R. Burstein, R. Noseda, and D. Borsook, "Migraine: multiple processes, complex pathophysiology," *Journal of Neuroscience*, vol. 35, no. 17, pp. 6619–6629, 2015.

[2] Y. Woldeamanuel and R. Cowan, "Worldwide migraine epidemiology: systematic review and meta-analysis of 302 community-based studies involving 6,216,995 participants (P6.100)," *Neurology*, vol. 86, no. 16, Article ID P6.100, 2016.

[3] R. C. Burch, D. C. Buse, and R. B. Lipton, "Migraine: epidemiology, burden, and comorbidity," *Neurologic Clinics*, vol. 37, no. 4, pp. 631–649, 2019.

[4] C.-T. Liu, B.-Y. Wu, Y.-C. Hung et al., "Decreased risk of dementia in migraine patients with traditional Chinese medicine use: a population-based cohort study," *Oncotarget*, vol. 8, no. 45, pp. 79680–79692, 2017.

[5] D. Millstine, C. Y. Chen, and B. Bauer, "Complementary and integrative medicine in the management of headache," *BMJ*, vol. 357, Article ID j1805, 2017.

[6] Y. Zhao, M. Martins-Oliveira, S. Akerman, and P. J. Goadsby, "Comparative effects of traditional Chinese and western migraine medicines in an animal model of nociceptive trigeminovascular activation," *Cephalalgia*, vol. 38, no. 7, pp. 1215–1224, 2018.

[7] S. Yu, Y. Ran, W. Xiao et al., "Treatment of migraines with Tianshu capsule: a multi-center, double-blind, randomized, placebo-controlled clinical trial," *BMC Complementary and Alternative Medicine*, vol. 19, no. 1, p. 370, 2019.

[8] T. Zhao, H. Tang, L. Xie et al., "*Scutellaria baicalensis* Georgi. (Lamiaceae): a review of its traditional uses, botany, phytochemistry, pharmacology and toxicology," *Journal of Pharmacy and Pharmacology*, vol. 71, no. 9, pp. 1353–1369, 2019.

[9] S. Hu, Y. Chen, Z. F. Wang et al., "The analgesic and anti-neuroinflammatory effect of baicalein in cancer-induced bone pain," *Evidence-Based Complementary and Alternative Medicine*, vol. 2015, Article ID 973524, 8 pages, 2015.

[10] S.-B. Yoon, Y.-J. Lee, S. K. Park et al., "Anti-inflammatory effects of Scutellaria baicalensis water extract on LPS-activated RAW 264.7 macrophages," *Journal of Ethnopharmacology*, vol. 125, no. 2, pp. 286–290, 2009.

[11] C. Waeber and M. A. Moskowitz, "Migraine as an inflammatory disorder," *Neurology*, vol. 64, no. 10, pp. S9–S15, 2005.

[12] K. J. Sufka, S. M. Staszko, A. P. Johnson, M. E. Davis, R. E. Davis, and T. A. Smitherman, "Clinically relevant behavioral endpoints in a recurrent nitroglycerin migraine model in rats," *Journal of Headache and Pain*, vol. 17, p. 40, 2016.

[13] C. Tassorelli, R. Greco, D. Wang, M. Sandrini, G. Sandrini, and G. Nappi, "Nitroglycerin induces hyperalgesia in rats—a time-course study," *European Journal of Pharmacology*, vol. 464, no. 2-3, pp. 159–162, 2003.

[14] C. Tassorelli and S. A. Joseph, "Systemic nitroglycerin induces Fos immunoreactivity in brainstem and forebrain structures of the rat," *Brain Research*, vol. 682, no. 1-2, pp. 167–181, 1995.

[15] F. Farajdokht, S. Babri, P. Karimi, and G. Mohaddes, "Ghrelin attenuates hyperalgesia and light aversion-induced by nitroglycerin in male rats," *Neuroscience Letters*, vol. 630, pp. 30–37, 2016.

[16] C. H. Chen, C. L. Lin, and C. H. Kao, "Gallbladder stone disease is associated with an increased risk of migraines," *Journal of Clinical Medicine*, vol. 7, no. 11, p. 455, 2018.

[17] Y. J. Wang, C. C. Liao, H. J. Chen, C. L. Hsieh, and T. C. Li, "The effectiveness of traditional Chinese medicine in treating patients with leukemia," *Evidence-Based Complementary and Alternative Medicine*, vol. 2016, Article ID 8394850, 12 pages, 2016.

[18] A. Nair and S. Jacob, "A simple practice guide for dose conversion between animals and human," *Journal of Basic and Clinical Pharmacy*, vol. 7, no. 2, pp. 27–31, 2016.

[19] A. Melo-Carrillo and A. Lopez-Avila, "A chronic animal model of migraine, induced by repeated meningeal nociception, characterized by a behavioral and pharmacological approach," *Cephalalgia*, vol. 33, no. 13, pp. 1096–1105, 2013.

[20] B. Vos, A. Strassman, and R. Maciewicz, "Behavioral evidence of trigeminal neuropathic pain following chronic constriction injury to the rat's infraorbital nerve," *The Journal of Neuroscience*, vol. 14, no. 5, pp. 2708–2723, 1994.

[21] H. M. Harris, J. M. Carpenter, J. R. Black, T. A. Smitherman, and K. J. Sufka, "The effects of repeated nitroglycerin administrations in rats; modeling migraine-related endpoints and chronification," *Journal of Neuroscience Methods*, vol. 284, pp. 63–70, 2017.

[22] C. Demartini, R. Greco, A. M. Zanaboni et al., "Nitroglycerin as a comparative experimental model of migraine pain: from animal to human and back," *Progress in Neurobiology*, vol. 177, pp. 15–32, 2019.

[23] C. A. Whyte and S. J. Tepper, "Adverse effects of medications commonly used in the treatment of migraine," *Expert Review of Neurotherapeutics*, vol. 9, no. 9, pp. 1379–1391, 2009.

[24] B. Dinda, S. Dinda, S. DasSharma, R. Banik, A. Chakraborty, and M. Dinda, "Therapeutic potentials of baicalin and its aglycone, baicalein against inflammatory disorders," *European Journal of Medicinal Chemistry*, vol. 131, pp. 68–80, 2017.

[25] H. Liao, J. Ye, L. Gao, and Y. Liu, "The main bioactive compounds of *Scutellaria baicalensis* Georgi. for alleviation of inflammatory cytokines: a comprehensive review," *Biomedicine & Pharmacotherapy*, vol. 133, Article ID 110917, 2020.

[26] J. W. Song, J. Y. Long, L. Xie et al., "Applications, phytochemistry, pharmacological effects, pharmacokinetics, toxicity of *Scutellaria baicalensis* Georgi. and its probably potential therapeutic effects on COVID-19: a review," *Chinese Medicine*, vol. 15, p. 102, 2020.

[27] J. Zhang, C. Teng, C. Li, and W. He, "Deliver anti-inflammatory drug baicalein to macrophages by using a crystallization strategy," *Frontiers in Chemistry*, vol. 8, p. 787, 2020.

[28] M. Zou, L. Yang, L. Niu et al., "Baicalin ameliorates *Mycoplasma gallisepticum*-induced lung inflammation in chicken by inhibiting TLR6-mediated NF-κB signalling," *British Poultry Science*, pp. 1–12, 2020.

[29] Y. Ji, J. Han, N. Lee et al., "Neuroprotective effects of baicalein, wogonin, and oroxylin A on amyloid beta-induced toxicity via NF-κB/MAPK pathway modulation," *Molecules*, vol. 25, no. 21, Article ID 5087, 2020.

[30] K.-C. Kim, S.-S. Kang, J.-S. Lee, D.-H. Park, and J.-W. Hyun, "Baicalein attenuates oxidative stress-induced expression of matrix metalloproteinase-1 by regulating the ERK/JNK/AP-1 pathway in human keratinocytes," *Biomolecules and Therapeutics*, vol. 20, no. 1, pp. 57–61, 2012.

[31] E. A. van Dam, J. E. van der Harst, C. J. F. ter Braak, R. A. J. Tegelenbosch, B. M. Spruijt, and L. P. J. J. Noldus, "An automated system for the recognition of various specific rat behaviours," *Journal of Neuroscience Methods*, vol. 218, no. 2, pp. 214–224, 2013.

[32] F. C. P. Simão, F. Martínez-Jerónimo, V. Blasco et al., "Using a new high-throughput video-tracking platform to assess behavioural changes in *Daphnia magna* exposed to neuroactive drugs," *Science of the Total Environment*, vol. 662, pp. 160–167, 2019.

[33] C.-C. Liao, J.-M. Li, C.-H. Chen, C.-L. Lin, and C.-L. Hsieh, "Effect of *Paeonia lactiflora*, a traditional Chinese herb, on migraines based on clinical application and animal behavior analyses," *Biomedicine & Pharmacotherapy*, vol. 118, Article ID 109276, 2019.

[34] C. C. Liao, J. M. Li, and C. L. Hsieh, "Auricular electrical stimulation alleviates headache through CGRP/COX-2/TRPV1/TRPA1 signaling pathways in a nitroglycerin-induced migraine rat model," *Evidence-Based Complementary and Alternative Medicine*, vol. 2019, Article ID 2413919, 10 pages, 2019.

[35] D. Vuralli, A. S. Wattiez, A. F. Russo, and H. Bolay, "Behavioral and cognitive animal models in headache research," *The Journal of Headache and Pain*, vol. 20, no. 1, p. 11, 2019.

[36] K. B. Digre and K. C. Brennan, "Shedding light on photophobia," *Journal of Neuro-Ophthalmology*, vol. 32, no. 1, pp. 68–81, 2012.

[37] F. Farajdokht, S. Babri, P. Karimi, M. R. Alipour, R. Bughchechi, and G. Mohaddes, "Chronic ghrelin treatment reduced photophobia and anxiety-like behaviors in nitroglycerin- induced migraine: role of pituitary adenylate cyclase-activating polypeptide," *European Journal of Neuroscience*, vol. 45, no. 6, pp. 763–772, 2017.

[38] S. Akerman, M. Romero-Reyes, N. Karsan et al., "Therapeutic targeting of nitroglycerin-mediated trigeminovascular neuronal hypersensitivity predicts clinical outcomes of migraine abortives," *Pain*, 2020.

[39] M. A. Louter, J. E. Bosker, W. P. van Oosterhout et al., "Cutaneous allodynia as a predictor of migraine chronification," *Brain*, vol. 136, no. 11, pp. 3489–3496, 2013.

Research Article

Acute and Subchronic Oral Safety Profiles of the Sudarshana Suspension

Weerakoon Achchige Selvi Saroja Weerakoon,[1] **Pathirage Kamal Perera** ,[2]
Kamani Samarasinghe,[3] **Dulani Gunasekera,**[4] **and Thusharie Sugandhika Suresh**[5]

[1]*Department of Ayurveda Obstetrics and Paediatrics, Institute of Indigenous Medicine, University of Colombo, Colombo, Sri Lanka*
[2]*Department of Ayurveda Pharmacology and Pharmaceutics, Institute of Indigenous Medicine, University of Colombo, Colombo, Sri Lanka*
[3]*Department of Pathology, Faculty of Medical Sciences, University of Sri Jayewardenepura, Nugegoda, Sri Lanka*
[4]*Department of Paediatrics, Faculty of Medical Sciences, University of Sri Jayewardenepura, Nugegoda, Sri Lanka*
[5]*Department of Biochemistry, Faculty of Medical Sciences, University of Sri Jayewardenepura, Nugegoda, Sri Lanka*

Correspondence should be addressed to Pathirage Kamal Perera; drkamalperera@yahoo.com

Sudarshana powder (SP) is an Ayurvedic preparation, which contains 53 herbal ingredients along with 50% of *Andrographis paniculata* and is clinically used with bees honey. This study was aimed to determine the safety profile of the SP, and its novel preparation Sudarshana suspension (SS) on male Wistar rats and tolerance studies were conducted for healthy adult volunteers. Acute and subacute toxicity studies of the SS and hot water extract of SP were assessed in Wistar rats by observing the general behavior, analyzing biochemical and haematological parameters, and pathological observation. Healthy consented adult volunteers ($n = 35$) of either sex were selected, and tolerance studies of SS were tested by measuring the biochemical and haematological parameters. There were no significant ($p > 0.05$) changes observed in the treated animals with SS and hot water extract of SP compared with control in body weights, food intake, and water consumption as well as the biochemical and haematological parameters. Histopathological studies revealed no significant ($p > 0.05$) changes in the liver, heart, and kidney tissues. The experimental results suggest that novel formulation SS was potentially safe for chronic administration in rats, and no significant differences ($p > 0.05$) were observed in tested parameters on day 3 and day 8 when compared to the day 0 (baseline) values in healthy volunteers. Healthy volunteers did not report any adverse effects or any other complications during the treatment period and the follow-up period. Therefore, it can be concluded that the novel preparation Sudarshana suspension does not cause any significant toxic effects on the blood parameters in animal and human models.

1. Introduction

Sudarshana powder (SP) is an effective antipyretic Ayurvedic preparation, widely used in Sri Lanka as well as in India from the very early beginning of Ayurveda treatment. Sudarshana powder (*Sudarshana churna*) is mentioned in the Ayurvedic Pharmacopeia complied under Sec. 41 (2) (c) of Ayurveda Act no 31 of 1961 by the Ayurvedic Pharmacopeia Committee under the direction of the Ayurvedic Research Committee. During the early beginning of

Ayurveda treatment in Sri Lanka, the main ingredient of the SP was *Swertia chirata* which was later replaced by *Andrographis paniculata* (Burm. F.) Nees in Sri Lanka. Presently, the SP contains *Andrographis paniculata* (Burm. F.) Nees (50%) along with other 52 ingredients (50%) [1]. This powder is being widely used with bees honey in all Ayurvedic hospitals and dispensaries for adults as well as in pediatric patients including National Ayurveda Teaching Hospital, Borella, Sri Lanka. Bees honey is recommended as an *Anupana* (vehicle) for SP in the pediatrics age group in

Ayurveda [2]. No reports on adverse effects have been reported of this mixer clinically.

It is recommended for all types of fever and common cold [3]. It is used traditionally as antimalarial, antiviral, and antipyretic formulation for which it is highly effective [1]. SP has been clinically used with bees honey to mask its bitter taste, but there is no ready-to-use product with the correct amount of bees honey in current dosage forms. Therefore, this powder was developed into user-friendly ready-to-use standard Ayurveda suspension using bees honey *viz* SS. SP and bees honey is the only ingredients of this novel preparation. There are no other added substances in this novel preparation. Suspension forms of drugs are an easy way to administer to the pediatrics and elderly who have difficulty in taking drugs in tablet or capsule forms. But, to date, there is no scientific research conducted for evaluating the safety of SP and SS. Thus, this study was aimed to determine the safety profile of the SP and SS effects after acute and chronic oral administration in male Wistar rats, and tolerance studies were conducted in healthy volunteers.

2. Materials and Methods

2.1. Collection of Materials and Preparation of Sudarshana Powder. All the ingredients were collected from the Ayurveda Drug Cooperation, Sri Lanka, and authentication of ingredients was done at the Institute of Indigenous Medicine, University of Colombo, Sri Lanka (Specimen no. 102). *Sudarshana* powder was prepared according to Ayurveda Pharmacopoeia [1, 4] at the pharmacy of the Institute of Indigenous Medicine, University of Colombo, Sri Lanka.

2.2. Preparation of Extracts. Aqueous extracts of SP were prepared by infusion with hot water, occasional shaking, and filtration (preparation method of Phanta Kasaya in Ayurveda medicine) [1].

2.3. Preparation of Suspension. *Sudarshana* powder is converted to *Sudarshana* suspension (SS) using bees honey, according to the Ayurvedic Mana *Paribhasha* (the method of syrup or suspension preparation) [5].

2.4. Animals. Healthy adult male Wistar rats (200–250 g) were used in the study. The animals were kept in plastic cages (two per cage) under standardized animal house conditions at the animal house, Faculty of Medical Sciences, University of Sri Jayewardenepura, Sri Lanka, with continuous access to standard pelleted feed and tap water.

2.5. Ethical Approval for Animal Studies. All experiments in rats were carried out in accordance with the recommendation of the guidelines for care and use of laboratory animals, and the project proposal was approved (no. 591/11) by the Ethics Review Committee of the Faculty of Medical Sciences, University of Sri Jayewardenepura, Sri Lanka (http://medical.sjp.ac.lk/index.php/ethics-review-committee-introduction).

2.6. Dosage and Administration of Drug to Animal Models. The doses of drugs corresponded to the normal therapeutic dose administered to adult humans as calculated, based on relative surface areas of humans and each individual animal. The dosage was calculated based on its weight, and then, it was multiplied by 6 (conversion factor, km: Factor for converting mg/kg dose to mg/m^2 dose) [6].

2.7. Acute Oral Toxicity Study. Wistar rats were kept for a minimum of 5 days prior to oral administration at the animal house, Faculty of Medical Sciences, University of Sri Jayewardenepura, Sri Lanka, to allow for their acclimatization to the animal house conditions. The animal room was ventilated with a 12°h cycle of day and night light conditions, and the temperature was maintained at approximately 25°C. Tap water and food were readily accessible to the rats throughout the study; however, prior to the oral administration of the single doses of Sudarshana suspension and infusion of Sudarshana powder, all animals were subjected to a short fasting period of 5 h [7, 8].

The acute toxicity [9] of SS and SP was compared with that of the control group, distilled water given at a rate of 1 ml/rat. There were 6 rats in each group. Test group 1 received a single dose of SS (4 ml/kg), and Test group 2 received a single dose of SP (0.5 g/kg). Treated animals were deprived of food and water for 2 h to assess the general behavior of rats and thereafter during a period of 48 h for dead animals. During a 48 h period of observation, the body weight changes and food and water intakes were recorded followed by observation for 2 weeks for possible signs of toxicity and deaths and the latency of death. Blood was collected for biochemical and haematological analyses after 48 h and 14 days, and creatinine, alkaline phosphatase, alanine aminotransferase (ALT), aspartate aminotransferase (AST), gamma-glutamyl transferase (γ-GT), and haemoglobin (Hb) levels were analyzed by the spectrophotometer. BIOLABO kits from France were purchased from Analytical Instrument (Pvt) Ltd., Colombo.

2.8. Subchronic Oral Toxicity Study. The SS and SP were compared with the control in three groups of rats, 6 rats in each. The control group received distilled water as a vehicle, Test group 1 received a single dose of SS (4 ml/kg), and Test group 2 received hot water extraction of SP (0.5 g/kg), single dose daily, for 42 consecutive days.

The body weights and the food and water intakes were recorded weekly. After 42 days of administration, blood was collected for haematological and biochemical analyses. The haematological parameters (i.e., WBC, RBC, Hb, PCV, MCV, MCH, MCHC, RDW, MPV, and platelets) and the biochemical parameters including creatinine, alkaline phosphatase, alanine aminotransferase (ALT), aspartate aminotransferase (AST), gamma-glutamyl transferase (γ-GT), and urea were evaluated. Reagent BIOLABO kits from France were used for the analysis, and the animals were sacrificed to harvest the liver, heart, and kidneys and weighed individually. Macroscopic and microscopic analyses were carried out.

2.9. Statistical Analysis. Results are presented as mean-±standard error of mean (SEM). Student's *t* test was used for statistical comparison of data between groups. Differences were considered significant at $p \leq 0.05$.

2.10. Ethical Clearance Process. The clinical study on healthy volunteers was approved by the Ethics Review Committee, Faculty of Medical Sciences, University of Sri Jayewardenepura, Sri Lanka (ref. no. 775/13), and Ethics Review Committee, Institute of Indigenous Medicine, University of Colombo (ref. no. ERC 12/11), Sri Lanka. A clinical study was registered at the Sri Lanka Clinical Trial Registry ((reg. no. SLCTR/2015/005) (http://slctr.lk/trials/304) and WHO International Clinical Trials Registry (http://apps.who.int/trialsearch/Trial2.aspx?TrialID=SLCTR/2015/005)).

2.11. Safety Effect of Sudarshana Suspension in Healthy Volunteers. Safety effect on hepatic and renal functions of the novel preparation Sudarshana suspension in healthy volunteers was tested by measuring the key hepatic enzymes alanine aminotransferase (ALT), aspartate aminotransferase (AST), gamma-glutamyl transferase (gamma GT), alkaline phosphatase, haemoglobin content (Hb), urea in serum, and creatinine.

2.12. Study Design. This study is an analytical interventional single-arm study where all volunteers were recruited until the required number was achieved.

2.13. Sample Size. Thirty-five healthy adult volunteers [10] were selected by an open advertisement.

2.13.1. Inclusion Criteria

(1) Age group of 18–60 years at the time of enrollment, of either sex with weight less than 60 kg

(2) Those having no known systemic disorders, such as hypertension, diabetes mellitus, hypercholesterolemia, and chronic arthritis

(3) Those having no history of drug allergy

(4) Those having no history of intolerance to SP or similar compounds

(5) Women should be neither pregnant and nor breast feeding

(6) Only those who can write and read languages of English or Sinhala.

2.13.2. Exclusion Criteria

(1) Less than 18 years of age and over 60 years at the time of enrollment, of either sex

(2) Weight more than 60 kg

(3) Concurrent treatment with any Ayurveda or Western medicine

2.14. Determination of Appropriate Dose of the SS. The dosage of the test drug was determined by calculating the dose per adult equivalent to the normal paediatric dosage proportionate with the body weight of a child.

2.15. The Procedures and Duration. Written consents were obtained from the participants before initiating the study, and the information sheets and diary sheets were distributed to the participants in their own language.

Sudarshana suspension was prepared at the pharmacy of the Institute of Indigenous Medicine, University of Colombo, Sri Lanka, and filled in 500 ml air-tight, amber, labeled glass bottles.

Adult volunteers were given four doses of drug at six-hour intervals per day for 7 consecutive days. The dosage of drug was determined according to the body weight of the volunteer. 3 ml of blood was drawn on days 0, 3, 8. The liver and renal functions tests (ALT, ALP, AST, γGT, creatinine, and urea) were done using the automated biochemical analyzer (Kone) at the Department of Biochemistry. Hb was analyzed by using the spectrophotometer at the Research Lab, Department of Biochemistry, FMS, USJ. BIOLABO kits were purchased from Analytical Instrument (Pvt) Ltd., Colombo. In each subject, basic epidemiological and anthropometric data (age, sex, and weight) were recorded. After the first and last doses, palatability was recorded using a modified five-point scale [11]:

0 = severely dislikes the taste and vomits

1 = dislikes the taste but does not vomit

2 = takes the drug rather unhappily

3 = takes the drug without any complaint

4 = likes the taste a lot

3. Results

3.1. Acute Oral Toxicity. The results of the acute toxicity study showed no signs of toxicity such as general behavioral changes or mortality. No abnormalities were detected in any of the tested blood parameters as well as body weights, food intake, and water consumption in the SS and SP groups when compared with the control group. The effects of SS and hot water extraction of SP after 48 hours of oral administration are summarized in Table 1.

The effects of SS and hot water extraction of SP in biochemical parameters after 14 days of oral administration are summarized in Table 2.

3.2. Subchronic Oral Toxicity

3.2.1. Effect of the Oral Administration of SP and SS on the General Behavior of the Rats. No significant changes in general behavior or other major physiological activities of rats were observed at any time point in this study. No significant changes were recorded in body weight and daily food intake in the treated rats as compared to the control. Both the control and treated rats appeared consistently healthy throughout the 42-day period of study. No death was also recorded in both the control and treated rats (Figure 1).

TABLE 1: Effects of SS and hot water extraction of SP after 48 hours of oral administration.

Biochemical parameters	Groups		
	Control	SP	SS
Haemoglobin (Hb) (g/dl)	14.15 ± 0.11	13.92 ± 0.24	14.02 ± 0.19
AST/GOT (IU/L)	86.05 ± 1.9	83.44 ± 1.92	84.75 ± 1.53
ALT/TGP (U/L)	30.92 ± 0.80	32.22 ± 1.78	34.04 ± 1.30
Gamma GT (IU/L)	3.9 ± 0.71	3.91 ± 0.50	3.90 ± 0.59
Alkaline phosphatase (IU/L)	131.64 ± 2.03	132.05 ± 3.0	131.92 ± 2.15
Urea (mmol/L)	28.63 ± 1.24	30.92 ± 1.84	32.73 ± 1.38
Creatinine (mg/dl)	0.59 ± 0.02	0.62 ± 0.02	0.65 ± 0.02

Values are expressed as mean $\pm$ SEM; $n = 35$.

TABLE 2: Effects of SS and hot water extraction of SP after 14 days of oral administration.

Biochemical parameters	Groups		
	Control	SP	SS
Haemoglobin (Hb) (g/dl)	14.12 ± 0.08	14.01 ± 0.21	14.05 ± 0.23
AST/GOT (IU/L)	85.41 ± 1.83	83.0 ± 1.92	85.32 ± 1.38
ALT/TGP (U/L)	30.2 ± 0.86	32.41 ± 1.21	33.24 ± 1.24
Gamma GT (IU/L)	4.12 ± 0.53	4.05 ± 0.36	4.05 ± 0.43
Alkaline phosphatase (IU/L)	133.64 ± 2.08	134.58 ± 2.75	134.47 ± 1.32
Urea (mg/dl)	28.59 ± 2.01	28.87 ± 1.43	31.23 ± 1.10
Creatinine (mg/dl)	0.60 ± 0.03	0.64 ± 0.01	0.63 ± 0.02

Values are expressed as mean $\pm$ SEM; $n = 35$.

3.2.2. Effect of Oral Administration of SP and SS on the Haematological and Biochemical Blood Parameters of the Rats. The haematological parameters (i.e., WBC, RBC, Hb, PCV, MCV, MCH, MCHC, RDW, MPV, and platelets) and the blood biochemical parameters (i.e., ALT, AST, ALP, ɤ-GT, urea, and creatinine) showed no significant changes ($p > 0.05$) in the treated rats compared to those in the the control rats, respectively. All levels were in consistent ranges until the termination of the study. The effects of SS and hot water extraction of SP after 42 days of oral administration are summarized in Tables 3–6.

3.2.3. Effect of Oral Administration of SP and SS on the Wet Weights, Heights, Length, and Width of Rat Organs after 42-Day Treatment Period. The wet weights of rats' organs of both treated and control groups are presented in Table 5. The subchronic oral ingestion of SP and SS over 42 days caused no significant changes in the wet weights of the organs (i.e., heart, kidneys, and liver) in the treated groups and was compared with the control rats. The height, length, and width of rats' organs (i.e., heart, kidneys, and liver) of both treated and control groups after 42 days of oral ingestion are presented in Table 6. There were no significant changes in the outline measurements of rats' organs when compared to the control group.

3.2.4. Histopathological Effect of Oral Administration of SP and SS on Selected Vital Organs after 42-Day Treatment Period. The liver, heart, and kidneys did not reveal any morphological changes on gross and histological examinations (Figures 2–4).

3.3. Clinical Study on Healthy Volunteers

3.3.1. Effect of SS on Renal and Hepatic Functions. According to the findings of the healthy volunteers' study, there were no statistically significant ($p > 0.05$) differences in the serum parameters (ALT, AST, ALP, γ-GT, urea, creatinine, and Hb) on days 3 and 8 when compared with the baseline values (day 0) as shown in Table 7.

Healthy volunteers did not get any adverse effects, such as vomiting, headache, diarrhoea, or any other abnormal feeling during the treatment period and also during the follow-up period.

4. Discussion

In Ayurveda, the majority of natural drugs are of plant origin. Different plant parts such as roots, seeds, flowers, stem, bark, wood, leaves, and the plant as a whole are used as medicine. The medicinal property of the crude drug is due to the biologically active chemical constituents. The development of these chemical constituents is greatly influenced by different environmental and ecological factors. Ayurveda, allopathic medicine, and homeopathy are popular in society to achieve the same. Its widespread use is further substantiated by the affordability, knowledge of medicinal plants, and belief that they are harmless [12]. The increase in the number of users as opposed to the scarcity of scientific evidence on the safety of the medicinal plants has raised concerns regarding toxicity and detrimental effects of these remedies [13], and the same applies for novel preparation Sudarshana suspension.
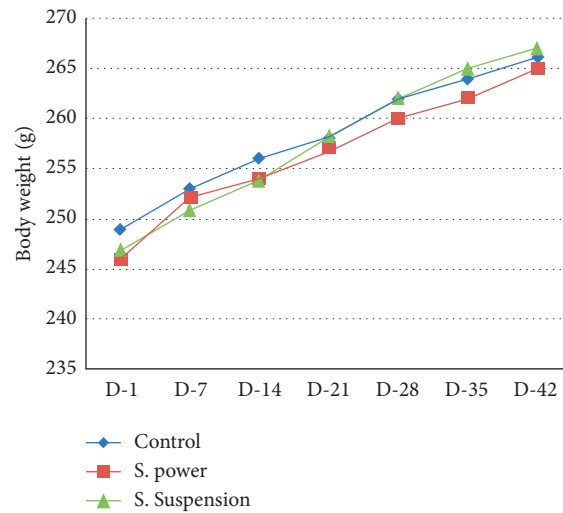
Figure 1: Mean body weights of rats during 42 days.

Table 3: Effects of oral administration of SP and SS on the biochemical parameters of rats' blood after 42-day period of oral administration.

Biochemical parameters	Groups		
	Control	S. powder	S. suspension
AST/GOT (IU/L)	85.97 ± 1.81	84.07 ± 1.86	85.17 ± 1.43
ALT/TGP (IU/L)	31.5 ± 0.62	32.92 ± 1.31	34.01 ± 1.76
Gamma GT (IU/L)	4.21 ± 0.61	4.37 ± 0.43	4.07 ± 0.43
Alkaline Phosphatase(IU/L)	135.81 ± 2.91	136 ± 3.91	133.51 ± 2.25
Urea UV (mg/dl)	32.57 ± 1.49	32.11 ± 1.77	33.25 ± 1.02
Creatinine (mg/dl)	0.62 ± 0.02	0.67 ± 0.01	0.67 ± 0.02

Values are expressed as mean ± SEM; $n = 6$.

Table 4: Effects of oral administration of SP and SS on the haematological parameters of rats' blood after 42-day period of oral administration.

Blood parameters	Groups		
	Control	S. powder	S. suspension
White blood cells (WBC) ($10^3/\mu$l)	8.18 ± 0.17	7.9 ± 0.13	8.02 ± 0.15
Neutrophil (%)	33.18 ± 3.2	28.65 ± 2.80	32.21 ± 2.82
Lymphocytes (%)	55.44 ± 1.84	59.54 ± 2.60	56.88 ± 2.58
Monocyte (%)	4.35 ± 1.23	5.92 ± 1.40	5.35 ± 1.0
Eosinophil (%)	2.54 ± 0.55	1.78 ± 0.18	2.07 ± 0.40
Basophil (%)	2.6 ± 0.70	3.8 ± 0.67	3.5 ± 0.53
Red blood cells (RBC) ($10^6/\mu$L)	8.29 ± 0.35	7.8 ± 0.19	7.9 ± 0.19
Haemoglobin (Hb)	14.18 ± 0.39	14.3 ± 0.20	14.18 ± 0.27
Packed cell volume (PCV) (%)	48.94 ± 1.85	48.65 ± 1.26	48.41 ± 1.93
Mean corpuscular volume (MCV) (fL)	53.61 ± 2.15	53.97 ± 1.78	56.37 ± 1.51
Mean corpuscular haemoglobin (MCH) (pg)	24.05 ± 1.27	23.37 ± 0.86	24.05 ± 0.97
Mean corpuscular haemoglobin conc. (MCHC) (pg)	27.34 ± 1.08	26.8 ± 0.91	25.87 ± 1.28
RDW (%)	14.81 ± 0.11	15.0 ± 0.19	14.52 ± 0.08
Platelets ($10^3/\mu$L)	636.42 ± 2.73	631.71 ± 2.02	635.42 ± 2.28
MPV (fL)	3.25 ± 0.42	2.61 ± 0.16	2.7 ± 0.11

Values are expressed as mean ± SEM; $n = 6$.

There are many traditional herbals or polyherbal medicines that have not been verified by clinical trials, and hence, their efficacy and safety are still questioned by consumers. Drug safety is a very basic and fundamental concept in medical practice, and hence, the safety profile of SS and SP was investigated on male Wistar rats and healthy volunteers. The results obtained from the acute toxicity study showed that the SP and SS did not exert any possible

TABLE 5: Wet weight of the heart, kidneys, and liver of rats chronically treated with SP and SS.

Groups	Organ weight (g)			
	Liver	Heart	R. kidney	L. kidney
Control	13.80 ± 0.40	1.12 ± 0.04	1.20 ± 0.02	1.13 ± 0.02
S. powder	13.66 ± 0.36	1.18 ± 0.04	1.23 ± 0.03	1.16 ± 0.04
S. suspension	14.17 ± 0.32	1.15 ± 0.03	1.23 ± 0.02	1.15 ± 0.01

Values are expressed as mean $\pm$ SEM; $n = 6$.

TABLE 6: Height, length, and width of rats' organs chronically treated with SP and SS.

Groups	Organ height $\times$ length $\times$ width (cm)			
	Liver	Heart	R. kidney	L. kidney
	2.18 ± 0.09	0.94 ± 0.02	0.88 ± 0.06	0.8 ± 0.04
Control	5.57 ± 0.32	1.85 ± 0.05	2.11 ± 0.10	1.92 ± 0.07
	4.6 ± 0.18	1.31 ± 0.03	1.24 ± 0.14	1.24 ± 0.09
	2.18 ± 0.07	0.8 ± 0.02	0.71 ± 0.02	0.67 ± 0.01
S. powder	5.57 ± 0.07	1.8 ± 0.03	1.88 ± 0.02	1.71 ± 0.04
	4.42 ± 0.02	1.28 ± 0.02	1.47 ± 0.03	1.38 ± 0.02
	2.1 ± 0.06	$0.8 \pm 0.03\pm$	0.7 ± 0.02	0.67 ± 0.01
S. suspension	5.11 ± 0.12	1.84 ± 0.02	1.94 ± 0.02	1.81 ± 0.02
	4.31 ± 0.06	1.27 ± 0.01	1.37 ± 0.01	1.32 ± 0.02

Values are expressed as mean $\pm$ SEM; $n = 6$.

(a)   (b)   (c)

FIGURE 2: Photomicrograph of the liver tissue of the rats: (a) control; (b) SP; (c) SS. All the groups have a normal lobular architecture, normal sinusoids, and normal limiting plate hepatocytes. No vascular congestion, hepatocyte necrosis, or tissue degeneration were observed.

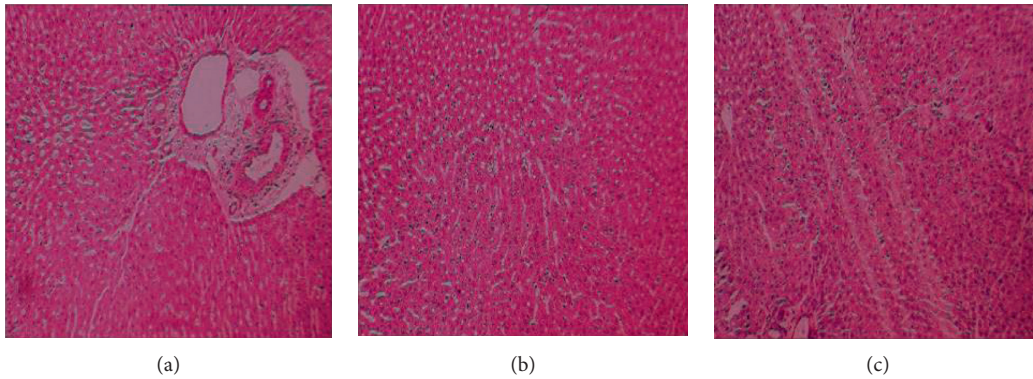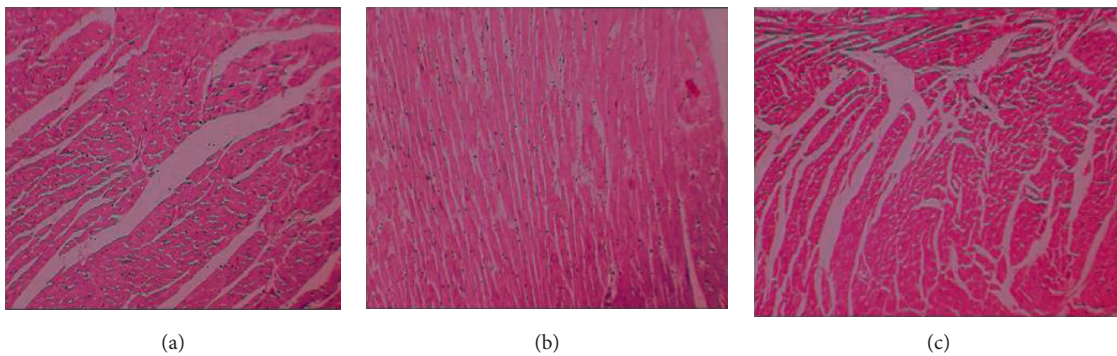

(a)   (b)   (c)

FIGURE 3: Photomicrograph of the heart tissue of the rats: (a) control; (b) SP; (c) SS. All the groups have a normal tissue structure.
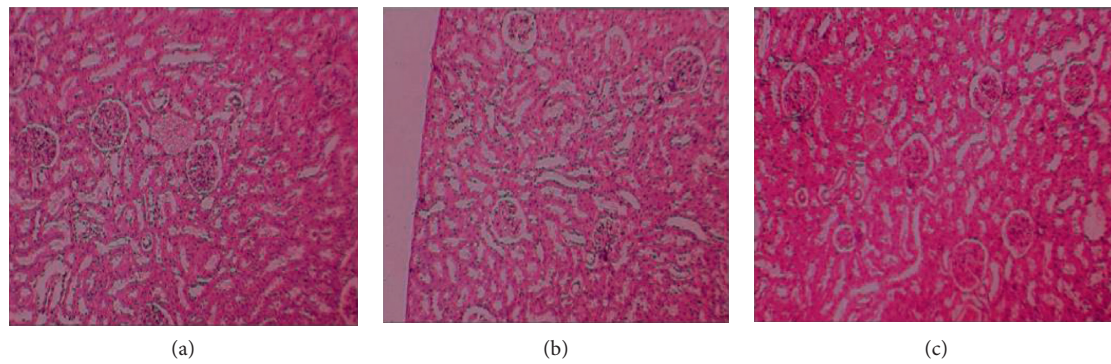
(a)

(b)

(c)

FIGURE 4: Photomicrograph of the kidney tissue of the rats: (a) control; (b) SP; (c) SS. All the groups have a normal tissue structure.

TABLE 7: Effect on renal and hepatic functions following 7 days of oral administration of SS.

Biochemical parameters	Testing days and p values				
	Day 0	Day 3	p value	Day 8	p value
Haemoglobin (Hb) (g/dl)	12.71 ± 0.24	12.70 ± 0.24	0.28	12.74 ± 0.23	0.19
AST/GOT (IU/L)	28.86 ± 0.68	28.57 ± 0.73	0.12	28.89 ± 0.69	0.46
ALT/TGP (U/L)	23.12 ± 1.44	22.76 ± 1.42	0.16	23.20 ± 1.43	0.4
Gamma GT (IU/L)	11.68 ± 0.85	11.54 ± 0.79	0.35	11.29 ± 0.81	0.7
Alkaline phosphatase (IU/L)	210.05 ± 8.44	209.13 ± 8.20	0.12	209.10 ± 8.15	0.11
Urea (mmol/L)	2.83 ± 0.13	2.80 ± 0.13	0.19	2.84 ± 0.12	0.4
Creatinine (mg/dl)	0.78 ± 0.01	0.78 ± 0.01	0.49	0.79 ± 0.01	0.25

All the values are expressed as mean ± SEM; $n = 35$. $p > 0.05$, not significant.

toxicity in rats with single doses of drug administration (Tables 1 and 2). In the subchronic toxicity study, when the extract was administered daily to the animals for a period of 42 days, no mortality or morbidity was observed (Table 3) and no significant changes occurred in the haematological parameters (Table 4). The SS and SP did not cause any significant change in body weight when compared with the control group (Figure 1). The gross examination of internal organs revealed no detectable inflammation, while the weight of the animals treated with the SS and SP was not significantly different when compared to the control group (Table 5). According to reports, body and internal organ weights are considered sensitive indices of nontoxicity after 42 consecutive days of drug administration (Table 6). Serum concentrations of alanine amino transaminase (ALT) and aspartate amino transaminase (AST) are known to increase significantly in liver toxicity [14, 15]. Since, in this study, the enzymes showed no appreciable increase in the treated animals, it implied that the SS and SP have no hepatotoxic effect. This was confirmed by the histological study in which tissue morphology showed no changes (Figures 2–4).

The serum creatinine and urea levels too were not significantly altered compared to the control indicating no possible nephrotoxicity which was confirmed by the histopathological study as well. When haematological parameters were evaluated, mean corpuscular volume (MCV), mean corpuscular haemoglobin (MCH), and mean corpuscular haemoglobin concentration (MCHC) showed no significant variations following the treatment with SS. The importance of MCH, MCV, and MCHC in the diagnosis of anaemia in most animals has been highlighted. From this result, it has been shown that the SS and SP did not significantly alter the calculated RBC indices. The inflammatory process is characterized by the involvement of multiple inflammatory WBC [16]. In this study, it has not been observed that WBC has altered significantly while lymphocytes, the main effector cells of the immune system [17], showed no significant differences, thus suggesting that the SS and SP did not exert any toxic effect.

The findings from this part of the study provided sufficient data on the therapeutic safety of this polyherbal drug. It was observed that SS and SP do not exert any hepatotoxic effect that would cause the liver to compromise its function. Furthermore, the indices pertaining to renal function showed no abnormalities. The findings were further supported by the histological study where the hepatic, renal, and cardiac tissues showed no changes following SS and SP treatment. This paved the way for the SS to be tested in human individuals.

In new drug development, Phase I studies are the studies where a drug is initially given to human beings. These studies with more benign drugs often use healthy volunteers. Drugs are then initiated at very low doses and slowly escalated to show safety at a level where some biological activities take place. Later, when pharmacological and safety information is available, the drug is introduced to the patient population, again with an emphasis on safety [18]. Therefore, based on the above guidance, Phase I study of SS was carried out with healthy volunteers. According to the findings of the Phase I

safety study, there were no statistically significant ($p > 0.05$) differences in the serum parameters (ALT, AST, ALP, γ-GT, urea, creatinine, and Hb) on days 3, 8 when compared with the baseline values (day 0) (Table 7).

Hence, *Sudarshana* suspension does not affect the above parameters when administered at 6 h intervals daily for 7 consecutive days. Therefore, it was revealed that it is well tolerated by the administered human therapeutic dose.

5. Conclusion

In conclusion, the hot water extract of SP and novel preparation SS given orally to male Wistar rats and healthy volunteers did not produce toxic effect at the therapeutic dose level when compared to the control. Therefore, SP and SS can be considered to be safe drugs for oral administration.

Data Availability

The data used to support the findings of this study are available from the corresponding author upon request.

Conflicts of Interest

The authors declare that they have no any conflicts of interest regarding the publication of this manuscript.

Acknowledgments

References

[1] Department of Ayurveda, *Ayurveda Pharmaco*, Department of Ayurveda, Maharagama, Sri Lanka, 1976.

[2] W. A. S. S. Weerakoon, P. K. Perera, D. Gunasekera, and T. S. Suresh, "Evaluation of the in vitro and in vivo antioxidant potentials of sudarshana powder," *Evidence-Based Complementary and Alternative Medicine*, vol. 2018, p. 1, Article ID 6743862, 2018.

[3] R. Bhaishajya, *Chaukhamba Sanskrit Sansthan*, Sanskrit, Chaukhamba, Varanasi, 2003.

[4] B. Sitaram, *Bavaprakasha of Bavamisra, Chowkhamba Orientalia*, Vol. 1, A house of Oriental and Antiquarian books, Varanasi, India, 2012.

[5] P. Nagodavthana, *Shri Sharangadara Samhita*, Vol. 2, Kanakanwadi Mahavidyala and Hospital, Varanasi, India, 1st edition, 2001.

[6] Guidance for Industry, "Estimating the maximum safe starting dose in initial clinical trials for therapeutics in adult healthy volunteers," 2005.

[7] J. E. Hilaly, Z. H. Israili, and B. Lyoussi, "Acute and chronic toxicological studies of ajuga iva in experimental animals," *Journal of Ethnopharmacology*, vol. 91, no. 1, pp. 43–50, 2004.

[8] J. T. Mukinda and J. A. Syce, "Acute and chronic toxicity of the aqueous extract of artemisia afra in rodents," *Journal of Ethnopharmacology*, vol. 112, no. 1, pp. 138–144, 2007.

[9] D. M. Lembè, J. Domkam, P. C. O. Oundoum et al., "Acute and subacute toxicity of Fagara heitzii in experimental animals," *Molecular & Clinical Pharmacology*, vol. 2, no. 1, pp. 44–54, 2012.

[10] L. E. Daly and G. J. Bourke, *Interpretation and Uses of Medical Statics, Chapter 8: Sample Size Determination*, Blackwell Science Ltd, Oxford, UK, 5th edition, 2000.

[11] J. McIntyre and D. Hull, "Comparing efficacy and tolerability of ibuprofen and paracetamol in fever," *Archives of Disease in Childhood*, vol. 74, no. 2, pp. 164–167, 1996.

[12] E. P. Springfield, P. K. F. Eagles, and G. Scott, "Quality assessment of South African herbal medicines by means of HPLC fingerprinting," *Journal of Ethnopharmacology*, vol. 101, no. 1–3, pp. 75–83, 2005.

[13] B. Saad, H. Azaizeh, G. Abu-Hijleh, and O. Said, "Safety of traditional Arab herbal medicine," *Evidence-based Complementary and Alternative Medicine*, vol. 2006, Article ID 762642, 2006.

[14] S. E. I. Adam, "Toxic effects ofFrancoeuria crispa in rats," *Phytotherapy Research*, vol. 12, no. 7, pp. 476–479, 1998.

[15] M. L. Hayes, "Guidelines for acute oral toxicity testing," in *Principles and Methods of Toxicology*, pp. 143–152, CRC Press, Boca Raton, FL, USA, 2nd edition, 1989.

[16] V.-P. Kytridis and Y. Manetas, "Mesophyll versus epidermal anthocyanins as potential in vivo antioxidants: evidence linking the putative antioxidant role to the proximity of oxy-radical source," *Journal of Experimental Botany*, vol. 57, no. 10, pp. 2203–2210, 2006.

[17] D. C. Mc Knight, R. G. Mills, J. J. Bray, and P. A. Crag, *Human Physiology*, Churchill Livingstone, London, UK, 4th edition, 1999.

[18] J. O. Quigley, M. Pepe, and L. Fisher, "Continual reassessment method: a practical design for phase I clinical trials in cancer," *Biometrics*, vol. 46, pp. 33–48, 1990.

Research Article

Investigating the Multitarget Mechanism of Traditional Chinese Medicine Prescription for Cancer-Related Pain by Using Network Pharmacology and Molecular Docking Approach

Jinyuan Chang,[1] Lixing Liu,[1] Yaohan Wang,[1] Yutong Sui,[1] Hao Li,[2] and Li Feng [1]

[1]*National Cancer Center, National Clinical Research Center for Cancer, Cancer Hospital,*
Chinese Academy of Medical Sciences and Peking Union Medical College, Beijing 100021, China
[2]*Beijing University of Traditional Chinese Medicine, Beijing 100029, China*

Correspondence should be addressed to Li Feng; fengli663@126.com

Gu-tong formula (GTF) has achieved good curative effects in the treatment of cancer-related pain. However, its potential mechanisms have not been explored. We used network pharmacology and molecular docking to investigate the molecular mechanism and the effective compounds of the prescription. Through the analysis and research in this paper, we obtained 74 effective compounds and 125 drug-disease intersection targets to construct a network, indicating that quercetin, kaempferol, and β-sitosterol were possibly the most important compounds in GTF. The key targets of GTF for cancer-related pain were Jun proto-oncogene (JUN), mitogen-activated protein kinase 1 (MAPK1), and RELA proto-oncogene (RELA). 2204 GO entries and 148 pathways were obtained by GO and KEGG enrichment, respectively, which proved that chemokine, MAPK, and transient receptor potential (TRP) channels can be regulated by GTF. The results of molecular docking showed that stigmasterol had strong binding activity with arginine vasopressin receptor 2 (AVPR2) and C-X3-C motif chemokine ligand 1 (CX3CL1) and cholesterol was more stable with p38 MAPK, prostaglandin-endoperoxide synthase 2 (PTGS2), and transient receptor potential vanilloid-1 (TRPV1). In conclusion, the therapeutic effect of GTF on cancer-related pain is based on the comprehensive pharmacological effect of multicomponent, multitarget, and multichannel pathways. This study provides a theoretical basis for further experimental research in the future.

1. Introduction

Cancer-related pain remains common and severe for many patients, especially in the advanced stage, while the prevalence is approximately more than 70% [1]. A large number of people suffer from mild to severe pain before they die, and only few patients with cancer pain are well managed because the pain is difficult to relieve. Cancer-related pain is an aggregation of many different cancer types, which is a mixed pain representing a homogenous pathological process, mainly including acute pain, inflammatory pain, nerve pain, and tumor-induced pain [2]. Currently, the principal strategy for cancer-related pain management has been based on an ordinal three-step analgesic ladder, but its clinical use is usually limited by the side effects of gastrointestinal bleeding, constipation, respiratory depression, and so on [3, 4].

In China, the application of Gu-tong Formula (GTF) in treatment of cancer-related pain has a history of decades, and it has been a patented prescription (Patent No.: 201410415620.1). GTF is prepared from a formula of nine Chinese medicines, including Radix Aconiti Lateralis Preparata (RALP), Cortex Cinnamomi (CC), Rhizoma Curculiginis (RC), Herba Asari (HA), Rhizoma Zingiberis (RZ), Radix Clematidis (CCO), Pseudobulbus Cremastrae seu Pleiones (PCSP), Scorpio (BMK), and Flos Caryophylli (FC). Preliminary clinical trials showed that GTF can observably reduce the frequency of breakthrough cancer pain and the requirements of medication [5]. However, the related

mechanisms of its analgesic effect have not been entirely explored.

It is known that the Chinese herbal formula has a characteristic of multicomponent, multitarget, and multipathways; it means traditional experimental methods cannot detect its complex mechanisms absolutely. Network pharmacology, as a combination of pharmacology and pharmacodynamics, emphasizing the integration of disease, gene, target, and drug, has been widely used for exploring the overall effect of drugs on the treatment of diseases from a macroscopic and systematic point of view. Therefore, we adopt the network pharmacology approach to discover potential mechanisms of GTF in the treatment of cancer-related pain and use molecular docking for reverse verification.

2. Methods

2.1. Active Ingredients and Related Targets in GTF

2.1.1. Pharmacokinetic Predictions. The active ingredients in GTF (except for BMK) were acquired from the Traditional Chinese Medicine Systems Pharmacology (TCMSP) database, a platform designed for herbs. Selecting oral bioavailability (OB) ≥30% and drug-likeness (DL) ≥0.18 as the screening criteria, the acquired active ingredients were searched for related protein targets from TCMSP and DrugBank databases [6, 7]. The active ingredients in BMK were obtained from the Traditional Chinese Medicine Information Database (TCMID) [8] and BATMAN-TCM [9]. Eventually, six effective compounds of BMK were collected, which were bufotoxin, chlorotoxin, katsutoxin, cholesterol, stearin, and 20-hexadecanoylingenol. Then, the chemical structure formula of the BMK active ingredients were downloaded from the PubChem database (https://pubchem.ncbi.nlm.nih.gov/), followed by importing to the PharmMapper database [10] and selecting the effective targets with high match (norm fit > 0.7).

2.1.2. Potential Target Genes of Cancer-Related Pain. The data for the target genes of cancer-related pain were acquired from the DisGeNET database [11], GeneCards [12], and the Online Mendelian Inheritance in Man (OMIM) database [13]. All the data were standardized through the *UniProt* database [14].

(1) DisGeNET database: search strategy—Set the disease name as "crushing pain, widespread chronic pain, postoperative pain, nerve pain, and intractable pain" in the *gene disease network* interface; 64 genes were collected (Table S1).

(2) GeneCards: search strategy—Set the keyword as "cancer related pain" and the score >4 after logging into GeneCards; 1093 genes were collected (Table S2).

(3) OMIM database: search strategy—Set the keyword as "cancer-related pain"; 22 genes were collected (Table S3).

2.1.3. Drug-Disease-Target Network Construction. Intersection genes, which may treat the disease, were obtained by intersecting the drug targets and disease targets. We used Cytoscape v3.7.2 to construct the drug-compound-disease intersection gene network and then carried out topology analysis [15]. Finally, we calculated the degree value of each node in the network by *cytoHubba* plug-in to screen out key pharmacodynamic molecules [16].

2.1.4. Protein-Protein Interaction (PPI) Data and Hub Gene Screening. We imported the intersection genes into the STRING database [17], and the species were set as *Homo sapiens*. The confidence score was set ≥0.9 to construct our PPI network [18], and the acquired network was imported into Cytoscape v3.7.2. The degree value of each node in the network was calculated using *cytoHubba* plug-in, and the top 10% was selected as the hub gene. Then, the biological process of GO was analyzed for the hub gene.

2.2. Enrichment Analysis

2.2.1. Gene Ontology (GO) and Kyoto Encyclopedia of Genes and Genomes (KEGG) Pathway Enrichment Analysis. ClusterProfiler package was used to perform GO and KEGG enrichment analysis of the intersection gene with $p < 0.05$ [19].

2.2.2. Molecular Docking Verification. AutoDock was used to perform the receptor-ligand docking simulation calculation of key pharmacodynamic molecules and screened core targets. The protein structure, downloaded from the PDB database, was imported into POCASA v1.1 [20]. Meanwhile, the position of the active site was investigated in the PubMed database to verify the predicted position by POCASA v1.1. The docking operation used the Lamarckian genetic algorithm, and the rigid receptor-flexible ligand docking pattern was used in the docking process. The number of runs was 50, and the maximum energy evaluation was 2,500,000 [21]. The ligand corresponding to the target protein was used as a positive control. After all the docking simulations were completed, heat maps were made according to the strongest affinity of key pharmacodynamic molecules and core targets.

3. Results and Discussion

In this study, we obtained 74 active compounds (Table S4) and 269 potential targets of GTF after deleting duplicates. The active compound-related targets in TCMSP and PharmMapper databases are listed in Tables S5 and S6, respectively. 1144 potential target genes of cancer-related pain were collected, and we obtained 125 drug-disease intersection targets (Figure 1(a)).

3.1. GTF Drug-Disease-Target Network. The intersection targets were imported into Cytoscape v3.7.2 to construct a drug-disease-target network (Figure 1(b)), including 163 nodes and 296 edges, with a network heterogeneity of 2.336
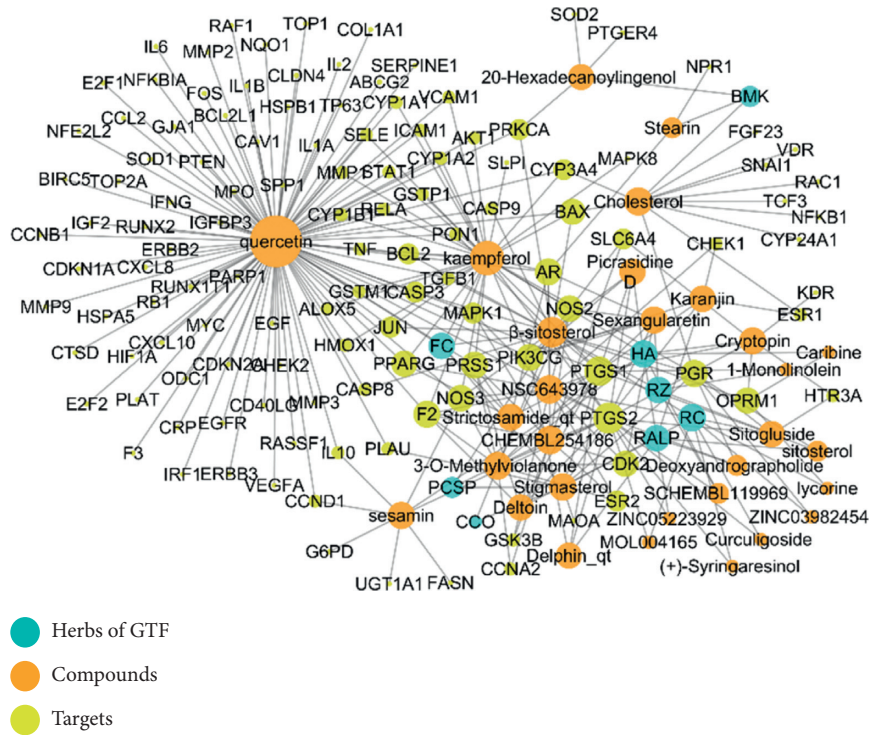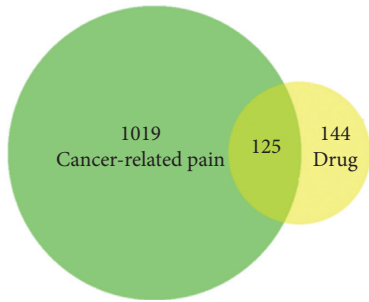
(a)

(b)
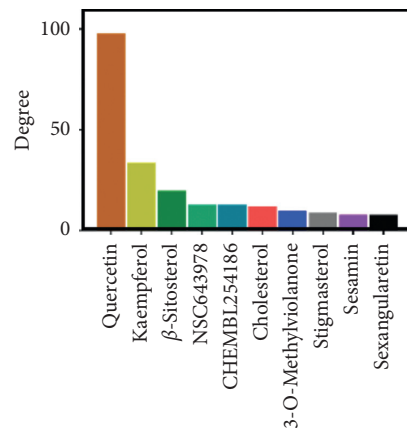
(c)

Figure 1: (a) Venn map of disease-related targets and drug targets. (b) Gu-tong formula (GTF) drug-disease-target network. Radix Aconiti Lateralis Preparata (RALP), Cortex Cinnamomi (CC), Rhizoma Curculiginis (RC), Herba Asari (HA), Rhizoma Zingiberis (RZ), Radix Clematidis (CCO), Pseudobulbus Cremastrae seu Pleiones (PCSP), Scorpio (BMK), and Flos Caryophylli (FC). (c) The top ten key pharmacodynamic molecules with the degree value.

and a network centralization of 0.590. It indicated that some nodes in the network were more concentrated than others. The network showed that compounds with most high connectivity were quercetin (degree = 98), kaempferol (degree = 34), and β-sitosterol (degree = 20), which were sorted by the degree value, suggesting that these three compounds were possibly the most important compounds in GTF (Figure 1(c)). Quercetin and kaempferol are flavonoids, and β-sitosterol is a phytosterol. All of them can regulate the way of cell apoptosis, proliferation, and phosphoinositide 3-kinase (PI3K)/protein kinase B (AKT) pathways to achieve the purpose of antitumor [22–24].

Moreover, they also have a strong inhibitory effect on inflammation through the inhibition of lipoxygenase and cyclooxygenase pathways. Among them, kaempferol has been used as a chemosensitizer in clinical research and has the potential of reducing toxicity and enhancing efficacy [25].

We preliminary analyzed the targets of the compounds in the network. NPR1 with a 0.672 disease-specific index (DSI) was targeted by stearin (extracted from BMK) and was important in crushing pain. ORPM1, which was targeted by β-sitosterol (extracted from FC, RZ, PCSP, CCO, and RC), caribine, cryptopine (extracted from HA), and lycorine

(extracted from RC), played an important role in nerve pain, and its DSI was 0.479. The DSI of CXCL8 targeted by quercetin (extracted from FC) in intractable pain was 0.342. These three types of pain were crucial in cancer-related pain.

3.2. PPI Network.

The intersection targets were imported into the STRING 11.0 database, and then, 104 nodes and 324 edges can be obtained, with an average degree of 5.18 for each node and an average neighbor of 6.231 for each edge (Figure 2(a)). As shown in Figure 2(b), the hub genes in the network screened by *cytoHubba* plug-in were JUN (degree = 28), MAPK1 (degree = 25), RELA (degree = 22), etc. Among them, RELA, RB1, NFKB1, TNF, and ESR1 had the function of regulating inflammatory response (GO: 0050727) and cellular response to reactive oxygen species (GO: 0034614). JUN, AKT1, FOS, and MAPK8 played the role of response to mechanical stimulus (GO: 0009612).

TNF mainly encoded a multifunctional proinflammatory cytokine, combination with the transient receptor potential vanilloid-1 (TRPV1), playing an important role in inflammatory pain and nerve pain [26, 27]. Downregulating TNF expression can effectively inhibit the occurrence of inflammatory pain and nerve pain [28]. Moreover, MAPK8, JUN, AKT1, and RELA can regulate cell proliferation and cell cycle, which was crucial in tumorigenesis. GTF can regulate the expression of these genes to affect the development of tumors.

3.3. GO Enrichment.

To further explore the multiple mechanisms of GTF, GO enrichment analysis (take biological process for example) was performed (Figure 3), and 2204 GO entries were enriched.

We found that GTF was involved in regulating the production of neuronal action potential via the regulation of membrane potential (GO: 0042391) and synaptic transmission (GO: 0050805). The activation of neurons and the conduction of electrical signals were the fundamental causes of nerve sensitization and pain [29]. GTF inhibited the conduction of pain by means of controlling the transmission of neurotransmitters to maintain the stability of the postsynaptic membrane.

What is more, GTF inhibited the secretion of inflammatory factors in the inflammatory response by means of regulating the prostaglandin (PG) biosynthetic process (GO: 0031392), cyclooxygenase pathway (GO: 0019371), inflammatory response (GO: 0050728), and cytokine production (GO: 0001818). Among them, PG induced inflammation and hyperalgesia, leading to the occurrence and aggravation of pain. In the first stage of three-step pain relief, it achieved the purpose of pain relief by inhibiting the target and cyclooxygenase pathway [2]. GTF also played a role in this pathway and the target and inhibited the occurrence of inflammatory pain. Moreover, it relieved the pain caused by tumor compression and sensitivity to cold stimulation after chemotherapy via the response to mechanical stimulus (GO: 0009612) and cold (GO: 0009409). Activation of the MAPK pathway was crucial in the development of pain [30], and

GTF-negative regulated the MAPK cascade (GO: 0043409) to restrain the occurrence of pain.

Cancer-related pain caused by bone metastasis and bone destruction is usually difficult to relieve [31]. It was believed that bone resorption and bone formation were the key factors of bone destruction caused by tumor [32]. Interestingly, we found that GTF protected bones through regulation of ossification (GO: 0030278), bone resorption (GO: 0045124), and remodeling (GO: 0046849). Detailed GO enrichment information is shown in Table 1. The multitarget and multifunctional characteristics of GTF played a certain role in alleviation of cancer-related pain by regulating nerves, reducing inflammation and mechanical stimulation, and protecting bone.

3.4. KEGG Enrichment.

We obtained 148 pathways in total, which belonged to several categories, including tumor, inflammation, infection, and other pathways. After analyzing the results of KEGG enrichment, we found that GTF mainly focused on the regulation of proinflammatory cytokines, damage associated molecular pattern (DAMP), neural sensitization, and pain-related protein kinase (Table 2).

GTF can regulate the synthesis and secretion of inflammatory factors by regulating IL-17 (hsa04657), TNF (hsa04668), and chemokine signaling pathways (hsa04062). IL-17, secreted by $CD4^+$ T cells, can induce epithelial cells and endothelial cells to synthesize IL-6, PG, and other cytokines, and combination with the TNF signaling pathway to promote inflammation [33]. Inhibition of IL-17 can effectively relieve pain and inhibit peripheral nerve sensitization [34]. C-X3-C motif chemokine ligand 1 (CX3CL1) is a kind of chemokine. It was found that CX3CL1 and its receptor CX3CR1 were very important in the development of neuropathic pain [35]. Soluble CX3CL1 bound to CX3CR1 on the surface of microglia, which lead to the increase of intracellular calcium concentration and the occurrence of neuropathic pain [36, 37]. In the study of network pharmacology of GTF, it was shown that the application of GTF can affect those pathways and inhibit the occurrence of pain. At the same time, we found that GTF can regulate the response of the body to DAMP by regulating Toll-like receptor (hsa04620), NOD-like receptor (hsa04621), and RIG-I-like receptor signaling pathways (hsa04622). It had been proven that Toll-like receptors were highly expressed in microglia of mice with neuropathy. When the Toll-like receptor signaling pathway was inhibited, it can effectively inhibit the occurrence of pain [38].

In the aspect of neurotransmitter transmission and central sensitization, GTF can regulate the release of neurotransmitters and maintain the stability of neuron membrane potential by influencing serotonergic (hsa04726) and dopaminergic synapse (hsa04728). Transient receptor potential (TRP) was widely distributed in nociceptive neurons and was related to the persistence of pain [39]. GTF regulated this pathway (hsa04750) to affect pain duration.

p38 MAPK was widely distributed in the spinal dorsal horn and can be activated by various external stimuli such as trauma stimulation and inflammatory factors [40] and
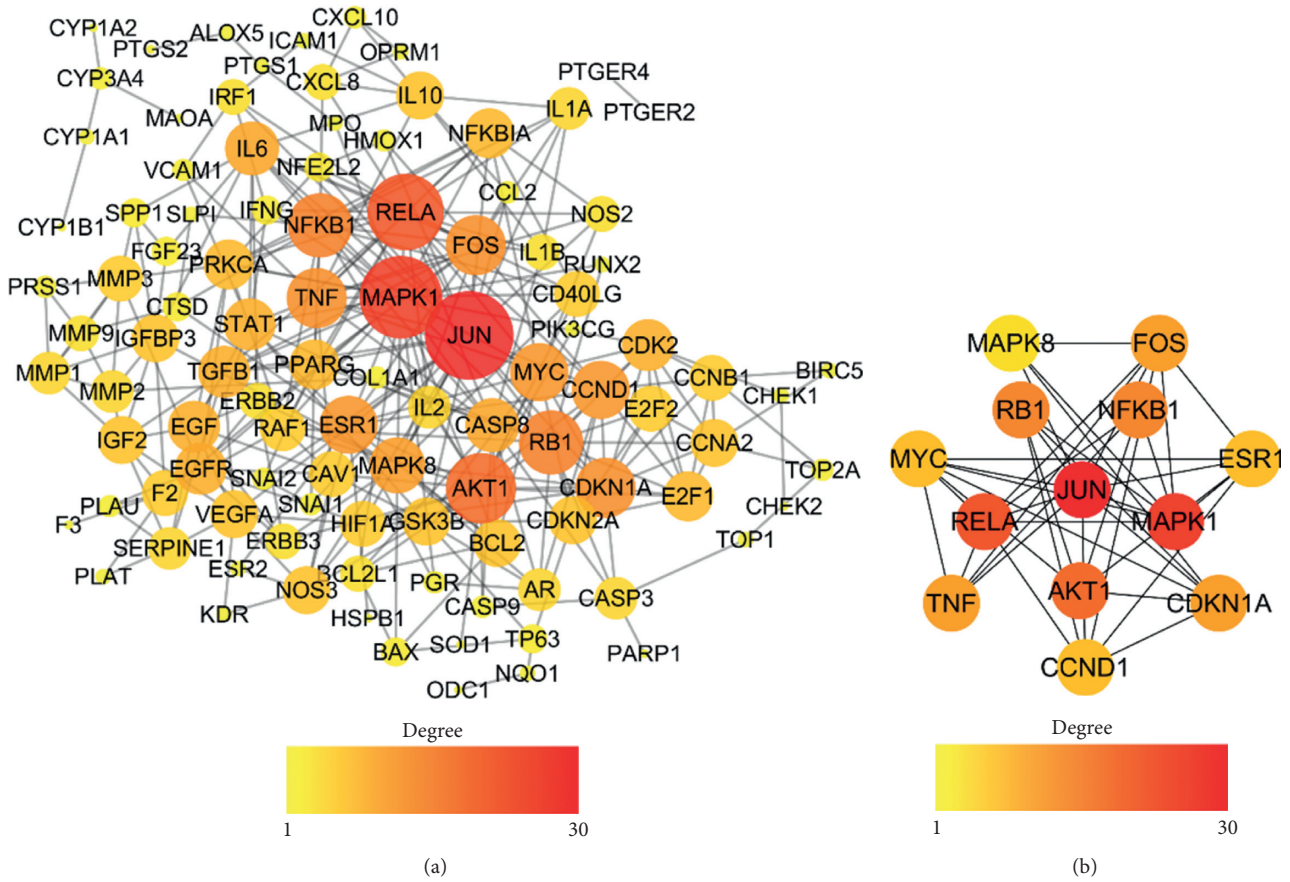
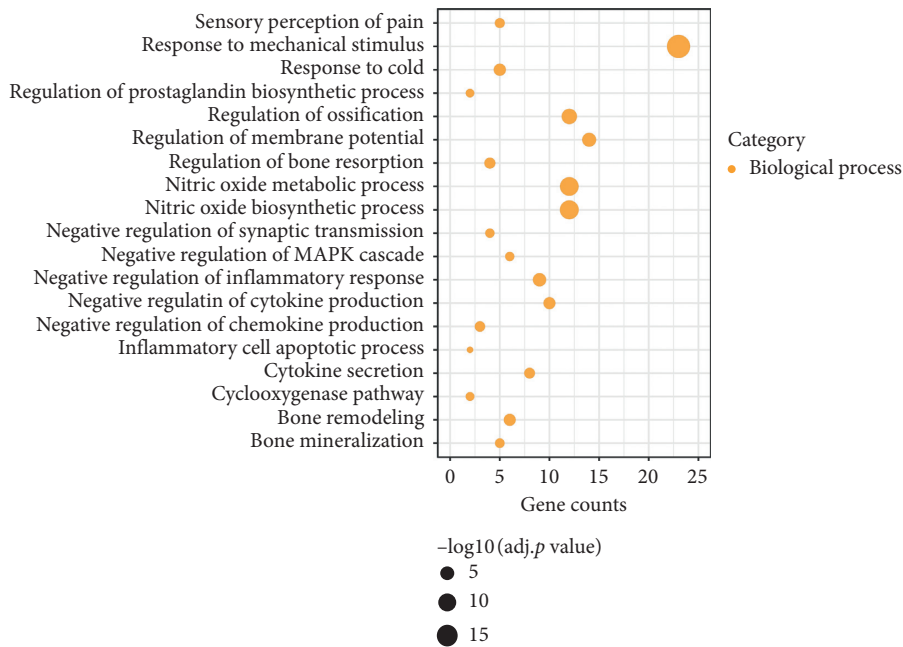Figure 2: (a) PPI network of the intersection targets. (b) The hub genes in the PPI network.

Figure 3: Gene Ontology (GO) enrichment result of GTF in treatment of cancer-related pain. The size of the bubble represents the different adjusted *p* value.

Table 1: Gene Ontology (GO) enrichment result.

ID	Description	p value	Count
GO:0009612	Response to mechanical stimulus	2.60×10^{-19}	23
GO:0006809	Nitric oxide biosynthetic process	5.86×10^{-12}	12
GO:0046209	Nitric oxide metabolic process	1.24×10^{-11}	12
GO:0030278	Regulation of ossification	1.55×10^{-7}	12
GO:0042391	Regulation of membrane potential	3.96×10^{-6}	14
GO:0050728	Negative regulation of inflammatory response	1.41×10^{-5}	9
GO:0009409	Response to cold	1.09×10^{-4}	5
GO:0001818	Negative regulation of cytokine production	1.52×10^{-4}	10
GO:0046849	Bone remodeling	1.55×10^{-4}	6
GO:0045124	Regulation of bone resorption	5.98×10^{-4}	4
GO:0050663	Cytokine secretion	8.37×10^{-4}	8
GO:0032682	Negative regulation of chemokine production	1.27×10^{-3}	3
GO:0019233	Sensory perception of pain	2.17×10^{-3}	5
GO:0030282	Bone mineralization	3.11×10^{-3}	5
GO:0050805	Negative regulation of synaptic transmission	4.09×10^{-3}	4
GO:0043409	Negative regulation of MAPK cascade	4.39×10^{-3}	6
GO:0019371	Cyclooxygenase pathway	6.38×10^{-3}	2
GO:0031392	Regulation of prostaglandin biosynthetic process	7.40×10^{-3}	2
GO:0006925	Inflammatory cell apoptotic process	2.02×10^{-2}	2

Table 2: Kyoto Encyclopedia of Genes and Genomes (KEGG) enrichment result.

ID	KEGG pathway	p value	Count
hsa04657	IL-17 signaling pathway	4.64×10^{-18}	21
hsa04668	TNF signaling pathway	9.66×10^{-18}	22
hsa04620	Toll-like receptor signaling pathway	4.63×10^{-12}	16
hsa04010	MAPK signaling pathway	3.76×10^{-11}	24
hsa04621	NOD-like receptor signaling pathway	2.40×10^{-7}	15
hsa04630	JAK-STAT signaling pathway	3.94×10^{-7}	14
hsa04726	Serotonergic synapse	2.15×10^{-5}	10
hsa04622	RIG-I-like receptor signaling pathway	2.35×10^{-5}	8
hsa04062	Chemokine signaling pathway	6.33×10^{-5}	12
hsa04728	Dopaminergic synapse	2.40×10^{-2}	6
hsa04750	Inflammatory mediator regulation of TRP channels	2.84×10^{-2}	5

participated in the occurrence of pain through phosphorylated voltage-gated sodium channels. The JAK-STAT pathway was activated by interleukin-6 (IL-6) involving in the occurrence of inflammation and pain [41]. GTF can regulate the release of PG and excitatory amino acids by regulating these two pathways, to reduce cancer pain.

3.5. Molecular Docking. POCASA v1.1 was used to predict the most likely docking pocket of protein, which was sorted according to the volume of the pocket (Figure S1, docking pocket from large to small: a–e). In addition, compared with the active sites reported in the PubMed database, the docking sites of protein targets were obtained. The detailed information for core protein is listed in Table S7.

Figure 4 shows the mapping of the strongest affinity of 10 key drug molecules and 10 core target proteins. We found that the binding energy between the molecule and the target protein was approximately between -3.59 and -9.43 kcal·mol^{-1}. It can be seen from Figure 4 that AVPR2, CX3CL1, p38 MAPK, prostaglandin-endoperoxide synthase 2 (PTGS2), and TRPV1 have stronger docking energy. It means that the compounds in GTF bind well to the above target proteins.

Arginine vasopressin (AVP), an important analgesic substance, can be synthesized and secreted by the paraventricular nucleus of the hypothalamus [42]. After external stimulation, the expression of AVP increased and transported to the midbrain aqueduct gray matter, nucleus raphe magnus, caudate nucleus, and other related nuclei, resulting in the secretion of endogenous opioid peptide, 5-hydroxytryptamine and acetylcholine, and activating vasopressin receptors in central and peripheral tissues, which played a crucial role in nociception. Studies had shown that high dose of AVP can increase the action potential of C-type nociceptive fibers and produce analgesic effect [43]. The receptors of AVP, including V1a, V1b, and V2, belong to G protein-coupled receptor [44]. The compounds contained in GTF can stably bind to G protein-coupled receptor, producing analgesic effect.

CX3CL1 and its receptor CX3CR1 were both expressed in the nervous system [35] and played a role in promoting the occurrence of pain, which had been confirmed in many experiments. The researchers believed that the painful behavior caused by CX3CL1 was achieved by exciting CX3CR1 on microglia and activating the p38 MAPK signaling pathway [45]. Interestingly, our molecular docking results

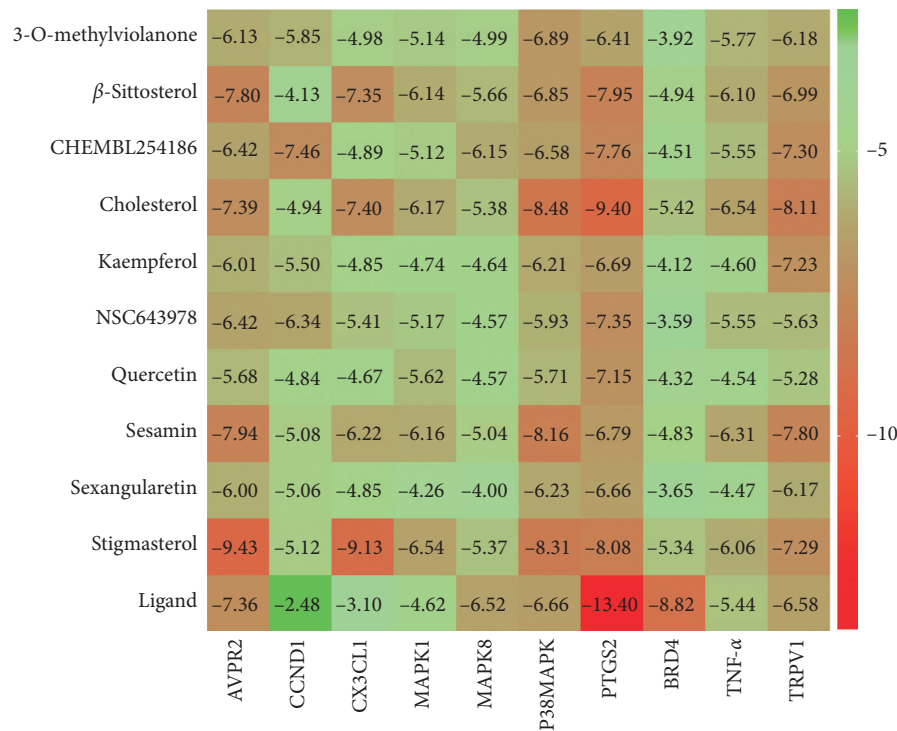|	AVPR2	CCND1	CX3CL1	MAPK1	MAPK8	P38MAPK	PTGS2	BRD4	TNF-α	TRPV1
3-O-methylviolanone	−6.13	−5.85	−4.98	−5.14	−4.99	−6.89	−6.41	−3.92	−5.77	−6.18
β-Sittosterol	−7.80	−4.13	−7.35	−6.14	−5.66	−6.85	−7.95	−4.94	−6.10	−6.99
CHEMBL254186	−6.42	−7.46	−4.89	−5.12	−6.15	−6.58	−7.76	−4.51	−5.55	−7.30
Cholesterol	−7.39	−4.94	−7.40	−6.17	−5.38	−8.48	−9.40	−5.42	−6.54	−8.11
Kaempferol	−6.01	−5.50	−4.85	−4.74	−4.64	−6.21	−6.69	−4.12	−4.60	−7.23
NSC643978	−6.42	−6.34	−5.41	−5.17	−4.57	−5.93	−7.35	−3.59	−5.55	−5.63
Quercetin	−5.68	−4.84	−4.67	−5.62	−4.57	−5.71	−7.15	−4.32	−4.54	−5.28
Sesamin	−7.94	−5.08	−6.22	−6.16	−5.04	−8.16	−6.79	−4.83	−6.31	−7.80
Sexangularetin	−6.00	−5.06	−4.85	−4.26	−4.00	−6.23	−6.66	−3.65	−4.47	−6.17
Stigmasterol	−9.43	−5.12	−9.13	−6.54	−5.37	−8.31	−8.08	−5.34	−6.06	−7.29
Ligand	−7.36	−2.48	−3.10	−4.62	−6.52	−6.66	−13.40	−8.82	−5.44	−6.58

Figure 4: The binding energy of 10 key drug molecules and 10 target proteins.

showed that GTF had better binding effect with CX3CL1 and p38 MAPK. In the pain model of bone tumor in rats made by injecting Walker 256 breast cancer cells into the tibial marrow cavity, intrathecal injection of CX3CR1 neutralizing antibody can reduce the development of pain and hyperalgesia, and blocking CX3CR1 can inhibit the activation of spinal microglia and the phosphorylation level of p38 MAPK [46]. It indicated the role of CX3CL1/CX3CR1/p38 MAPK pathway in the formation and development of cancer pain. This further showed that GTF can affect the occurrence and development of pain by regulating the above pathways.

PTGS2, also known as cyclooxygenase-2 (COX-2), was the second isozyme of cyclooxygenase. COX was an important rate-limiting enzyme for PG. COX-2 can be induced by a variety of inflammatory mediators and cytokines and participated in tissue inflammation and cell differentiation and proliferation. Upregulation of COX-2 was also related to antiapoptosis and tumor angiogenesis [47]. The results of molecular docking showed that the pharmacodynamic molecules selected in GTF had stronger binding energy to COX-2, which meant that the active ingredients in GTF can regulate the development of inflammatory pain and tumors through COX-2.

TRPV1 was a heat-activated cation channel protein, which was expressed on primary afferent neurons and upregulated after inflammation and nerve injury and was closely related to inflammation and acute and chronic pain [48]. Inhibition of TRPV1 activity was one of the pain treatment methods. In the preclinical study, it has the potential to be a receptor of nonopioid analgesics [49]. The results of molecular docking showed that the compounds contained in GTF can better combine with TRPV1 and played an analgesic role.

According to the docking energy results, we selected the 2 compounds with the strongest protein docking results from the 5 proteins, respectively. Stigmasterol had the strongest affinity with AVPR2, CX3CL1, and cholesterol with PTGS2, p38 MAPK, and TRPV1. The binding patterns of compounds and proteins were plotted, and then the interaction between compounds and binding sites and surrounding amino acid residues was observed (Figure 5). Cholesterol and stigmasterol both occupied the docking pocket of the protein and bound stably. The analysis of the docking effect of compounds and receptor proteins is shown in Table 3.

All the five protein targets are able to form hydrophobic interaction and van der Waals force with compounds and stable binding. Stigmasterol (with AVPR2 and CX3CL1) and cholesterol (with p38 MAPK and TRPV1) can form hydrogen bonds on Gly87, His162, Leu171, and Arg557 residues, respectively, which made the binding more robust. CX3CL1 (with stigmasterol) and PTGS2 (with cholesterol) can form Pi-Sigma interaction on His3 and His389 residues, respectively, which increased the binding stability.

Stigmasterol is a common phytosterol. Modern pharmacological studies showed that it can effectively relieve acute and chronic pain and had neuroprotective effect on ischemic/reperfusion injury and good anti-inflammatory effect [50, 51]. In the process of molecular docking, the stigmasterol also had strong binding activity with AVPR2 and CX3CL1. It also suggested that stigmasterol in GTF was also an effective component in relieving cancer pain.

Cholesterol, widely consisted in vivo, a precursor of neurosteroid biosynthesis, is an endogenous produced molecule that inhibits TRPV1 activity and plays an

(a)

(b)

(c)

(d)

(e)
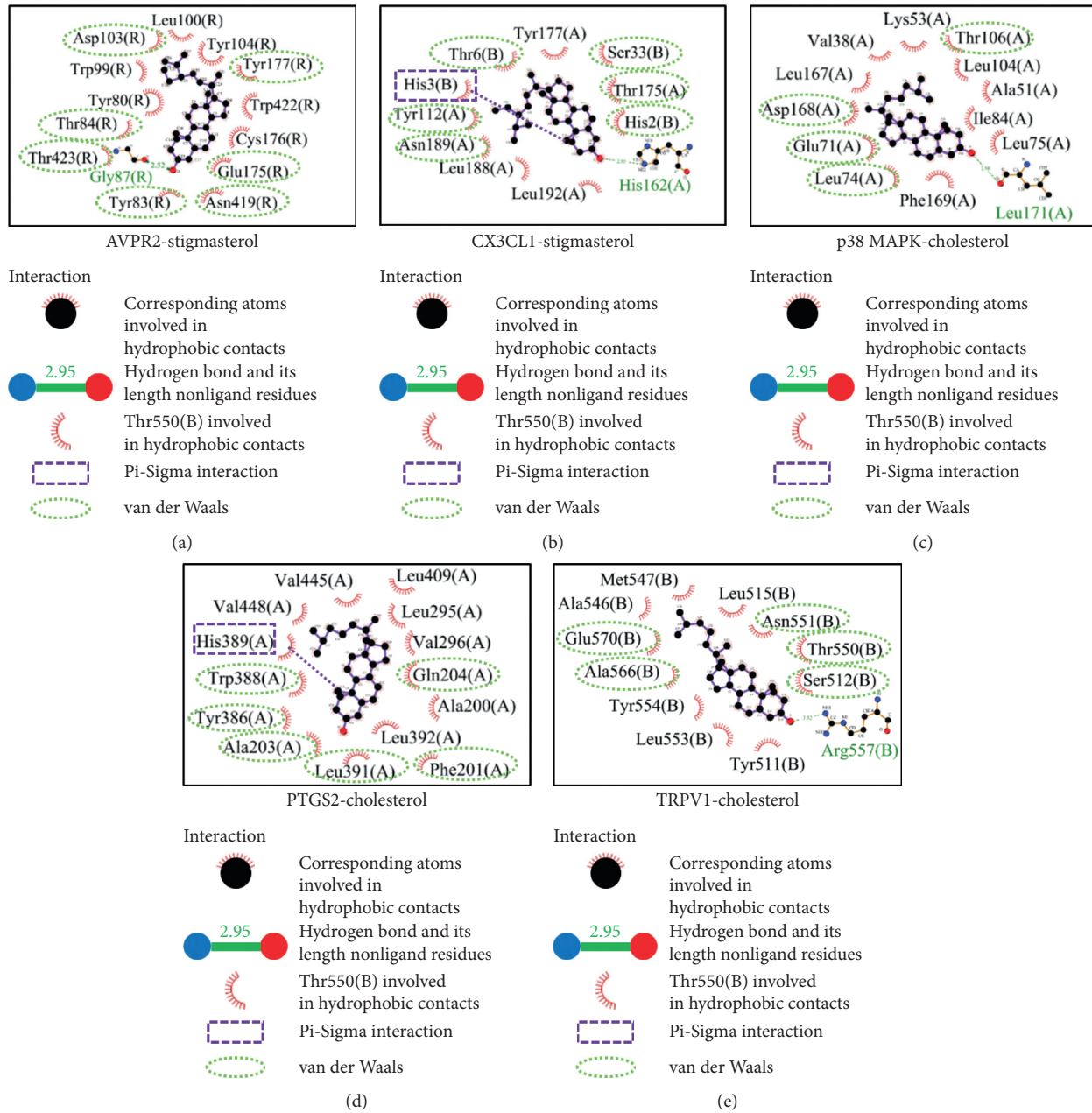
FIGURE 5: Binding mode of protein and compounds.

TABLE 3: Docking effect analysis of compounds and targets.

Compound	Target	Binding energy (kcal/mol)	Hydrogen bonding interaction	Hydrophobic interaction
Stigmasterol	AVPR2	−9.43	Cly87	Tyr80, Tyr83, Tyr84, Trp99, Leu100, Asp103, Tyr104, Glu175, Cys176, Tyr177, Asn419, Trp422, Thr423
	CX3CL1	−9.13	His162	Chain (A): Tyr112, Thr175, Tyr177, Leu188, Asn189, Leu192; China (B): His2, His3, Thr6, Ser33
	p38 MAPK	−8.48	Leu171	Val38, Ala51, Lys53, Glu71, Leu74, Leu75, Ile84, Leu104, Thr106, Leu167, Asp168, Phe169
Cholesterol	PTGS2	−9.4	Not formed	Ala200, Phe201, Ala203, Gln204, Leu295, Val296, Tyr386, Tyr388, His389, Leu391, Leu392, Leu409, Val445, Val448
	TRPV1	−8.11	Arg557	Tyr511, Ser512, Leu515, Ala546, Met547, Thr550, Asn551, Leu553, Tyr554, Ala566, Glu570

important role in the regulation of nervous system injury and disorder [52]. Little is known about its role in neuropathic pain. Recent studies have shown that in inflammatory animal models, transcutaneous cholesterol delivery can alleviate allergic reactions and cholesterol homeostasis can help regulate inflammation and pain [53]. Increasing cholesterol content can inhibit the expression of PTGS2 and the secretion of PG [54], while decreasing cholesterol content can enhance p38 MAPK and inflammatory activity [55]. In molecular docking research, we found that cholesterol contained in GTF can stably target PTGS2, p38 MAPK, and TRPV1, which may play an analgesic role through MAPK and chemokine pathways.

4. Conclusion

To sum up, we revealed the potential pharmacological mechanism of GTF in the treatment of cancer pain from a systematic perspective, which may involve the secretion of inflammatory cytokines, membrane potential, bone protection, and other biological processes by regulating chemokine, MAPK, and TRP channels. The cholesterol and stigmasterol in GTF can be the key pharmacodynamic molecules for analgesia in molecular docking screening. This study provides clues for understanding the synergistic effect of GTF in relieving cancer pain. However, considering that this study is mainly based on data analysis and molecular docking, further experiments are necessary to verify the results.

Abbreviations

GTF: Gu-tong formula
JUN: Jun proto-oncogene
MAPK: Mitogen-activated protein kinase
RELA: RELA proto-oncogene
AVPR2: Arginine vasopressin receptor 2
CX3CL1: C-X3-C motif chemokine ligand 1
PTGS2: Prostaglandin-endoperoxide synthase 2
TRPV1: Transient receptor potential vanilloid-1
RALP: Radix Aconiti Lateralis Preparata
CC: Cortex Cinnamomi
RC: Rhizoma Curculiginis
HA: Herba Asari
RZ: Rhizoma Zingiberis
CCO: Radix Clematidis
PCSP: Pseudobulbus Cremastrae seu Pleiones
BMK: Scorpio
FC: Flos Caryophylli
TCMSP: Traditional Chinese Medicine Systems Pharmacology
OB: Bioavailability
DL: Drug-likeness
TCMID: Traditional Chinese Medicine Information Database
BATMAN-TCM: A Bioinformatics Analysis Tool for Molecular mechANism of Traditional Chinese Medicine
OMIM: Online Mendelian Inheritance in Man
PPI: Protein-protein interaction
GO: Gene Ontology
KEGG: Kyoto Encyclopedia of Genes and Genomes
PI3K/AKT: Phosphoinositide 3-kinase/protein kinase B
PG: Prostaglandin
DSI: Disease-specific index
NPR1: Natriuretic peptide receptor 1
OPRM1: Opioid receptor mu 1
CXCL8: Interleukin-8
RB1: Retinoblastoma-associated protein
CDKN1A: Cyclin-dependent kinase inhibitor 1
FOS: Proto-oncogene c-Fos
TNF: Tumor necrosis factor
ESR1: Estrogen receptor
MYC: Myc proto-oncogene protein
DAMP: Damage associated molecular pattern
IL-6: Interleukin-6
JAK-STAT: Janus kinase-signal transducer and activator of transcription
COX-2: Cyclooxygenase-2.

Data Availability

The data used to support the findings of this study are included within the article and the supplementary information files.

Conflicts of Interest

The authors declare that they have no conflicts of interest.

Authors' Contributions

Li Feng conceived and designed the research. Jinyuan Chang collected the data and drafted the manuscript. Lixing Liu, Yaohan Wang, and Hao Li analyzed the data and provided valuable suggestions on the investigation. Yutong Sui critically reviewed the manuscript and assisted in the final write-up of the manuscript. All authors read and approved the final manuscript.

Acknowledgments

Supplementary Materials

Figure S1. The docking pocket of target proteins predicted by POCASA v1.1, and the order of pocket volume is from large to small: a–e. Table S1. The targets of cancer-related pain in DisGeNET. Table S2. The targets of cancer-related pain in GeneCards. Table S3. The targets of cancer-related pain in OMIM. Table S4. All the GTF compounds. Table S5. Potential targets of GTF compounds downloaded from TCMSP database. Table S6. Potential targets of BMK active

compounds downloaded from PharmMapper database. Table S7. The PDB information for core protein. (*Supplementary Materials*)

References

[1] R. K. Portenoy, "Treatment of cancer pain," *The Lancet*, vol. 377, no. 9784, pp. 2236–2247, 2011.

[2] M. Fallon, R. Giusti, F. Aielli et al., "Management of cancer pain in adult patients: ESMO clinical practice guidelines," *Annals of Oncology*, vol. 29, no. 4, pp. iv166–iv191, 2018.

[3] E. Eisenberg, C. S. Berkey, D. B. Carr, F. Mosteller, and T. C. Chalmers, "Efficacy and safety of nonsteroidal antiinflammatory drugs for cancer pain: a meta-analysis," *Journal of Clinical Oncology*, vol. 12, no. 12, pp. 2756–2765, 1994.

[4] J. Gaertner, U. M. Stamer, C. Remi et al., "Metamizole/dipyrone for the relief of cancer pain: a systematic review and evidence-based recommendations for clinical practice," *Palliative Medicine*, vol. 31, no. 1, pp. 26–34, 2017.

[5] J. Tian, *Clinical Observation of Bone-Pain Plaster in the Treatment of Cancerous Somatic Pain of Yin Cold Stagnation Type Master*, Beijing University of Traditional Chinese Medicine, Beijing, China, 2015, https://kns.cnki.net/kcms/detail/detail.aspx?FileName=1015386149.nh&DbName=CMFD2015.

[6] J. Ru, P. Li, J. Wang et al., "TCMSP: a database of systems pharmacology for drug discovery from herbal medicines," *Journal of Cheminformatics*, vol. 6, no. 1, p. 13, 2014.

[7] D. S. Wishart, Y. D. Feunang, A. Marcu et al., "HMDB 4.0: the human metabolome database for 2018," *Nucleic Acids Research*, vol. 46, no. D1, pp. D608–D617, 2018.

[8] R. Xue, Z. Fang, M. Zhang, Z. Yi, C. Wen, and T. Shi, "TCMID: traditional Chinese medicine integrative database for herb molecular mechanism analysis," *Nucleic Acids Research*, vol. 41, pp. D1089–D1095, 2013.

[9] Z. Liu, F. Guo, Y. Wang et al., "BATMAN-TCM: a bioinformatics analysis tool for molecular mechanism of traditional Chinese medicine," *Scientific Reports*, vol. 6, no. 1, p. 21146, 2016.

[10] X. Wang, Y. Shen, S. Wang et al., "PharmMapper 2017 update: a web server for potential drug target identification with a comprehensive target pharmacophore database," *Nucleic Acids Research*, vol. 45, no. W1, pp. W356–W360, 2017.

[11] J. Piñero, J. M. Ramírez-Anguita, J. Saüch-Pitarch et al., "The DisGeNET knowledge platform for disease genomics: 2019 update," *Nucleic Acids Research*, vol. 48, no. D1, pp. D845–D855, 2020.

[12] G. Stelzer, N. Rosen, I. Plaschkes et al., "The GeneCards suite: from gene data mining to disease genome sequence analyses," *Current Protocols in Bioinformatics*, vol. 54, no. 1, p. 1, 2016.

[13] A. Hamosh, A. F. Scott, J. Amberger, D. Valle, and V. A. McKusick, "Online mendelian inheritance in man (OMIM)," *Human Mutation*, vol. 15, no. 1, pp. 57–61, 2000.

[14] The UniProt Consortium, "UniProt: a worldwide hub of protein knowledge," *Nucleic Acids Research*, vol. 47, no. D1, pp. D506–D515, 2019.

[15] D. Otasek, J. H. Morris, J. Bouças, A. R. Pico, and B. Demchak, "Cytoscape automation: empowering workflow-based network analysis," *Genome Biology*, vol. 20, no. 1, p. 185, 2019.

[16] C.-H. Chin, S.-H. Chen, H.-H. Wu, C.-W. Ho, M.-T. Ko, and C.-Y. Lin, "CytoHubba: identifying hub objects and subnetworks from complex interactome," *BMC Systems Biology*, vol. 8, no. 4, p. S11, 2014.

[17] D. Szklarczyk, A. L. Gable, D. Lyon et al., "STRING v11: protein-protein association networks with increased coverage, supporting functional discovery in genome-wide experimental datasets," *Nucleic Acids Research*, vol. 47, no. D1, pp. D607–D613, 2019.

[18] Y. Song, H. Wang, Y. Pan, and T. Liu, "Investigating the multi-target pharmacological mechanism of hedyotis diffusa willd acting on prostate cancer: a network pharmacology approach," *Biomolecules*, vol. 9, no. 10, p. 591, 2019.

[19] G. Yu, L.-G. Wang, Y. Han, and Q.-Y. He, "Clusterprofiler: an R package for comparing biological themes among gene clusters," *Omics: A Journal of Integrative Biology*, vol. 16, no. 5, pp. 284–287, 2012.

[20] J. Yu, Y. Zhou, I. Tanaka, and M. Yao, "Roll: a new algorithm for the detection of protein pockets and cavities with a rolling probe sphere," *Bioinformatics*, vol. 26, no. 1, pp. 46–52, 2010.

[21] G. M. Morris, R. Huey, W. Lindstrom et al., "AutoDock4 and AutoDockTools4: automated docking with selective receptor flexibility," *Journal of Computational Chemistry*, vol. 30, no. 16, pp. 2785–2791, 2009.

[22] A. Rauf, M. Imran, I. A. Khan et al., "Anticancer potential of quercetin: a comprehensive review," *Phytotherapy Research*, vol. 32, no. 11, pp. 2109–2130, 2018.

[23] M. Imran, B. Salehi, J. Sharifi-Rad et al., "Kaempferol: a key emphasis to its anticancer potential," *Molecules*, vol. 24, no. 12, p. 2277, 2019.

[24] S. M. Bin Sayeed and S. S. Ameen, "Beta-sitosterol: a promising but orphan nutraceutical to fight against cancer," *Nutrition and Cancer*, vol. 67, no. 8, pp. 1214–1220, 2015.

[25] Q. Li, L. Wei, S. Lin, Y. Chen, J. Lin, and J. Peng, "Synergistic effect of kaempferol and 5fluorouracil on the growth of colorectal cancer cells by regulating the PI3K/Akt signaling pathway," *Molecular Medicine Reports*, vol. 20, no. 1, pp. 728–734, 2019.

[26] M. Leo, M. Schulte, L. I. Schmitt, M. Schäfers, C. Kleinschnitz, and T. Hagenacker, "Intrathecal resiniferatoxin modulates TRPV1 in DRG neurons and reduces TNF-induced pain-related behavior," *Mediators of Inflammation*, vol. 2017, Article ID 2786427, 8 pages, 2017.

[27] R. Li, C. Zhao, M. Yao, Y. Song, Y. Wu, and A. Wen, "Analgesic effect of coumarins from radix angelicae pubescentis is mediated by inflammatory factors and TRPV1 in a spared nerve injury model of neuropathic pain," *Journal of Ethnopharmacology*, vol. 195, pp. 81–88, 2017.

[28] D. Zhao, D. F. Han, S. S. Wang, B. Lv, X. Wang, and C. Ma, "Roles of tumor necrosis factor-α and interleukin-6 in regulating bone cancer pain via TRPA1 signal pathway and beneficial effects of inhibition of neuro-inflammation and TRPA1," *Molecular Pain*, vol. 15, pp. 1–10, 2019.

[29] I. Gilron, R. Baron, and T. Jensen, "Neuropathic pain: principles of diagnosis and treatment," *Mayo Clinic Proceedings*, vol. 90, no. 4, pp. 532–545, 2015.

[30] L. Al-Olabi, S. Polubothu, K. Dowsett et al., "Mosaic RAS/MAPK variants cause sporadic vascular malformations which respond to targeted therapy," *Journal of Clinical Investigation*, vol. 128, no. 11, p. 5185, 2018.

[31] M. Futakuchi, K. Fukamachi, and M. Suzui, "Heterogeneity of tumor cells in the bone microenvironment: mechanisms and therapeutic targets for bone metastasis of prostate or breast cancer," *Advanced Drug Delivery Reviews*, vol. 99, pp. 206–211, 2016.

[32] P. Curtin, H. Youm, and E. Salih, "Three-dimensional cancer-bone metastasis model using ex-vivo co-cultures of live

calvarial bones and cancer cells," *Biomaterials*, vol. 33, no. 4, pp. 1065–1078, 2012.

[33] A. Hot, F. Lavocat, V. Lenief, and P. Miossec, "Simvastatin inhibits the pro-inflammatory and pro-thrombotic effects of IL-17 and TNF-α on endothelial cells," *Annals of the Rheumatic Diseases*, vol. 72, no. 5, pp. 754–760, 2013.

[34] H. Luo, H.-Z. Liu, W.-W. Zhang et al., "Interleukin-17 regulates neuron-glial communications, synaptic transmission, and neuropathic pain after chemotherapy," *Cell Reports*, vol. 29, no. 8, pp. 2384–2397, 2019.

[35] E. A. Old, S. Nadkarni, J. Grist et al., "Monocytes expressing CX3CR1 orchestrate the development of vincristine-induced pain," *Journal of Clinical Investigation*, vol. 124, no. 5, pp. 2023–2036, 2014.

[36] C. Mecca, I. Giambanco, R. Donato, and C. Arcuri, "Microglia and aging: the role of the TREM2-DAP12 and CX3CL1-CX3CR1 axes," *International Journal of Molecular Sciences*, vol. 19, no. 1, p. 318, 2018.

[37] J. Lindia, E. McGowan, N. Jochnowitz, and C. Abbadie, "Induction of CX3CL1 expression in astrocytes and CX3CR1 in microglia in the spinal cord of a rat model of neuropathic pain," *The Journal of Pain*, vol. 6, no. 7, pp. 434–438, 2005.

[38] Y. Peng, X. Zhang, T. Zhang et al., "Lovastatin inhibits Toll-like receptor 4 signaling in microglia by targeting its co-receptor myeloid differentiation protein 2 and attenuates neuropathic pain," *Brain, Behavior, and Immunity*, vol. 82, pp. 432–444, 2019.

[39] L. Basso and C. Altier, "Transient receptor potential channels in neuropathic pain," *Current Opinion in Pharmacology*, vol. 32, pp. 9–15, 2017.

[40] M. Tsuda, A. Mizokoshi, Y. Shigemoto-Mogami, S. Koizumi, and K. Inoue, "Activation of p38 mitogen-activated protein kinase in spinal hyperactive microglia contributes to pain hypersensitivity following peripheral nerve injury," *Glia*, vol. 45, no. 1, pp. 89–95, 2004.

[41] C.-P. Ding, Y.-J. Guo, H.-N. Li, J.-Y. Wang, and X.-Y. Zeng, "Red nucleus interleukin-6 participates in the maintenance of neuropathic pain through JAK/STAT3 and ERK signaling pathways," *Experimental Neurology*, vol. 300, pp. 212–221, 2018.

[42] J. Yang, P. Li, X.-Y. Zhang et al., "Arginine vasopressin in hypothalamic paraventricular nucleus is transferred to the caudate nucleus to participate in pain modulation," *Peptides*, vol. 32, no. 1, pp. 71–74, 2011.

[43] P.-E. Juif and P. Poisbeau, "Neurohormonal effects of oxytocin and vasopressin receptor agonists on spinal pain processing in male rats," *Pain*, vol. 154, no. 8, pp. 1449–1456, 2013.

[44] G. Decaux, A. Soupart, and G. Vassart, "Non-peptide arginine-vasopressin antagonists: the vaptans," *The Lancet*, vol. 371, no. 9624, pp. 1624–1632, 2008.

[45] S. A. O'Sullivan, F. Gasparini, A. K. Mir, and K. K. Dev, "Fractalkine shedding is mediated by p38 and the ADAM10 protease under pro-inflammatory conditions in human astrocytes," *Journal of Neuroinflammation*, vol. 13, no. 1, p. 189, 2016.

[46] J.-H. Hu, J.-P. Yang, L. Liz et al., "Involvement of CX3CR1 in bone cancer pain through the activation of microglia p38 MAPK pathway in the spinal cord," *Brain Research*, vol. 1465, pp. 1–9, 2012.

[47] S. J. Desai, B. Prickril, and A. Rasooly, "Mechanisms of phytonutrient modulation of cyclooxygenase-2 (COX-2) and inflammation related to cancer," *Nutrition and Cancer*, vol. 70, no. 3, pp. 350–375, 2018.

[48] J. K. Bujak, D. Kosmala, I. M. Szopa, K. Majchrzak, and P. Bednarczyk, "Inflammation, cancer and immunity-implication of TRPV1 channel," *Frontiers in Oncology*, vol. 9, p. 1087, 2019.

[49] M. R. Sapio, J. K. Neubert, D. M. LaPaglia et al., "Pain control through selective chemo-axotomy of centrally projecting TRPV1$^+$ sensory neurons," *Journal of Clinical Investigation*, vol. 128, no. 4, pp. 1657–1670, 2018.

[50] S. L. Morales-Lázaro and T. Rosenbaum, "Cholesterol as a key molecule that regulates TRPV1 channel function," *Advances in Experimental Medicine and Biology*, vol. 1135, pp. 105–117, 2019.

[51] Y. Liu, D. Flores, R. Carrisoza-Gaytán, and R. Rohatgi, "Cholesterol affects flow-stimulated cyclooxygenase-2 expression and prostanoid secretion in the cortical collecting duct," *American Journal of Physiology-Renal Physiology*, vol. 308, no. 11, pp. F1229–F1237, 2015.

[52] A. Martin-Segura, A. Casadome-Perales, P. Fazzari et al., "Aging increases hippocampal DUSP2 by a membrane cholesterol loss-mediated RTK/p38MAPK activation mechanism," *Frontiers in Neurolofy*, vol. 10, p. 675, 2019.

[53] M. Amsalem, C. Poilbout, G. Ferracci, P. Delmas, and F. Padilla, "Membrane cholesterol depletion as a trigger of Nav1.9 channel-mediated inflammatory pain," *The EMBO Journal*, vol. 37, no. 8, Article ID e97349, 2018.

[54] M. M. Leitão, J. A. S. Radai, I. C. Ferrari et al., "Effects of an ethanolic extract and fractions from *Piper glabratum* (Piperaceae) leaves on pain and inflammation," *Regulatory Toxicology and Pharmacology*, vol. 117, Article ID 104762, 2020.

[55] J. Sun, X. Li, J. Liu, X. Pan, and Q. Zhao, "Stigmasterol exerts neuro-protective effect against ischemic/reperfusion injury through reduction of oxidative stress and inactivation of autophagy," *Neuropsychiatric Disease and Treatment*, vol. 15, pp. 2991–3001, 2019.

Review Article

The Pivotal Potentials of Scorpion *Buthus Martensii Karsch*-Analgesic-Antitumor Peptide in Pain Management and Cancer

Seidu A. Richard (ID),[1] **Sylvanus Kampo,**[2] **Marian Sackey,**[3] **Maite Esquijarosa Hechavarria,**[2] **and Alexis D. B. Buunaaim**[4]

[1]*Department of Medicine, Princefield University, P.O. Box MA128, Ho, Ghana*
[2]*Department of Anesthesia and Critical Care, School of Medicine, University of Health and Allied Sciences, Ho, Ghana*
[3]*Department of Pharmacy, Ho Teaching Hospital, P.O. Box MA-374, Ho, Ghana*
[4]*Department of Surgery, School of Medicine and Health Science, University for Development Studies, Tamale, Ghana*

Correspondence should be addressed to Seidu A. Richard; gbepoo@gmail.com

Scorpion *Buthus martensii Karsch* -analgesic-antitumor peptide (BmK AGAP) has been used to treat diseases like tetanus, tuberculosis, apoplexy, epilepsy, spasm, migraine headaches, rheumatic pain, and cancer in China. AGAP is a distinctive long-chain scorpion toxin with a molecular mass of 7142 Da and composed of 66 amino acids cross-linked by four disulfide bridges. Voltage-gated sodium channels (VGSCs) are present in excitable membranes and partakes in essential roles in action potentials generation as compared to the significant function of voltage-gated calcium channels (VGCCs). A total of nine genes ($Na_v1.1$–$Na_v1.9$) have been recognized to encode practical sodium channel isoforms. $Na_v1.3$, $Na_v1.7$, $Na_v1.8$, and $Na_v1.9$ have been recognized as potential targets for analgesics. $Na_v1.8$ and $Na_v1.9$ are associated with nociception initiated by inflammation signals in the neuronal pain pathway, while $Na_v1.8$ is fundamental for neuropathic pain at low temperatures. AGAP has a sturdy inhibitory influence on both viscera and soma pain. AGAP potentiates the effects of MAPK inhibitors on neuropathic as well as inflammation-associated pain. AGAP downregulates the secretion of phosphorylated p38, phosphorylated JNK, and phosphorylated ERK 1/2 *in vitro*. AGAP has an analgesic activity which may be an effective therapeutic agent for pain management because of its downregulation of PTX3 via NF-κB and Wnt/beta-catenin signaling pathway. In cancers like colon cancer, breast cancer, lymphoma, and glioma, rAGAP was capable of blocking the proliferation. Thus, AGAP is a promising therapy for these tumors. Nevertheless, research is needed with other tumors.

1. Introduction

Scorpion *Buthus martensii Karsch* (BmK) constitutes an integral portion of Chinese traditional medicine for the treatment of several diseases like tetanus, tuberculosis, apoplexy, epilepsy, spasm, migraine headaches, rheumatic pain, and cancer [1, 2]. Scorpions venom composes of a complex combination of low molecular weight bioactive molecules as well as small peptides and enzymes [1–4]. Several distinctive toxic peptides extracted from scorpion venom have diverse functions [1, 3, 4]. Analgesic-antitumor peptide (AGAP) was extracted from the venom of Scorpion

BmK approximately 20 years ago [1, 3, 4]. Studies on the expression as well as purification of AGAP were conducted using *Escherichia coli* (*E. coli*), while the biological action of AGAP was experimented in mice [5].

Recombinant AGAP (rAGAP) is made up of small ubiquitin-related modifier-AGAP (SUMO-AGAP) which is associated with a hexahistidine tag by *E. coli* [6]. Thus, rAGAP is a fusion protein comprising a hexahistidine (His6) tag, SUMO, and AGAP. Also, rAGAP was oversecreted in *E. coli* [3]. Studies demonstrated that AGAP may be a Na^+-channel specific inhibitor because it was capable of inhibiting mRNA transcription of voltage-gated sodium channels

(Na_v) [6, 7]. Electrophysiological studies using $hNa_v1.4$, $hNa_v1.5$, $hNa_v1.7$, and $hNa_v1.8$ revealed that AGAP is possibly a β-type scorpion toxin rather than an α-type toxin [8].

AGAP lengthens the survival of mice with engrafted *Ehrlich ascites* (*E. ascites*) tumor cells significantly and also subdued the growth of S-180 fibrosarcoma effectively [4]. In comparison with cyclophosphamide, it was observed that AGAP had more affinity for tumor cells and less harm for healthy cells [4]. Studies have demonstrated that AGAP has analgesic and antitumor potentials [1–4, 6]. Although scorpion toxin contains numerous toxic polypeptides with dissimilar functions as reviewed by Wang et al. [9], this review explicitly focuses on AGAP. We elucidate the cardinal analgesic and antitumor potentials of AGAP with a focus on the key signaling mechanisms via which it functions. Most of the articles reviewed were indexed in PubMed and PubMed Central with strict inclusion criteria being analgesic and antitumor potentials of BmK AGAP. The "Boolean logic" was utilized to search for articles on the subject matter. The key search words were analgesia and/or AGAP, cancer/tumor and/or AGAP, anticancer/antitumor and/or AGAP as well as AGAP signaling pathways. None peer-reviewed articles and news files were excluded.

2. Structure and Functions of BmK AGAP

AGAP is a distinctive long-chain scorpion toxin with a molecular mass of 7142 Da. It composes of 66 amino acids cross-linked by four disulfide bridges such as Cys12–Cys63, Cys16–Cys36, Cys22–Cys46, and Cys26-Cys48 [10]. This structure suggests that AGAP is a suitable model to identify an analgesic domain. AGAP demonstrated soluble secretions in *E. coli* after it was refined and duplicated. Subsequently, its bioactivity was investigated in an animal experiment [4, 11]. Nevertheless, the structure-functional association between Na_vs and AGAP, leading to the analgesic effects, still needs further studies. A total of four disulfide bridges in AGAP existed after analysis with site-directed mutagenesis in an *E. coli* model [10]. The four disulfide bonds in the AGAP were modified using 12 mutants, comprising 8 single mutants and 4 double mutants, in which Ser was substituted for Cys [10]. Also, disulfide bonds are the only common covalent cross-links in polypeptide chains [10].

The polypeptide chain in AGAP can assume numerous conformations and the sequence of its amino acid residues targets folding in a specific conformation [10]. The fundamental components associated with folding were the formation of disulfide bonds which restricts the quantity of folded conformations of a polypeptide chain [10, 12]. Furthermore, the principal consequence of disulfide bonds was stabilizing the protein foisted distance as well as angle restrictions between the C^β and S^γ atoms of the joined cysteine residues [10, 13]. The protein structure, conformational stability, catalytic activity, and folding are thus useful for further studies into AGAP [10, 14]. Also, mutants in the disulfide bridges regulating the analgesic action are visible on the molecule exterior in two domains (core and NC domains). The Core domain comprises Gly-17, Arg-18, Trp-38, and Asn-44. The Gly-17 and Arg-18 are in the long-loop linking the secondary structure motifs of the molecule α/β-core. On the other hand, NC-domain comprises five-residue-turn (residues 8–12) as well as the C-terminal region (residues 56–64) [10, 15].

3. BmK AGAP and Voltage-Gated Channels

Voltage-gated sodium channels (VGSCs) facilitate the internal sodium current in the brain and peripheral nerves [16]. VGSCs are thus crucial in triggering as well as propagation of action potentials in excitable tissues such as the brain and peripheral nerves [17]. AGAP is an ion channel regulator with diverse activities on a variation of neuronal ion channels such as high-voltage-activated (HVA), low-voltage-activated (LVA) calcium channels as well as tetrodotoxin-resistant (TTX-R) sodium channels [16]. A total of nine genes ($Na_v1.1$–$Na_v1.9$) have been recognized to encode practical sodium channel isoforms [8]. $Na_v1.4$ encoded by SCN4A was primarily secreted by skeletal muscle. It was necessary for the initiation as well as propagation of the action potential necessary for skeletal muscle contraction. On the other hand, $Na_v1.3$, $Na_v1.7$, $Na_v1.8$, and $Na_v1.9$ have been recognized as potential targets for analgesics [8].

Studies have demonstrated that peripheral nerve injury often aggravates chronic pain which was associated with hyperexcitability of sensory neurons in dorsal root ganglia (DRG) [16, 18–20]. Caffrey et al. identified two types of sodium currents in small-diameter neurons of rat DRG [21]. Furthermore, studies have shown that $Na_v1.8$ and $Na_v1.9$ are composed of the basic pattern of TTX-R sodium channel subtypes that are extremely secreted in peripheral sensory neurons [16, 18, 22]. They are both believed to partake in significant functions during ectopic expression via neuronal bodies as well as axons subsequent to peripheral nerve injury [22]. These characteristics perhaps make them possible molecular targets for analgesic drugs [16, 23]. Studies have further shown that both TTX-R subtypes, $Na_v1.8$ and $Na_v1.9$, are associated with nociception initiated by inflammation signals in neuronal pain pathway while $Na_v1.8$ was fundamental for neuropathic pain at low temperatures [24, 25].

Li et al. confirmed that AGAP might attenuate pain by blocking TTX-R channels in small-diameter DRG neurons [16]. They demonstrated that 1000 nM AGAP decreased the Nav1.8 as well as $Na_v1.9$ currents while the inhibitory proportion of $Na_v1.8$ as well as $Na_v1.9$ currents were 59.4 ± 5.1 and $33.7 \pm 6.6\%$, correspondingly. They further suggested that the consequence of AGAP on $Na_v1.8$ channels was greater than that of $Na_v1.9$ channels [16]. Jarvis et al. indicated that $Na_v1.8$ was essential in the development and/or continuation of nerve injury-induced pain [26]. They specified that numerous $Na_v1.8$-specific blockers are associated with analgesic activities in neuropathic pain [26]. Li et al. established that $Na_v1.8$ might be a potential target of AGAP in inflammatory as well as neuropathic antinociceptive targets [16]. Genetic and functional studies have demonstrated that $Na_v1.7$ was predominantly involved in

pain signaling in humans [27]. Studies further showed that $Na_v1.7$ was linked with erythromelalgia, paroxysmal life-threatening pain disorder, and congenital insensitivity to pain [27, 28]. Xu et al. demonstrated that AGAP potently blocked the action of both $hNa_v1.7$ and $hNa_v1.8$, signifying that both channel isoforms were involved in the analgesic mechanisms of AGAP [8].

Furthermore, studies have shown that $Na_v1.9$ channels are crucial intermediators of inflammation than neuropathic pain and participation in hyperexcitability of nociceptors during inflammatory pain [16, 29–31]. Also, hyperexcitability occurred during the silencing of $Na_v1.9$ resulting in the loss of depolarizing subsequent to hyperpolarizing shift in resting potential and eradicated resting inactivation on TTX-S NaCl channels [32]. Xu et al. demonstrated that AGAP showed a notable blockade influence on both $hNa_v1.4$ and $hNa_v1.5$, which accounts for its toxicity in skeletal and cardiac muscles [8]. They further proved that W38G mutation drastically reduced the blockade of I_{Nap} with an augmented calculated IC_{50} value of 60,000-fold for $hNa_v1.4$ and 420-fold for $hNa_v1.5$, respectively. They again indicated that the decreased blockade of W38G on $hNa_v1.4$ and $hNa_v1.5$ appeared as a result of its decreased inhibitory activities on both channels than its alteration on kinetic activities. Nevertheless, they explained that Trp^{38} could be the fundamental amino acid that aids in AGAP communication with $hNa_v1.4$ and $hNa_v1.5$ [8].

Liu et al. indicated that AGAP potently blocked voltage-gated calcium channels (VGCCs), particularly high-voltage triggered calcium currents in rat DRG neurons [33]. Studies have shown that AGAP reduced HVA calcium channels, specifically N-type calcium currents, while N-type calcium channels are secreted at the presynaptic level and may have more effects on EPSC/EPSP than other calcium channel types [16, 34]. Nevertheless, voltage-gated L-type calcium channels are capable of sustaining longer-lasting depolarizations leading to decreased firing threshold, control repetitive firing, and influencing regenerative action potentials [16]. Li et al. indicated that antinociceptive consequence of AGAP might be due to its precise alteration of voltage-gated ion channels of sensory neurons [16]. Payandeh et al. indicated that VGSCs are present in excitable membranes and partakes in essential roles in action potentials generation as compared to the significant function of VGCCs [17].

4. Nerve Conduction and the Role of AGAP in Pain

Studies have proven that nerve injury can trigger painful hyperalgesia subsequent to allodynia [1, 35, 36]. Also, sensitization of the peripheral nociceptor triggered by inflammation or injury manifests as hyperalgesia [1]. Hyperalgesia is an exaggerated pain reaction to a noxious stimulus, while allodynia is the perception of a nonnoxious stimulus as noxious [1, 37]. Furthermore, peripheral sensitization facilitates the firing of small-diameter sensory neurons that communicate information regarding noxious stimuli to the dorsal horn of the spinal cord and augments synaptic activities [36, 38]. This in turn triggers central sensitization, a major cellular mechanism resulting in the transformation of acute nociceptive injuries into chronic pain [1].

Central sensitization is depicted with upsurges in the excitability of neurons and augmentation of reactions to nociceptive or/and nonnociceptive stimuli [1, 37]. Central sensitization plays a crucial role in the pathogenesis of chronic pain [39]. The initiation and continuance of central sensitization are determined by maladaptive modifications in the secretion, distribution, and action of ion channels, receptors, and intracellular signal transduction pathways [1, 39]. Central sensitization is also one of the principal triggers of behavior hyperalgesia under pathologic conditions [37, 39]. Liu et al. indicated that AGAP had a sturdy inhibitory influence on both viscera and soma pain [4].

Mao et al. demonstrated that preintraplantar administration AGAP inhibited inflammatory pain triggered by formalin in a dose-dependent manner [5]. They indicated that formalin-triggered inflammatory pain was associated with the initiation of peripheral and spinal mitogen-activated protein kinases (MAPKs) both in Phase I and II [5]. Nevertheless, the above reaction was blocked by pretreatment with AGAP. Thus, they concluded that pretreatment with AGAP blocked the spinal Fos secretion triggered by formalin. Their study also revealed that AGAP potentiated the consequences of the inhibitors of MAPKs on inflammatory pain (Figure 1) [5].

Ruan et al. demonstrated that intrathecal administration of AGAP both inhibited and reversed chronic constrictive injury (CCI)-triggered by thermal hyperalgesia and mechanical allodynia [1]. They further indicated that triggering CCI augmented secretion of p-MAPKs and spinal Fos which was also inhibited or reversed by treated AGAP. Furthermore, AGAP relieved pain linked with formalin-triggered inflammation and regulated formalin-related augmented secretion of p-MAPK and spinal Fos (Figure 1). Thus, they concluded that AGAP potentiates the effects of MAPK inhibitors on neuropathic and inflammation-associated pain [1].

5. Mechanisms via Which BmK AGAP Elicits Analgesia

Liu et al. indicated that intrathecal administration of AGAP in a dose-determined manner reduced formalin-triggered spontaneous nociceptive behaviors as well as spinal c-Fos secretion in rats [40]. Ma et al. demonstrated that rAGAP and its 12 mutants were notably dissimilar from the negative control with respect to analgesic action [10]. They explained that the region responsible for analgesic action was numerous and mutants in disulfide bridges with partially damaged sections still have a native-like structure. Nevertheless, they found out that the analgesic actions of the 12 mutants were lower than those of rAGAP, which suggested that the existence of all disulfide bonds appeared to be essential for the analgesic action of the rAGAP [10].

Also, two mutants in Cys22S, Cys46S, and Cys16S, Cys36S had relatively lower actions, which means that the region of analgesic action was obviously disrupted [10].
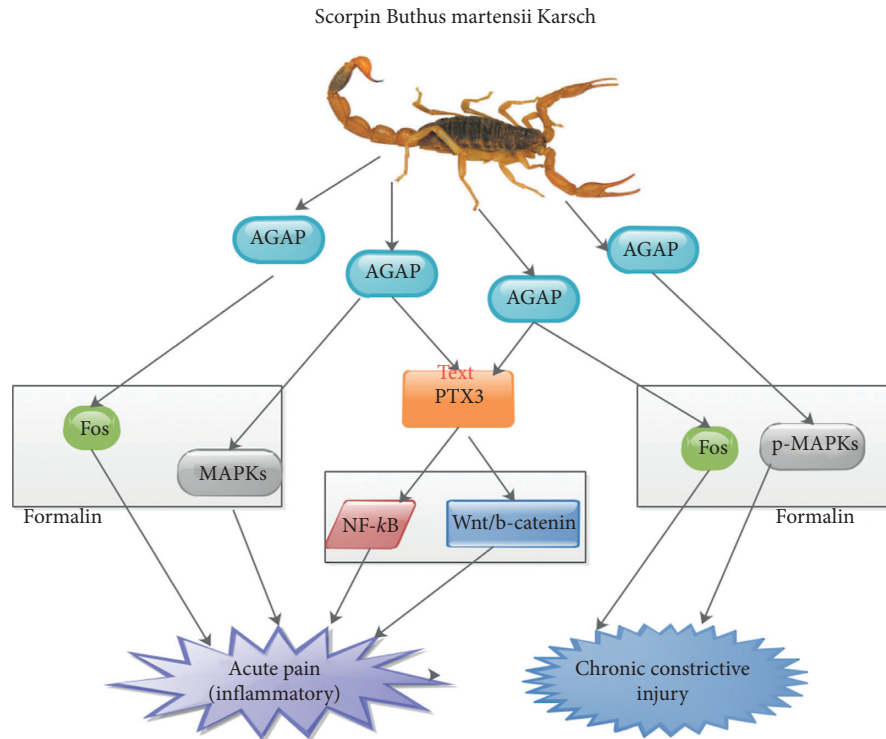
FIGURE 1: An illustration showing the inhibitory pathways via which AGAP elicited analgesia. AGAP is capable of resolving acute inflammatory pain and chronic constrictive injury via MAPS and Fos pathways in formalin.

Furthermore, the disulfide bond Cys16-Cys36 was associated with the long-loop of the β-strand II, while the bridge Cys22-Cys46 was associated with the α-helix of the β-strand II. The β-strand II was linked to the β-strand III to form a $\beta\alpha\beta$ motif comprising six key-chain hydrogen bonds [10, 41]. Ma et al. indicated that, in Cys16-Cys36 and Cys22-Cys46, the disulfide bonds were interrupted and the six key-chain hydrogen bonds also fragmented leading to augmented flexibility of the long-loop as well as β-turn II [10].

Mutants in Cys26S and Cys22S had a substantial effect on the analgesic action of AGAP. Also, amino acids Cys22 and Cys26 were detected in the α-helix which was associated with the β-strand III to form the α/β skeleton [42]. This framework was well-maintained in all the long-chain scorpion toxins described in the literature [42]. Furthermore, in mutants Cys22S and Cys26S, the entire structure may generate a major change, mainly in the analgesic region leading to a decrease in analgesic action [42].

On the other hand, Cys46S preserved 99.46% mutational action relatively, which indicated that the domain of analgesic action was practically unbroken [10]. Moreover, it was observed that, though the β-strand content of Cys36S generated a relatively reduced analgesic activity, it preserved 90.36% relative analgesic action. Also, Cys36 sited in the β-strand II may contribute to structural stability [10]. The analgesic action of its replacement did not reduce tersely, which means that the disulfide bonds played a crucial role in its regulatory activity [10, 43]. Kampo et al. demonstrated that AGAP had an analgesic activity which may be an effective therapeutic agent for pain management because of its

downregulation of PTX3 via NF-κB and Wnt/β-catenin signaling pathway (Figure 1) [44]. Further studies are required in this direction.

6. Signing Pathways via Which BmK AGAP Function

Studies have proven that modulation of MAPKs contributed to distinctive nociceptive activities and peripheral central sensitization triggered by distinctive noxious stimuli [45–48]. MAPKs, comprising p38, extracellular signal-regulated protein kinase (ERK), and Jun N-terminal kinase (JNK), are a family of serine/threonine protein kinases that transduce extracellular stimuli into intracellular posttranslational and transcriptional reactions (Figure 1) [46, 47]. Ruan et al. found that MAPKs signaling facilitated the function of AGAP via inhibiting neuropathic and inflammation-associated pain [1]. Also, AGAP potentiated the actions of MAPK inhibitors in regulating inflammation-associated pain (Figure 1) [1].

AGAP was capable of downregulating the secretion of phosphorylated p38 (p-p38), phosphorylated JNK (p-JNK), and phosphorylated ERK 1/2 *in vitro* (Figure 1) [7]. Ruan et al. demonstrated that intraplantar administration of AGAP enhanced formalin-triggered impulsive nociceptive behavior, followed by reduced secretion of peripheral as well as spinal phosphorylated (p)-MAPKs [1]. Therefore, it was likely that MAPKs, downregulatory effectors, contributed to the modifying of spinal nociceptive activities associated with AGAP [1]. Nevertheless, spinal ERK signaling was triggered

via phosphorylation and phosphorylated ERK which happens to be a marker of pain behavior-related neuronal sensitization [1, 49].

Fos protein secretory levels have been used as markers for neuronal stimulation in the central nervous system [5, 50]. It has extensively been used as a marker for the practical mapping of neuronal circuits in reaction to numerous described stimuli [50, 51]. There was a positive correlation between the amount of Fos protein secretion and the grade of sensitization triggered by nociceptive stimuli in spinal cord neurons [5]. Studies have shown that prolong triggering of the c-fiber-evoked firing of broad active collection neurons in the spinal dorsal horn in reaction to taming stimulation of afferent fibers was accompanied by the frequency-dependent upsurge of c-fos-labeled cells in superficial, intermediate, and a deep laminate of the dorsal horn on the stimulated end [5, 50, 51]. Also, AGAP was capable of inhibiting formalin-induced spinal c-Fos secretion (Figure 1) [1, 5]. Mao et al. affirmed further that pre-intraplantar administration of AGAP inhibited the secretion of spinal Fos protein in the formalin pain model (Figure 1) [5]. The reduced secretion of spinal Fos protein affirmed the antinociceptive function of pretreatment with AGAP [5].

Studies have shown that β-catenin was very crucial in mediating the cross-regulation of NF-κB via the GSK- 3β pathway [52, 53]. Kampo et al. discovered that rAGAP blocked pGSK-3β, GSK-3β, and β-catenin in vitro and in vivo (Figure 2). They indicated that AGAP was capable of reducing the secretion of p-p65/NF-κB, TNF-α, and PTX3 in breast cancer cells (Figure 30 in [44]). They thus concluded that AGAP mediated the downregulation of PTX3 via the NF-κB signaling pathway. They further observed that reduced secretion of β-catenin, Oct4, Sox2, and Snail1 and augmentation in the secretion of E-cadherin by AGAP both in vitro and in vivo were capable of decreasing breast cancer cell stemness and epithelial-mesenchymal transition (Figure 2) [44]. Further signing studies are needed to establish a link between AGAP and morphine and other pain receptors.

7. BmK AGAP and Apoptosis

Studies have demonstrated that p27 and PTEN/PI3K/Akt pathways are crucial during cell cycle succession. On the other hand, Bcl-2 family proteins modulate mitochondrial membrane permeability and mitochondrial apoptosis pathway [6, 54]. The Bcl-2 family proteins comprise anti-apoptotic protein like Bcl-xl, Bcl-2, KSHV-Bcl-2, and Bcl-w and proapoptotic proteins like Bax, Bad, and Bid [55]. Gu et al. demonstrated that rAGAP was capable of influencing apoptosis. They indicated that the secretion of cell apoptosis associated proteins like Bcl-2, Bax, and PTEN/PI3K/Akt pathway was crucial in the molecular mechanism of apoptosis stimulation [6].

Also, AGAP was capable of triggering downregulation of Bcl-2, upregulation of caspase-3, and reduced cell cycle associated protein cyclin D in MCF-7 cells and human lymphoma cells [56]. Gu et al. demonstrated that rAGAP upregulated the secretion of Bax and triggered the concurrent downregulation of Bcl-2, thus reducing the Bcl-2/Bax proportion. Moreover, the PTEN/PI3K/Akt pathway was also implicated in cell apoptosis succession [6]. They indicated that rAGAP appreciably augmented secretion of PTEN and reduced secretion of PI3K and phosphorylation stimulation of Akt [6].

8. BmK AGAP and Cell Cycle

Cell cycle comprises the pre-DNA synthesis phase G1, DNA synthesis phase (S), DNA postsynthetic phase G2, and the phase of mitosis M. It was proven that cells are capable of halting mitosis and moving from the G1 phase of the cell cycle into G0 phase which is usually a temporary stationary phase [57]. Cell cycle arrest is the crucial mechanisms via which antitumor medication elicits the function. Also, if the cell cycle is inhibited at the G1 phase, the unlimited proliferation of tumor cells would be modulated [58]. Gu et al. demonstrated that rAGAP was capable of inhibiting the adaptability of SW480 cells. They further indicated that rAGAP triggers SW480 cell cycle arrest at the G0/G1 phase, followed by a decrease in the S phase but no substantial modification in the G2/M phase [6]. Thus, the cell cycle did attain the G1/S restriction phase and was blocked from going through the G1 to S phase [59, 60].

p27, a member of the CDK blocker family, is a tumor suppressor gene that inhibits phosphorylation of the Rb protein and accordingly blocks cell growth and proliferation [6]. Studies have shown that the PI3K pathway played a critical role during cell cycle progression. This pathway was triggered in the G1/S transition leading to cell proliferation, growth, and resistance to cancer therapy [61, 62]. Furthermore, PTEN was a tumor suppressor gene regulated via the PI3K/Akt pathway [63]. Studies have proven that p-Akt phosphorylates proteins like NFκB, mTOR, Bad, GSK-3β, and MDM-2 leading to the augmentation of cell growth, metabolism, survival, and proliferation once it was activated [64, 65]. Moreover, the PTEN/PI3K/Akt pathway blocked G1/S cell cycle progression and G2/M transition resulting in defects in DNA damage checkpoint control when it was constitutively activated [66].

Gu et al. demonstrated that rAGAP upregulated the secretion of p27 and PTEN, while it downregulated PI3K and p-Akt secretion. They established that rAGAP was capable of increasing the quantity of p27 protein and blockade PI3K/Akt signal transduction resulting in G0/G1 cell cycle arrest in SW480 cells [6]. Zhao demonstrated that the cell cycle was triggered by rAGAP in SHG-44 cell arrested in the G1 phase, followed by a decrease in the S phase with no alteration in the G2/M phase [7]. They further indicated that the cell cycle from G1 to S phase was modulated via cyclin D/CDK4 (CDK6) or cyclin E/CDK2 multiplexes. Cyclin/CDK multiplexes intermediated RB phosphorylation in the late G1 phase, and hyperphosphorylated RB triggered the secretion of transcription factor E2F, leading to cell cycle progression to S phase [7]. Also, the downregulation of p-AKT resulted in a decreased secretion of CDK2 and CDK6 leading to a decrease in the protein levels of p-RB. Thus, this pathway was capable of influencing cell cycle arrest in the G1 phase and blockade of the proliferation of SHG-44 cells [7].
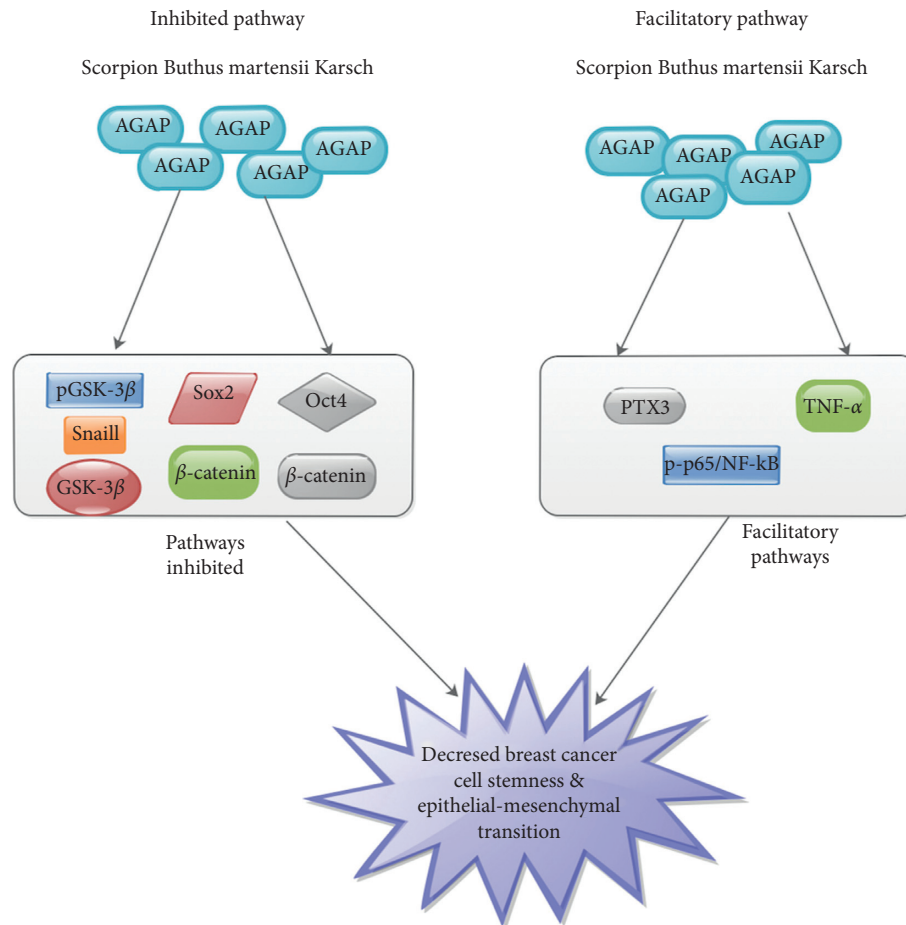
Figure 2: An illustration showing the inhibitory and facilitatory pathways via which AGAP is decreasing breast cancer cell stemness and epithelial-mesenchymal transition.

9. BmK AGAP and Cancer

Liu et al. indicated that AGAP has an antitumor effect against *E. ascites* tumor and S-180 fibrosarcoma. They further indicated that AGAP was more effective for tumor cells and less harmful for healthy cells than cyclophosphamide [4]. Additionally, rAGAP was capable of blocking the proliferation of lymphoma and glioma [3]. Thus, rAGAP is a promising antitumor therapy [3]. Hence, further studies are needed in this direction. Also, comparative studies between the antitumor potentials and already established anticancer medications are warranted. Gu et al. indicated that the intrinsic apoptotic pathway modulating the Bcl-2 family and the PTEN/PI3K/Akt pathway was associated with rAGAP-triggered SW480 colon cancer cell (CRC) apoptosis (Figure 3). Thus, rAGAP was a potential therapeutic agent for CRC [6].

Zhao et al. demonstrated that AGAP downregulated the protein secretion of p-AKT and p-Erk1/2 resulting in a decrease in the protein concentrations of CDK2, CDK6, and p-RB, leading to G1 cell cycle arrest (Figure 3) [7]. These alterations resulted in the blockade of SHG-44 cells proliferation. They further indicated that AGAP was capable of blocking the proliferation and migration of SHG-44 cells leading to suppressing of protein secretory levels of VEGF

and MMP-9 via downregulation of NF-kB and BCL-2 which were modulated via the triggering of p-AKT, p-p38, and p-c-Jun (Figure 3) [7]. They concluded that, when the concentrations of rAGAP were elevated, the protein levels of NF-kB and BCL-2 in treated SHG-44 cells were gradually downregulated via suppressing the protein secretory levels of p-AKT, p-Erk1/2, p-c-Jun, and p-p38 in a dose-dependent manner [7]. Nevertheless, there was a decrease in the concentration of VEGF and MMP-9 via the modulation of NF-kB and BCL-2. Zhao et al. further revealed that the migration of SHG-44 cells in a wound healing assay was associated with Erk, p38, c-Jun, MAPK, and AKT pathway (Figure 3). Thus, rAGAP was capable of blocking the proliferation of SHG-44 cells via suppressing the modulation of p-Erk1/2. They stressed in their experiments involving the DNA ladder that rAGAP induced SHG-44 cells in a dose- and time-dependent manner, but the DNA ladder did not occur [7].

PTX3 was capable of triggering inflammation activities as well as complement [67]. Also, PTX3 was capable of recruiting leukocyte into inflamed tissues and clearance of apoptotic cells [68]. Bonavita et al. demonstrated that PTX3 influences tumor associated inflammation and chemo-resistance during breast cancer treatment [69]. Basile et al. established that NF-κB binding site, p65/NF-κB was
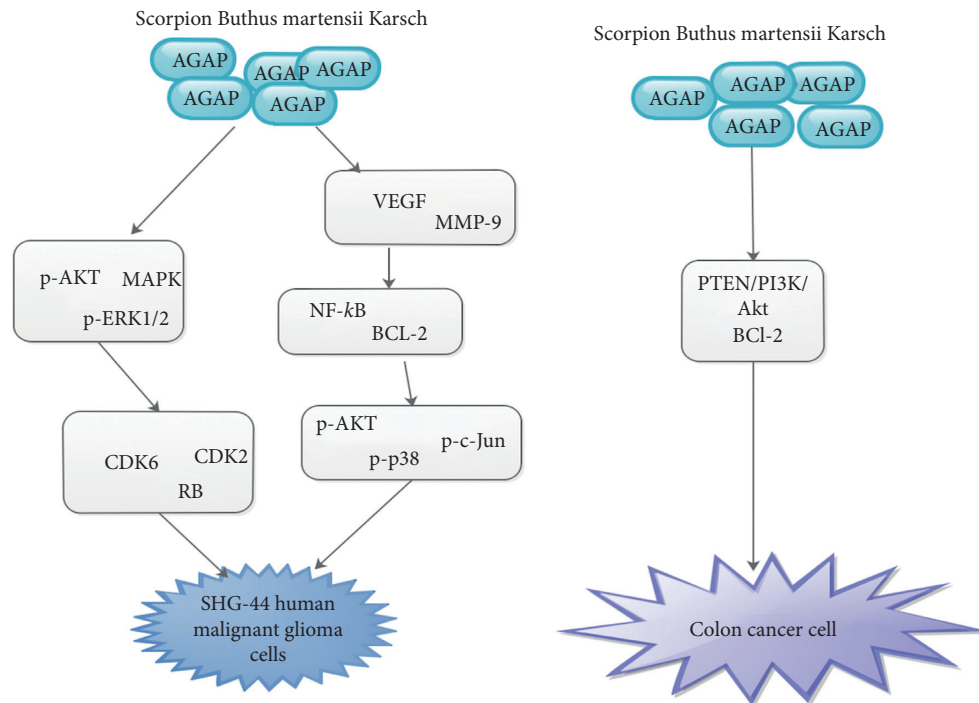
FIGURE 3: An illustration showing the pathways via which AGAP influence SHG-44 Human Malignant Glioma Cells and colon cancer cell.

functionally significant in PTX3 promoter such as TNF-α. They indicated that the activities of NF-κB in TNF-α were essential for the molecular mechanisms vital for the modulation of PTX3 [70]. Nevertheless, the secretion of PTX3 in breast cancer was elevated and linked to stem-like structures, epithelial-mesenchymal transition, migration, invasion, and metastasis [71]. Kampo et al. demonstrated that AGAP blocked cancer stemness and epithelial-mesenchymal transition via downregulating PTX3 secretion in breast cancer [44]. They indicated that AGAP intermediated downregulation of PTX3 via NF-κB and Wnt/beta-catenin signaling pathways. They concluded that AGAP had analgesic activity which may be an effective therapeutic agent for cancer [44].

10. Conclusion

Our review points clearly to the fact that AGAP has analgesic and antitumor potentials. AGAP had a sturdy inhibitory influence on both viscera and soma pain. VGSCs are present in excitable membranes and partake in essential roles in action potentials generation as compared to the significant function of VGCCs. AGAP potentiates the effects of MAPK inhibitors on neuropathic and inflammation-associated pain. AGAP has more affinity for tumor cells and has less harmful effects on healthy cells. In cancers like colon cancer, breast cancer, lymphoma, and glioma, rAGAP was capable of blocking proliferation. Thus, AGAP is a promising analgesic and antitumor therapy for these tumors. Nevertheless, research is needed with other tumors.

Data Availability

No data were used to support this paper.

Conflicts of Interest

The authors declare that they have no conflicts of interest.

Authors' Contributions

All authors contributed toward literature search, drafting, and critical revision of the paper and agreed to be accountable for all aspects of the work.

References

[1] J.-P. Ruan, Q.-H. Mao, W.-G. Lu et al., "Inhibition of spinal MAPKs by scorpion venom peptide BmK AGAP produces a sensory-specific analgesic effect," *Molecular Pain*, vol. 14, 2018.

[2] J. Shao, R. Zhang, X. Ge, B. Yang, and J. Zhang, "Analgesic peptides in Buthus martensii Karsch: a traditional Chinese animal medicine," *Asian Traditional Medicine*, vol. 2, no. 2, pp. 45–50, 2007.

[3] P. Cao, J. Yu, W. Lu et al., "Expression and purification of an antitumor-analgesic peptide from the venom of Mesobuthus martensii Karsch by small ubiquitin-related modifier fusion in *Escherichia coli*," *Biotechnology Progress*, vol. 26, no. 5, pp. 1240–1244, 2010.

[4] Y.-F. Liu, R.-L. Ma, S.-L. Wang et al., "Expression of an antitumor-analgesic peptide from the venom of Chinese scorpion Buthus martensii karsch in *Escherichia coli*," *Protein Expression and Purification*, vol. 27, no. 2, pp. 253–258, 2003.

[5] Q. Mao, J. Ruan, X. Cai et al., "Antinociceptive effects of analgesic-antitumor peptide (AGAP), a neurotoxin from the scorpion Buthus martensii Karsch, on formalin-induced inflammatory pain through a mitogen-activated protein kinases–dependent mechanism in mice," *PLoS One*, vol. 8, no. 11, Article ID e78239, 2013.

[6] Y. Gu, S.-L. Liu, W.-Z. Ju, C.-Y. Li, and P. Cao, "Analgesic-antitumor peptide induces apoptosis and inhibits the proliferation of SW480 human colon cancer cells," *Oncology Letters*, vol. 5, no. 2, pp. 483–488, 2013.

[7] Y. Zhao, X. Cai, T. Ye et al., "Analgesic-antitumor peptide inhibits proliferation and migration of SHG-44 human malignant glioma cells," *Journal of Cellular Biochemistry*, vol. 112, no. 9, pp. 2424–2434, 2011.

[8] Y. Xu, X. Meng, X. Hou et al., "A mutant of theButhus martensiiKarsch antitumor-analgesic peptide exhibits reduced inhibition to hNav1.4 and hNav1.5 channels while retaining analgesic activity," *Journal of Biological Chemistry*, vol. 292, no. 44, pp. 18270–18280, 2017.

[9] J. Wang, H. Zhang, S. Gao, and J. Wang, "Review on pharmacological activities of the peptides from scorpion Buthus martensii Karsch," *Journal of Pharmaceutics & Drug Development*, vol. 3, no. 2, pp. 1–6, 2015.

[10] R. Ma, Y. Cui, Y. Zhou et al., "Location of the analgesic domain in Scorpion toxin BmK AGAP by mutagenesis of disulfide bridges," *Biochemical and Biophysical Research Communications*, vol. 394, no. 2, pp. 330–334, 2010.

[11] Y. Cui, G.-L. Guo, L. Ma et al., "Structure and function relationship of toxin from Chinese scorpion Buthus martensii Karsch (BmKAGAP): gaining insight into related sites of analgesic activity," *Peptides*, vol. 31, no. 6, pp. 995–1000, 2010.

[12] C. B. Anfinsen, "Principles that govern the folding of protein chains," *Science*, vol. 181, no. 4096, pp. 223–230, 1973.

[13] C. N. Pace, G. R. Grimsley, J. A. Thomson, and B. J. Barnett, "Conformational stability and activity of ribonuclease T1 with zero, one, and two intact disulfide bonds," *Journal of Biological Chemistry*, vol. 263, no. 24, pp. 11820–11825, 1998.

[14] T. A. Klink, K. J. Woycechowsky, K. M. Taylor, and R. T. Raines, "Contribution of disulfide bonds to the conformational stability and catalytic activity of ribonuclease A," *European Journal of Biochemistry*, vol. 267, no. 2, pp. 566–572, 2004.

[15] I. Karbat, F. Frolow, O. Froy et al., "Molecular basis of the high insecticidal potency of scorpion α-toxins," *Journal of Biological Chemistry*, vol. 279, no. 30, pp. 31679–31686, 2004.

[16] C.-L. Li, X.-F. Liu, G.-X. Li et al., "Antinociceptive effects of AGAP, a recombinant neurotoxic polypeptide: possible involvement of the tetrodotoxin-resistant sodium channels in small dorsal root ganglia neurons," *Frontiers in Pharmacology*, vol. 7, p. 496, 2016.

[17] J. Payandeh, T. Scheuer, N. Zheng, and W. A. Catterall, "The crystal structure of a voltage-gated sodium channel," *Nature*, vol. 475, no. 7356, pp. 353–358, 2011.

[18] S. D. Dib-Hajj, T. R. Cummins, J. A. Black, and S. G. Waxman, "Sodium channels in normal and pathological pain," *Annual Review of Neuroscience*, vol. 33, no. 1, pp. 325–347, 2010.

[19] L. Djouhri, X. Fang, S. Koutsikou, and S. N. Lawson, "Partial nerve injury induces electrophysiological changes in conducting (uninjured) nociceptive and nonnociceptive DRG neurons: possible relationships to aspects of peripheral neuropathic pain and paresthesias," *Pain*, vol. 153, no. 9, pp. 1824–1836, 2012.

[20] A. Ebersberger, G. Natura, A. Eitner, K.-J. Halbhuber, R. Rost, and H.-G. Schaible, "Effects of prostaglandin D2 on tetrodotoxin-resistant Na+ currents in DRG neurons of adult rat," *Pain*, vol. 152, no. 5, pp. 1114–1126, 2011.

[21] J. Caffrey, D. Eng, J. Black, S. Waxman, and J. Kocsis, "Three types of sodium channels in adult rat dorsal root ganglion neurons," *Brain Research*, vol. 592, no. 1-2, pp. 283–297, 1992.

[22] Y.-Q. Yu, F. Zhao, S.-M. Guan, and J. Chen, "Antisense-mediated knockdown of Nav1. 8, but not Nav1. 9, generates inhibitory effects on complete Freund's adjuvant-induced inflammatory pain in rat," *PLoS One*, vol. 6, no. 5, Article ID e19865, 2011.

[23] T. Berta, O. Poirot, M. Pertin, R.-R. Ji, S. Kellenberger, and I. Decosterd, "Transcriptional and functional profiles of voltage-gated Na+ channels in injured and non-injured DRG neurons in the SNI model of neuropathic pain," *Molecular and Cellular Neuroscience*, vol. 37, no. 2, pp. 196–208, 2008.

[24] K. Zimmermann, A. Leffler, A. Babes et al., "Sensory neuron sodium channel Nav1.8 is essential for pain at low temperatures," *Nature*, vol. 447, no. 7146, pp. 856–859, 2007.

[25] J. Lai, F. Porreca, J. C. Hunter, and M. S. Gold, "Voltage-gatedsodiumchannels and hyperalgesia," *Annual Review of Pharmacology and Toxicology*, vol. 44, no. 1, pp. 371–397, 2004.

[26] M. F. Jarvis, P. Honore, C.-C. Shieh et al., "A-803467, a potent and selective Nav1.8 sodium channel blocker, attenuates neuropathic and inflammatory pain in the rat," *Proceedings of the National Academy of Sciences*, vol. 104, no. 20, pp. 8520–8525, 2007.

[27] S. Yang, Y. Xiao, D. Kang et al., "Discovery of a selective NaV1.7 inhibitor from centipede venom with analgesic efficacy exceeding morphine in rodent pain models," *Proceedings of the National Academy of Sciences*, vol. 110, no. 43, pp. 17534–17539, 2013.

[28] S. D. Dib-Hajj, Y. Yang, J. A. Black, and S. G. Waxman, "The NaV1.7 sodium channel: from molecule to man," *Nature Reviews Neuroscience*, vol. 14, no. 1, pp. 49–62, 2012.

[29] F. Amaya, I. Decosterd, T. A. Samad et al., "Diversity of expression of the sensory neuron-specific TTX-resistant voltage-gated sodium ion channels SNS and SNS2," *Molecular and Cellular Neuroscience*, vol. 15, no. 4, pp. 331–342, 2000.

[30] B. T. Priest, B. A. Murphy, J. A. Lindia et al., "Contribution of the tetrodotoxin-resistant voltage-gated sodium channel NaV1.9 to sensory transmission and nociceptive behavior," *Proceedings of the National Academy of Sciences*, vol. 102, no. 26, pp. 9382–9387, 2005.

[31] J. A. R. Östman, M. A. Nassar, J. N. Wood, and M. D. Baker, "GTP up-regulated persistent Na+current and enhanced nociceptor excitability require NaV1.9," *The Journal of Physiology*, vol. 586, no. 4, pp. 1077–1087, 2008.

[32] T. R. Cummins and S. G. Waxman, "Downregulation of tetrodotoxin-resistant sodium currents and upregulation of a rapidly repriming tetrodotoxin-sensitive sodium current in small spinal sensory neurons after nerve injury," *The Journal of Neuroscience*, vol. 17, no. 10, pp. 3503–3514, 1997.

[33] X. Liu, C. Li, J. Chen et al., "AGAP, a new recombinant neurotoxic polypeptide, targets the voltage-gated calcium channels in rat small diameter DRG neurons," *Biochemical and Biophysical Research Communications*, vol. 452, no. 1, pp. 60–65, 2014.

[34] K. Tsuzuki, H. Xing, J. Ling, and J. G. Gu, "Menthol-induced Ca2+ release from presynaptic Ca2+ stores potentiates sensory synaptic transmission," *Journal of Neuroscience*, vol. 24, no. 3, pp. 762–771, 2004.

[35] M. Devor, "The pathophysiology of damaged peripheral nerves," *In Fernando Cervero, Troels S. Jensen; Handbook of Clinical Neurology*, vol. 81, pp. 261–276, 2006, Elsevier, Amsterdam, Netherlands.

[36] C. J. Woolf, "Central sensitization," *Anesthesiology*, vol. 106, no. 4, pp. 864–867, 2007.

[37] H. Ikeda, B. Heinke, R. Ruscheweyh, and J. Sandkühler, "Synaptic plasticity in spinal lamina I projection neurons that mediate hyperalgesia," *Science*, vol. 299, no. 5610, pp. 1237–1240, 2003.

[38] M. Zimmermann, "Pathobiology of neuropathic pain," *European Journal of Pharmacology*, vol. 429, no. 1–3, pp. 23–37, 2001.

[39] R. Melzack, T. J. Coderre, J. Katz, and A. L. Vaccarino, "Central neuroplasticity and pathological pain," *Annals of the New York Academy of Sciences*, vol. 933, no. 1, pp. 157–174, 2001.

[40] T. Liu, X.-Y. Pang, F. Jiang, Z.-T. Bai, and Y.-H. Ji, "Antinociceptive effects induced by intrathecal injection of BmK AS, a polypeptide from the venom of Chinese-scorpion Buthus martensi Karsch, in rat formalin test," *Journal of Ethnopharmacology*, vol. 117, no. 2, pp. 332–338, 2008.

[41] X.-L. He, H.-M. Li, Z.-H. Zeng, X.-Q. Liu, M. Wang, and D.-C. Wang, "Crystal structures of two α-like scorpion toxins: non-proline cis peptide bonds and implications for new binding site selectivity on the sodium channel," *Journal of Molecular Biology*, vol. 292, no. 1, pp. 125–135, 1999.

[42] S. Mouhat, B. Jouirou, A. Mosbah, M. De Waard, and J.-M. Sabatier, "Diversity of folds in animal toxins acting on ion channels," *Biochemical Journal*, vol. 378, no. 3, pp. 717–726, 2004.

[43] M. E. Moghaddam and H. Naderi-Manesh, "Role of disulfide bonds in modulating internal motions of proteins to tune their function: molecular dynamics simulation of scorpion toxin Lqh III," *Proteins: Structure, Function, and Bioinformatics*, vol. 63, no. 1, pp. 188–196, 2006.

[44] S. Kampo, B. Ahmmed, T. Zhou et al., "Scorpion venom analgesic peptide, BmK AGAP inhibits stemness, and epithelial-mesenchymal transition by down-regulating PTX3 in breast cancer," *Frontiers in Oncology*, vol. 9, p. 21, 2019.

[45] R.-R. Ji, H. Baba, G. J. Brenner, and C. J. Woolf, "Nociceptive-specific activation of ERK in spinal neurons contributes to pain hypersensitivity," *Nature Neuroscience*, vol. 2, no. 12, pp. 1114–1119, 1999.

[46] S.-X. Jin, Z.-Y. Zhuang, C. J. Woolf, and R.-R. Ji, "p38 mitogen-activated protein kinase is activated after a spinal nerve ligation in spinal cord microglia and dorsal root ganglion neurons and contributes to the generation of neuropathic pain," *The Journal of Neuroscience*, vol. 23, no. 10, pp. 4017–4022, 2003.

[47] K. Obata and K. Noguchi, "MAPK activation in nociceptive neurons and pain hypersensitivity," *Life Sciences*, vol. 74, no. 21, pp. 2643–2653, 2004.

[48] R.-R. Ji, R. W. Gereau, M. Malcangio, and G. R. Strichartz, "MAP kinase and pain," *Brain Research Reviews*, vol. 60, no. 1, pp. 135–148, 2009.

[49] Y.-J. Gao and R.-R. Ji, "c-Fos or pERK, which is a better marker for neuronal activation and central sensitization after noxious stimulation and tissue injury?" *The Open Pain Journal*, vol. 2, no. 1, p. 11, 2009.

[50] Z. Wang, Y. Zhang, and Z. Zhao, "Inhibition of tetanically sciatic stimulation-induced LTP of spinal neurons and Fos expression by disrupting glutamate transporter GLT-1," *Neuropharmacology*, vol. 51, no. 4, pp. 764–772, 2006.

[51] J.-P. Ruan, H.-X. Zhang, X.-F. Lu, Y.-P. Liu, and J.-L. Cao, "EphrinBs/EphBs signaling is involved in modulation of spinal nociceptive processing through a mitogen-activated protein kinases-dependent mechanism," *Anesthesiology*, vol. 112, no. 5, pp. 1234–1249, 2010.

[52] N. D. Perkins, "The diverse and complex roles of NF-κB subunits in cancer," *Nature Reviews Cancer*, vol. 12, no. 2, pp. 121–132, 2012.

[53] J. Deng, W. Xia, S. A. Miller, Y. Wen, H.-Y. Wang, and M.-C. Hung, "Crossregulation of NF-κB by the APC/GSK-3β/β-catenin pathway," *Molecular Carcinogenesis*, vol. 39, no. 3, pp. 139–146, 2004.

[54] Y. Guo, S. M. Srinivasula, A. Druilhe, T. Fernandes-Alnemri, and E. S. Alnemri, "Caspase-2 induces apoptosis by releasing proapoptotic proteins from mitochondria," *Journal of Biological Chemistry*, vol. 277, no. 16, pp. 13430–13437, 2002.

[55] A. M. Petros, E. T. Olejniczak, and S. W. Fesik, "Structural biology of the Bcl-2 family of proteins," *Biochimica et Biophysica Acta (BBA)-Molecular Cell Research*, vol. 1644, no. 2-3, pp. 83–94, 2004.

[56] W. Li, Y. Li, Y. Zhao, J. Yuan, and W. Mao, "Inhibition effects of scorpion venom extracts (Buthus matensii Karsch) on the growth of human breast cancer MCF-7 cells," *African Journal of Traditional, Complementary and Alternative Medicines*, vol. 11, no. 5, pp. 105–110, 2014.

[57] M. A. Chaudhry, "Base excision repair of ionizing radiation-induced DNA damage in G1 and G2 cell cycle phases," *Cancer Cell International*, vol. 7, no. 1, p. 15, 2020.

[58] J. C. Sitko, B. Yeh, M. Kim et al., "SOCS3 regulates p21 expression and cell cycle arrest in response to DNA damage," *Cellular Signalling*, vol. 20, no. 12, pp. 2221–2230, 2008.

[59] K. Narbonne-Reveau and M. Lilly, "The Cyclin-dependent kinase inhibitor Dacapo promotes genomic stability during premeiotic S phase," *Molecular Biology of the Cell*, vol. 20, no. 7, pp. 1960–1969, 2009.

[60] S. Liu and H. Yamauchi, "p27-Associated G1 arrest induced by hinokitiol in human malignant melanoma cells is mediated via down-regulation of pRb, Skp2 ubiquitin ligase, and impairment of Cdk2 function," *Cancer Letters*, vol. 286, no. 2, pp. 240–249, 2009.

[61] S. M. Jones and A. Kazlauskas, "Growth-factor-dependent mitogenesis requires two distinct phases of signalling," *Nature Cell Biology*, vol. 3, no. 2, pp. 165–172, 2001.

[62] J. Liang, J. Zubovitz, T. Petrocelli et al., "PKB/Akt phosphorylates p27, impairs nuclear import of p27 and opposes p27-mediated G1 arrest," *Nature Medicine*, vol. 8, no. 10, pp. 1153–1160, 2002.

[63] A. Carnero, "The PKB/AKT pathway in cancer," *Current Pharmaceutical Design*, vol. 16, no. 1, pp. 34–44, 2020.

[64] J. A. Engelman, J. Luo, and L. C. Cantley, "The evolution of phosphatidylinositol 3-kinases as regulators of growth and metabolism," *Nature Reviews Genetics*, vol. 7, no. 8, pp. 606–619, 2006.

[65] G. Song, G. Ouyang, and S. Bao, "The activation of Akt/PKB signaling pathway and cell survival," *Journal of Cellular and Molecular Medicine*, vol. 9, no. 1, pp. 59–71, 2007.

[66] J. Liang and J. M. Slingerland, "Multiple roles of the PI3K/PKB (Akt) pathway in cell cycle progression," *Cell Cycle*, vol. 2, no. 4, pp. 336–342, 2020.

[67] B. Bottazzi, A. Inforzato, M. Messa et al., "The pentraxins PTX3 and SAP in innate immunity, regulation of inflammation and tissue remodelling," *Journal of Hepatology*, vol. 64, no. 6, pp. 1416–1427, 2016.

[68] K. Daigo, A. Mantovani, and B. Bottazzi, "The yin-yang of long pentraxin PTX3 in inflammation and immunity," *Immunology Letters*, vol. 161, no. 1, pp. 38–43, 2014.

[69] E. Bonavita, S. Gentile, M. Rubino et al., "PTX3 is an extrinsic oncosuppressor regulating complement-dependent inflammation in cancer," *Cell*, vol. 160, no. 4, pp. 700–714, 2015.

[70] A. Basile, A. Sica, E. d'Aniello et al., "Characterization of the promoter for the human long pentraxin PTX3 role of NF-κB in tumor necrosis factor-α and interleukin-1β regulation," *Journal of Biological Chemistry*, vol. 272, no. 13, pp. 8172–8178, 1997.

[71] S.-H. Chan, J.-P. Tsai, C.-J. Shen, Y.-H. Liao, and B.-K. Chen, "Oleate-induced PTX3 promotes head and neck squamous cell carcinoma metastasis through the up-regulation of vimentin," *Oncotarget*, vol. 8, no. 25, p. 41364, 2017.